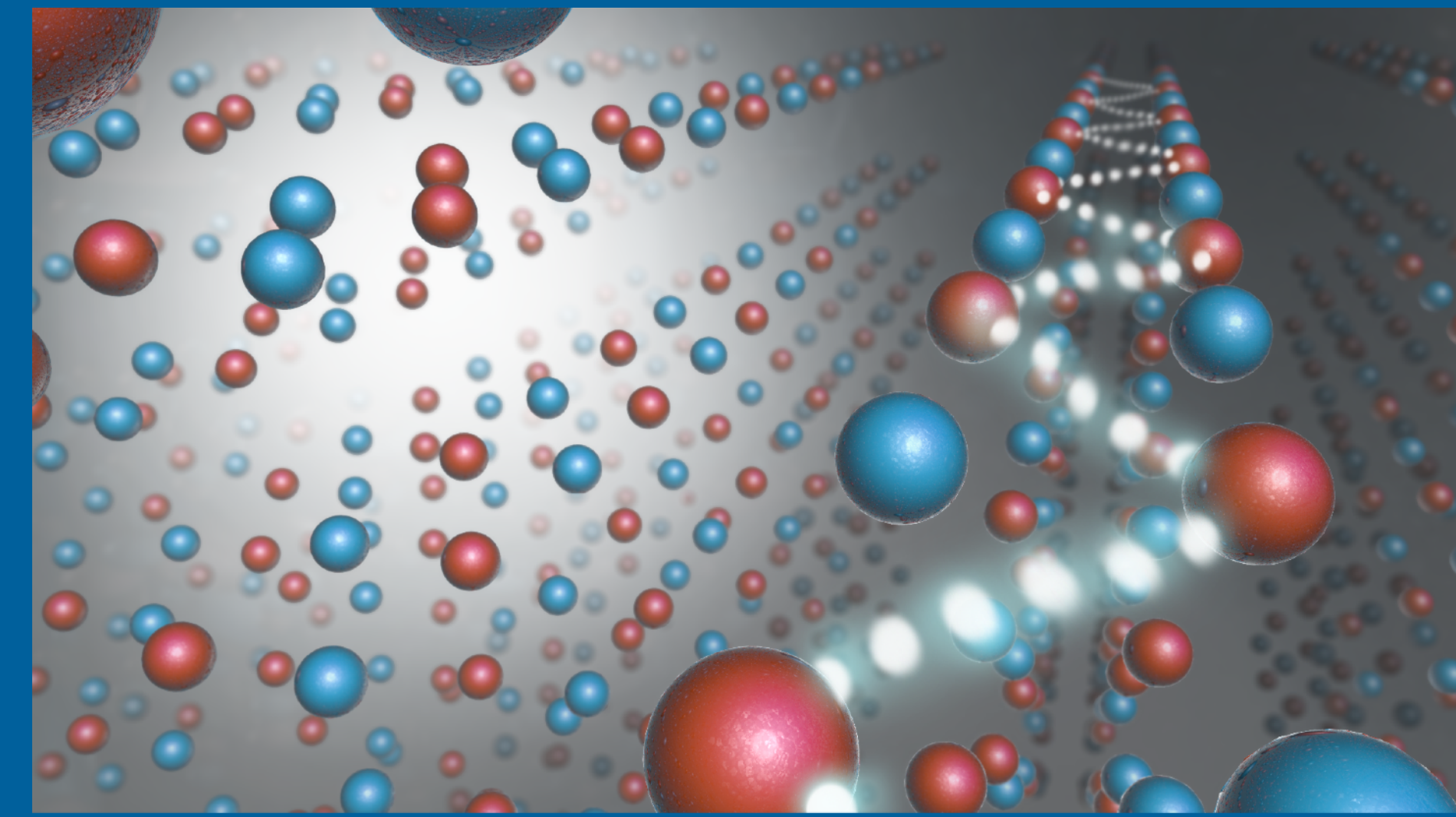


SINGLE CRYSTAL DIFFUSE SCATTERING



RAYMOND OSBORN

Neutron & X-ray Scattering Group
Materials Science Division

Acknowledgements: Stephan Rosenkranz and Matthew Krogstad



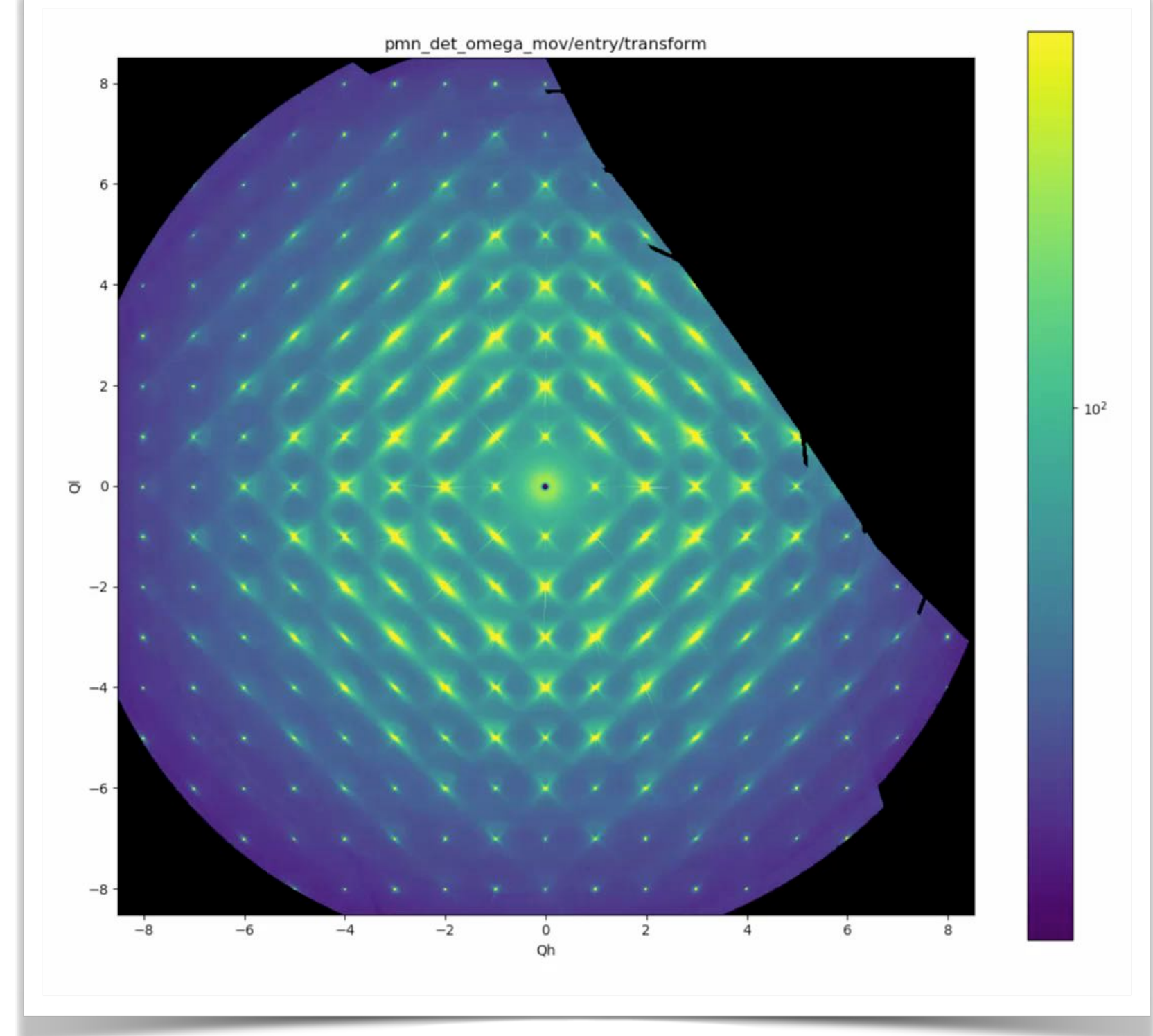
Argonne National Laboratory is a
U.S. Department of Energy laboratory
managed by UChicago Argonne, LLC.

Work supported by the U.S. Department of Energy,
Office of Science, Materials Sciences and Engineering Division.

Neutron & X-ray School
July 21, 2022

OUTLINE

- What is diffuse scattering?
 - What causes it?
- What is it good for?
 - A random walk through disordered materials
- How do I model it?
 - A few equations
- How do I measure it?
- Case Study 1: Diffuse scattering from vacancies in mullite
- Case Study 2: 3D- Δ PDF in sodium-intercalated V_2O_5
- How do I look at static disorder?
 - Diffuse scattering with elastic discrimination

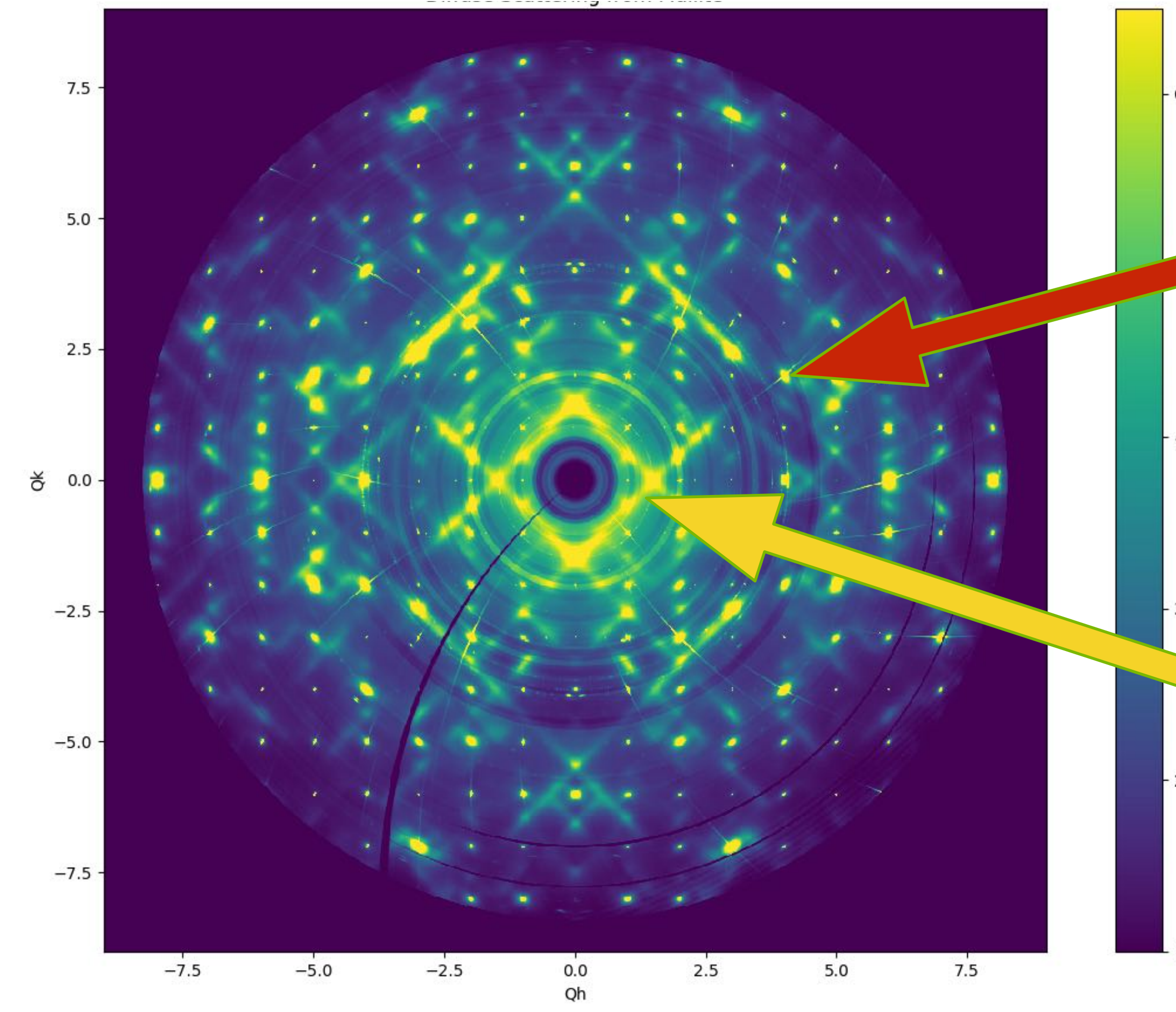


WHAT IS DIFFUSE SCATTERING?



U.S. DEPARTMENT OF
ENERGY
Argonne National Laboratory is a
U.S. Department of Energy laboratory
managed by UChicago Argonne, LLC.





Bragg Scattering
Average Structure

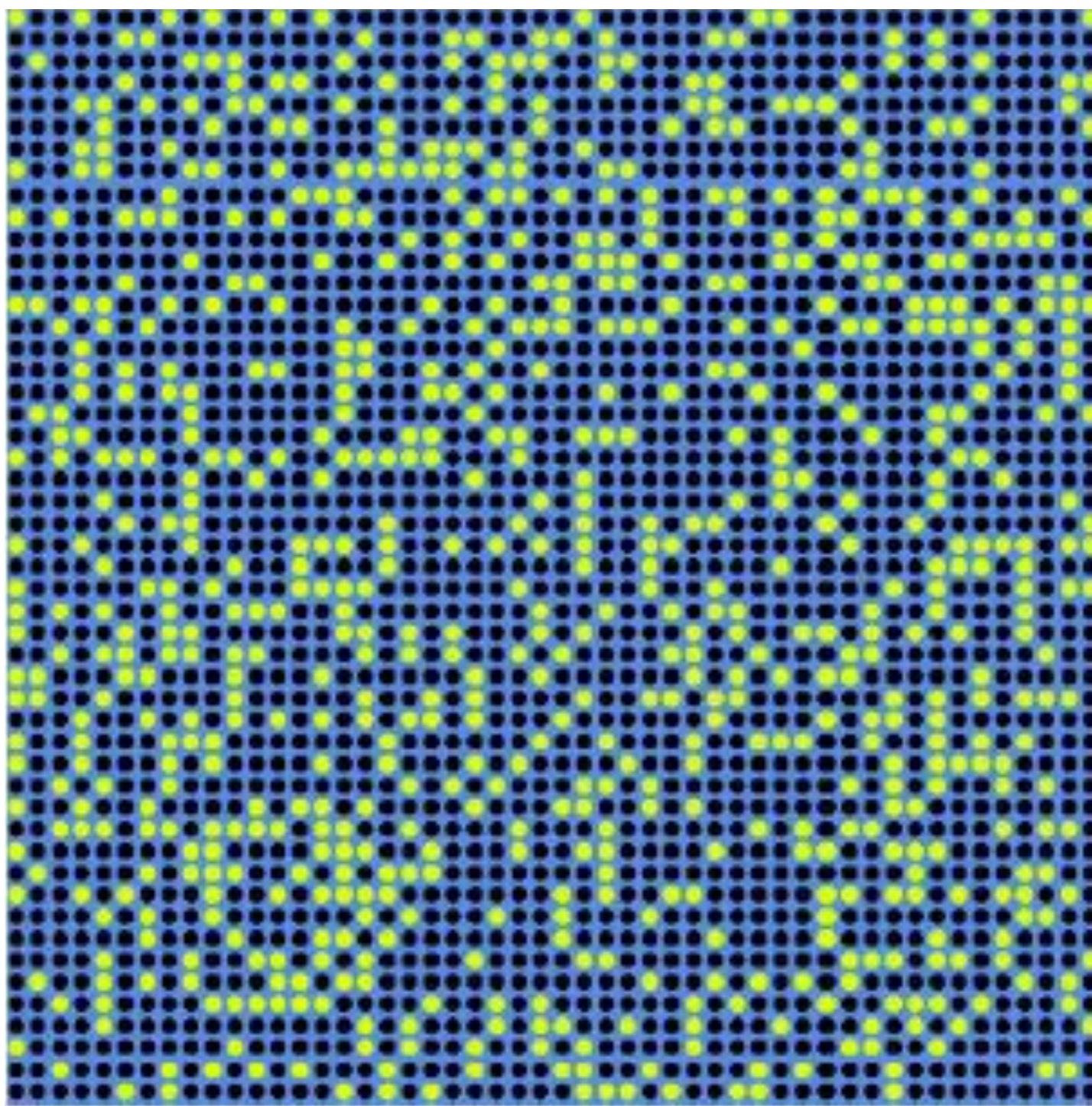
Diffuse Scattering
Deviations from the Average Structure

DIFFUSE SCATTERING

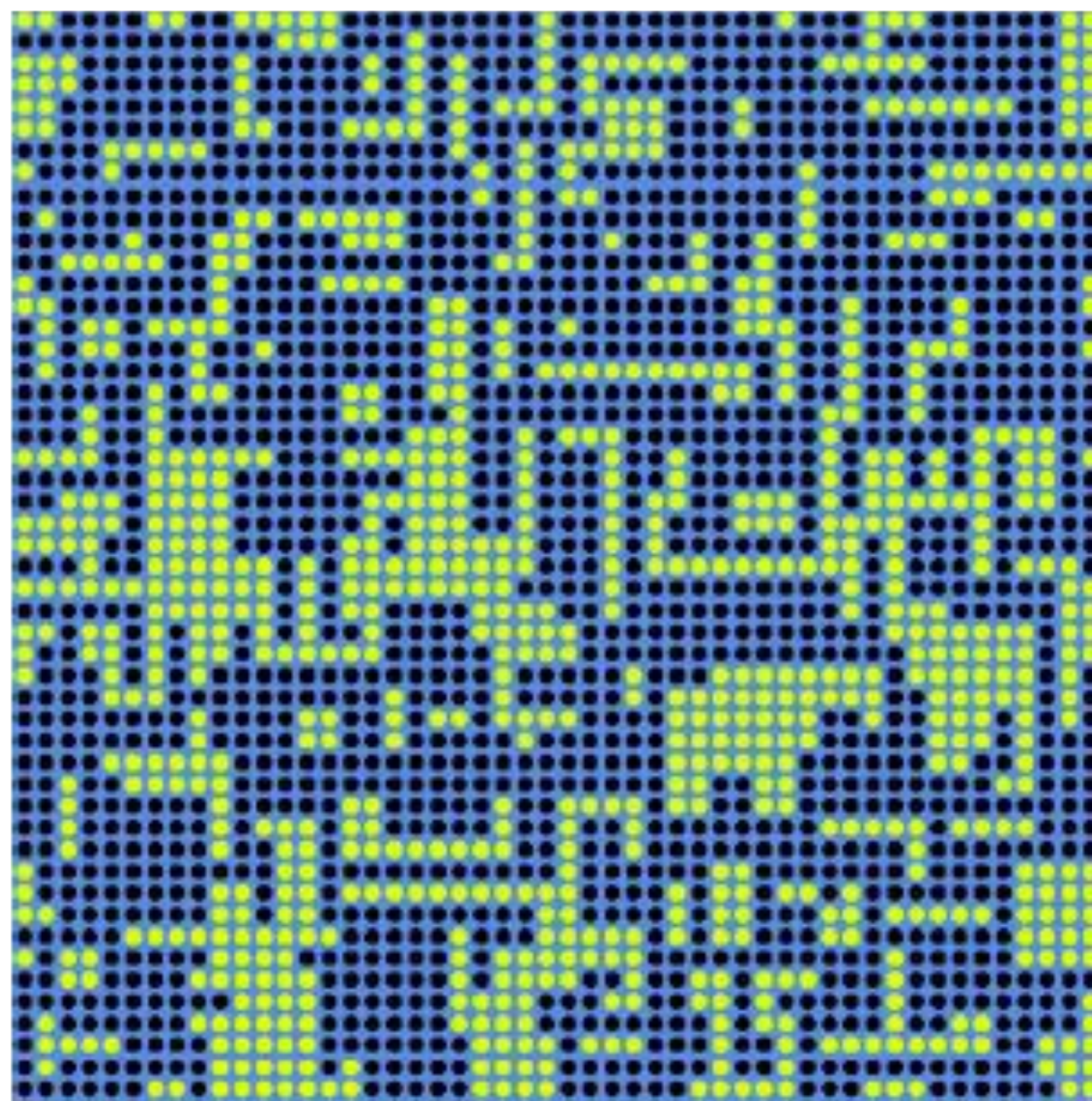
SIMPLE EXAMPLE OF DISORDER

Replace 30% of atoms (blue dots) by vacancies (green dots)

Random Vacancies



Vacancy Clusters

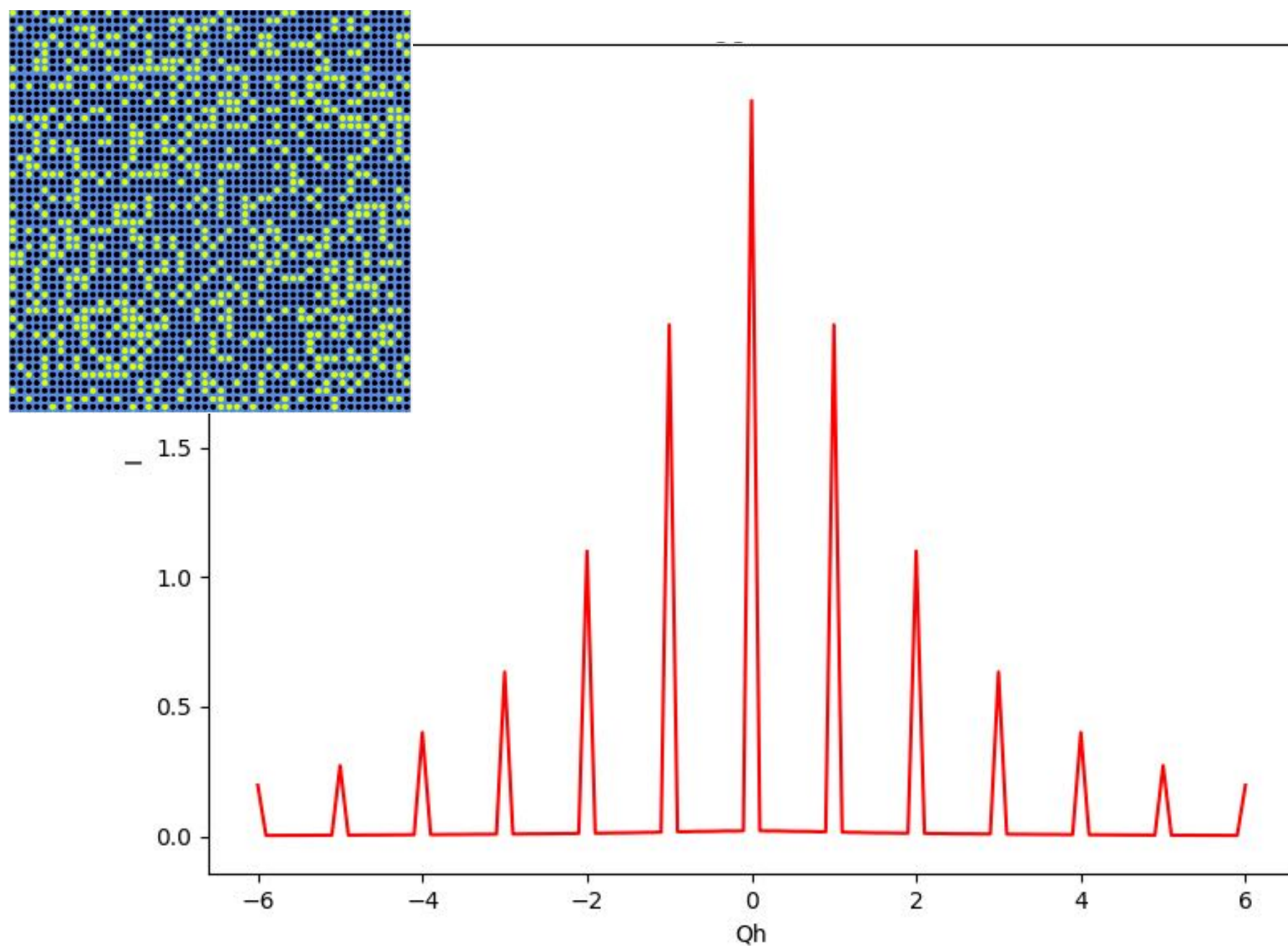


Model due to Thomas Proffen

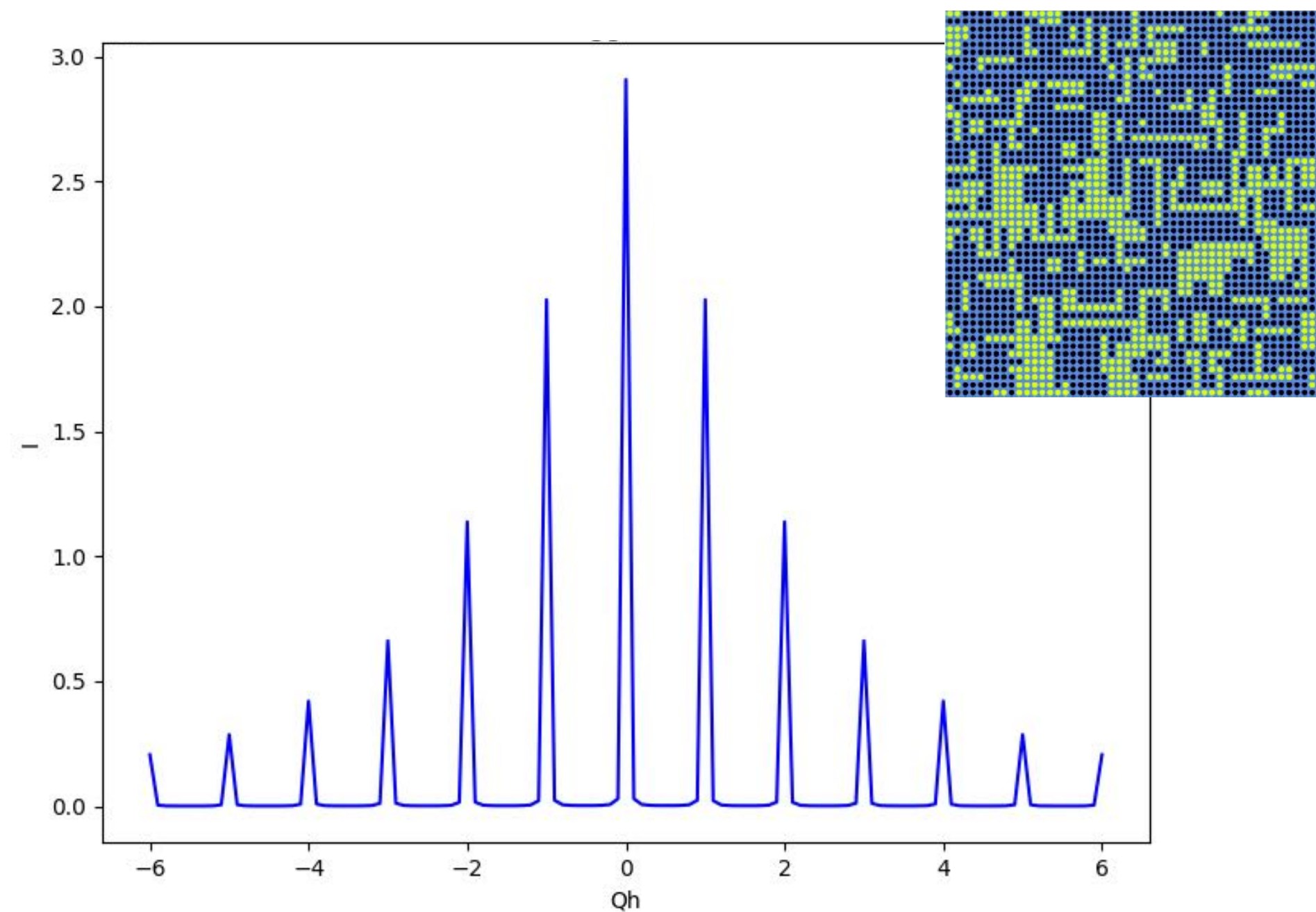
BRAGG SCATTERING

The average occupancy is unchanged \Rightarrow Bragg peaks are identical

Random Vacancies



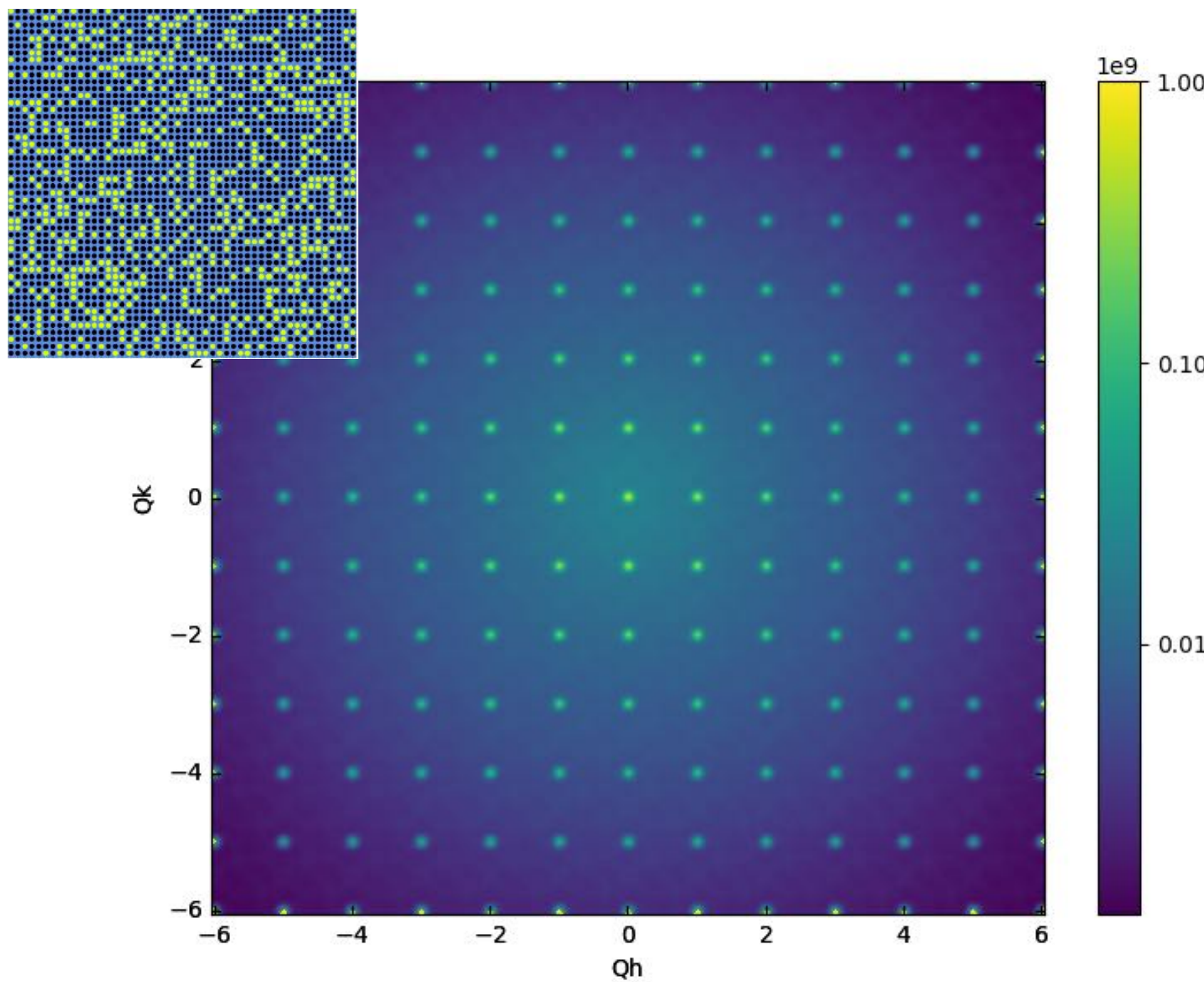
Vacancy Clusters



DIFFUSE SCATTERING

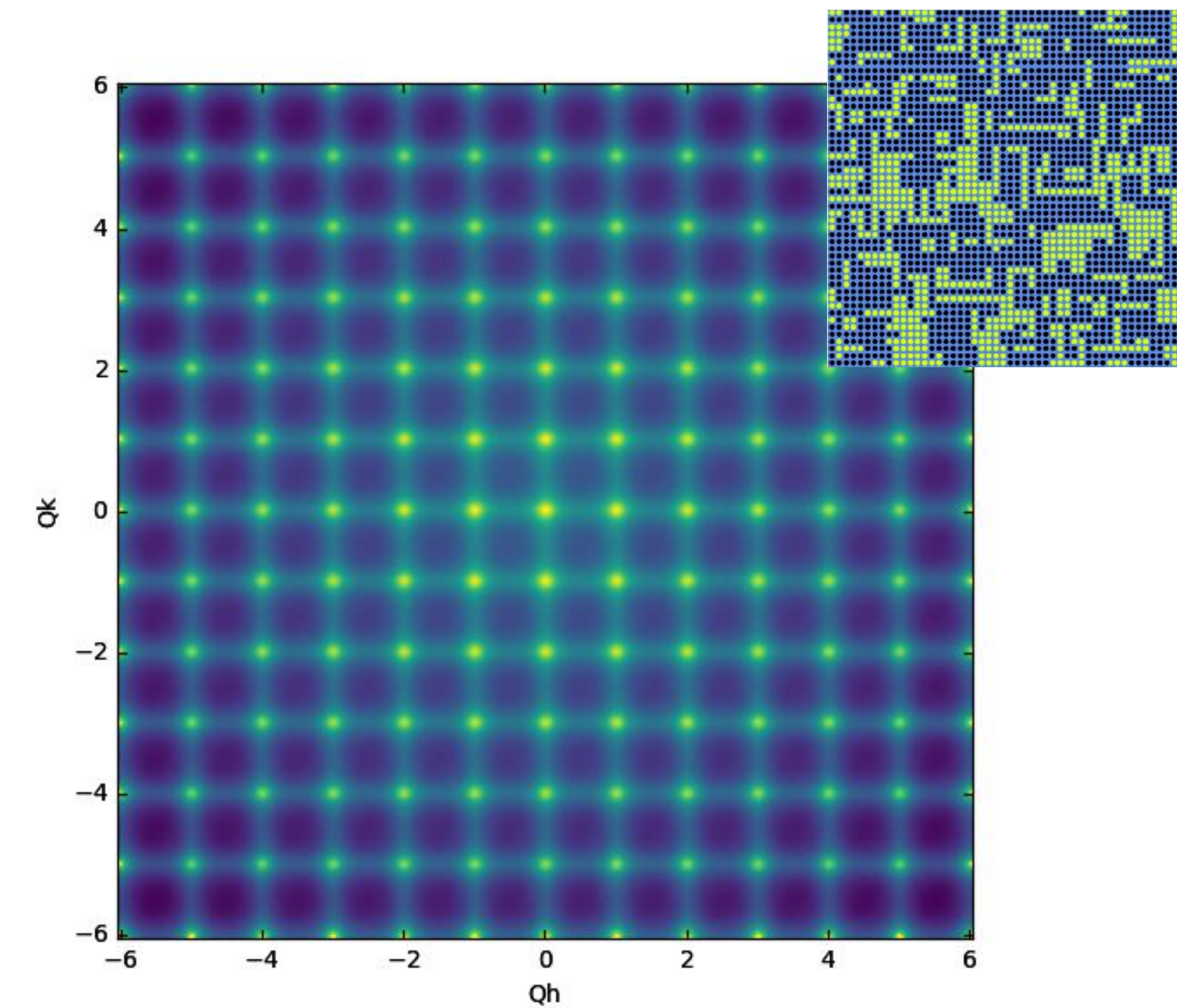
The diffuse scattering is quite different.

Random Vacancies



Laue Monotonic Scattering

Vacancy Clusters



Substitutional Diffuse Scattering

WHAT IS IT GOOD FOR?

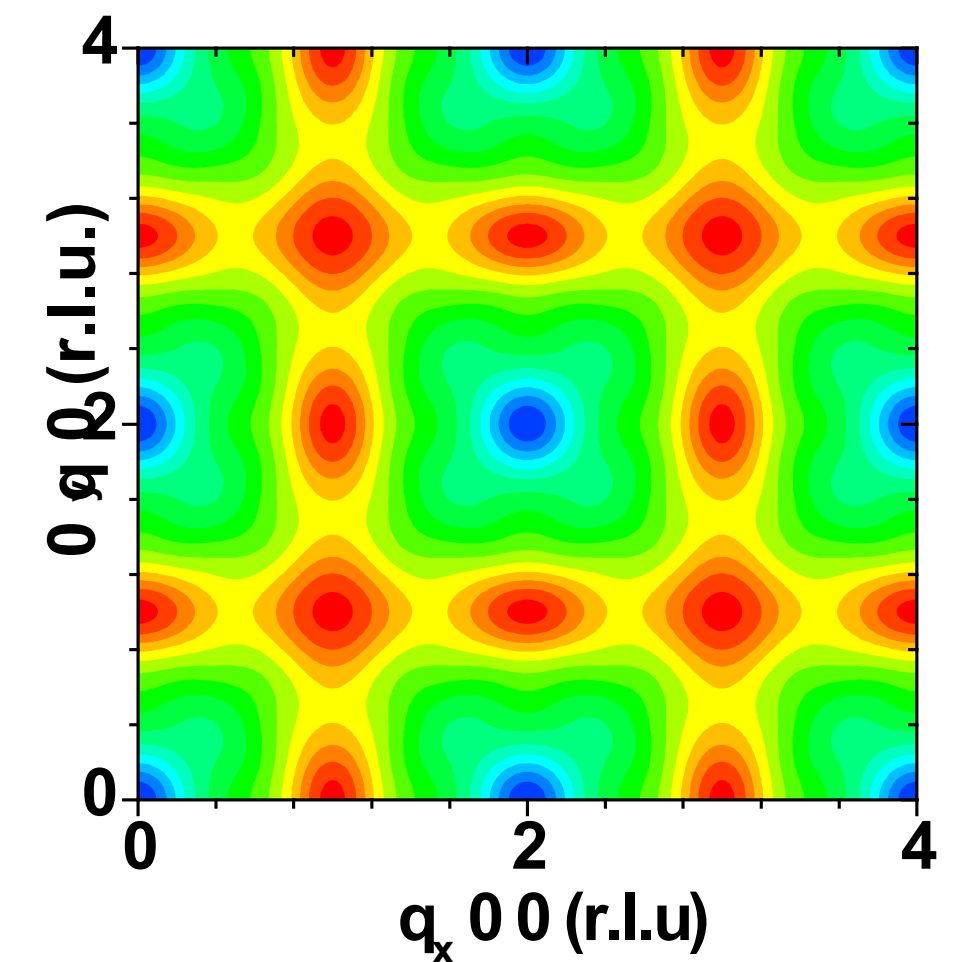
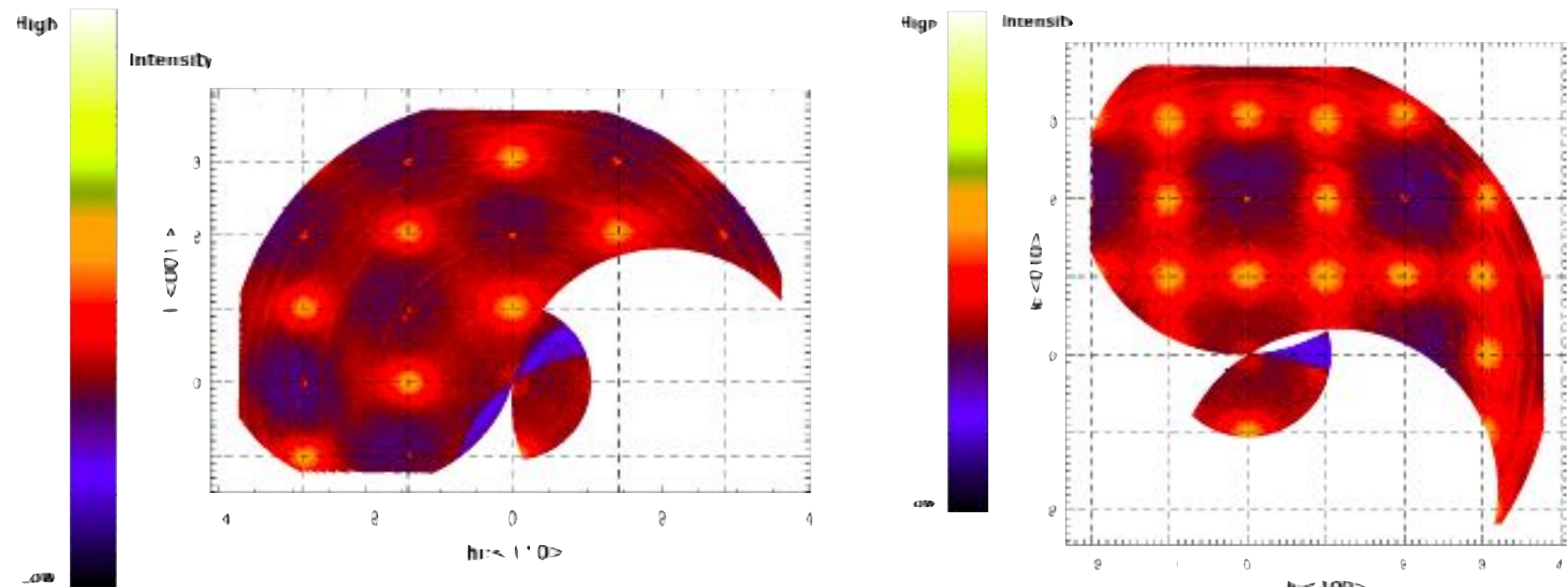


Argonne National Laboratory is a
U.S. Department of Energy laboratory
managed by UChicago Argonne, LLC.



DIFFUSE SCATTERING FROM METALLIC ALLOYS

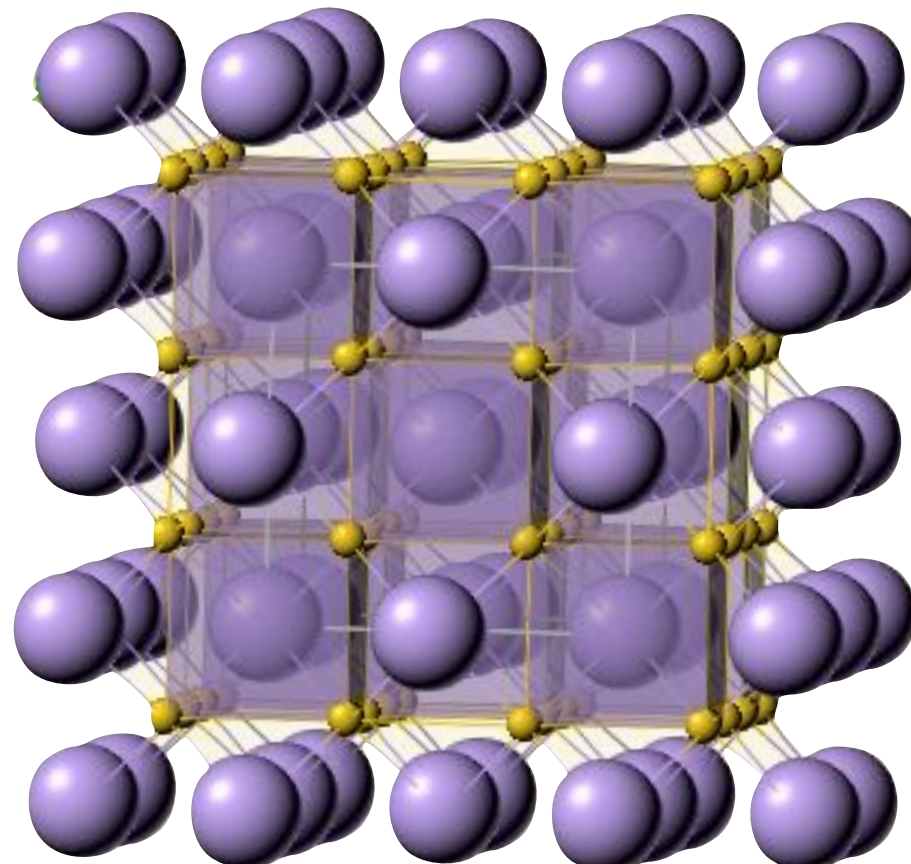
Short-range Order in Null Matrix $^{62}\text{Ni}_{0.52}\text{Pt}_{0.52}$



J. A. Rodriguez, *et al.*, Phys. Rev. B 74, 104115

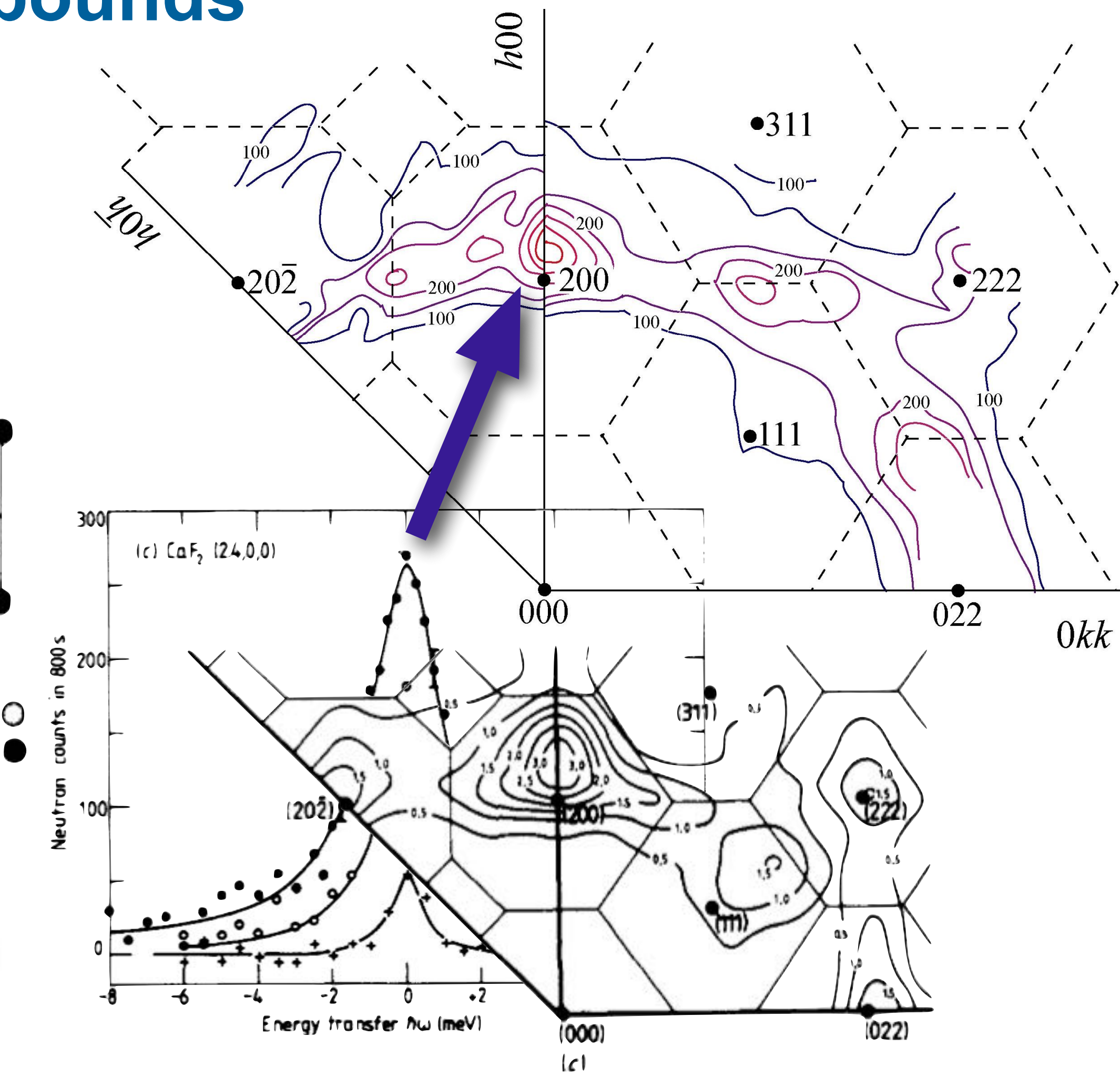
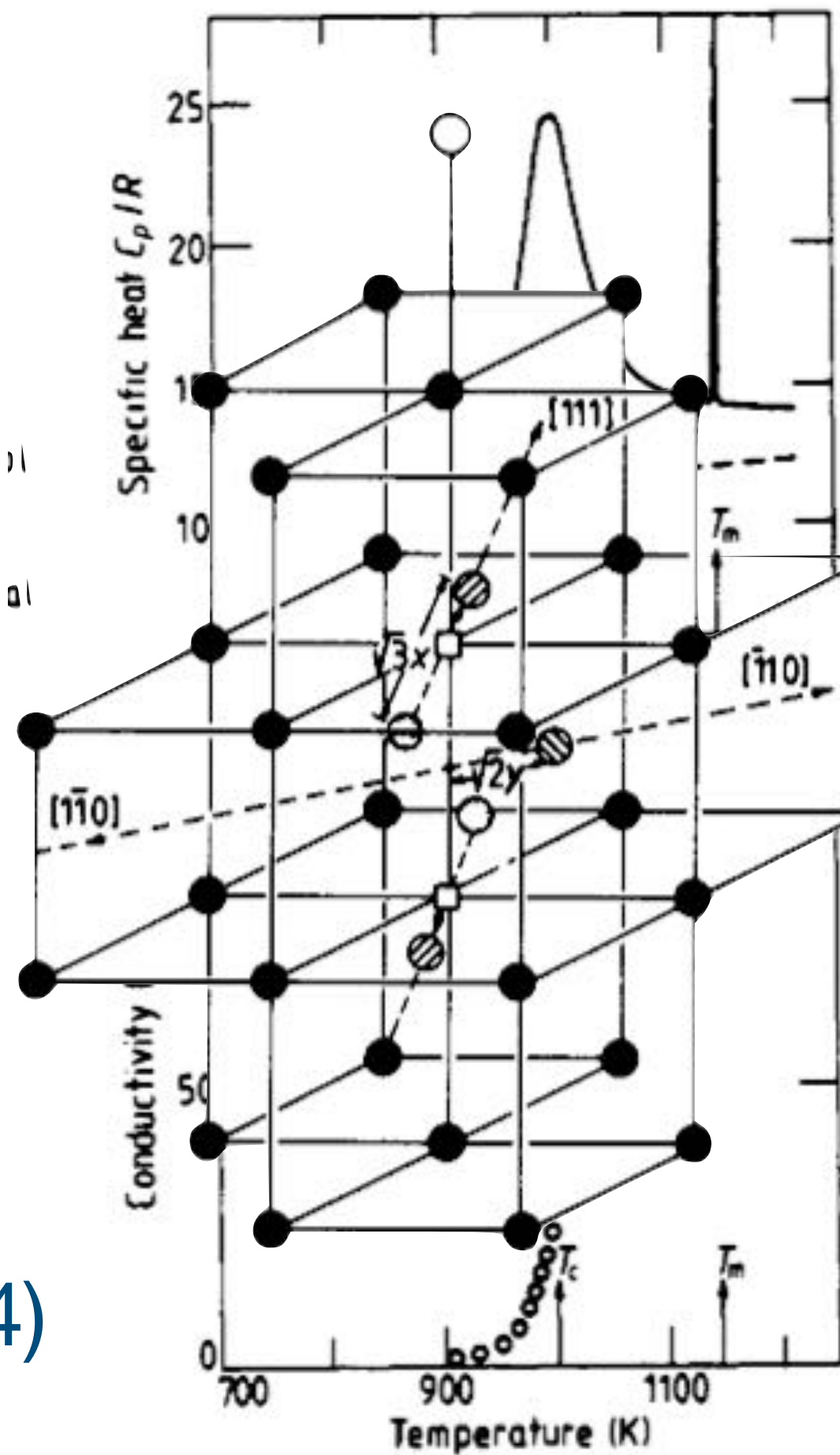
DIFFUSE SCATTERING FROM A FAST-ION CONDUCTOR

Sublattice Melting in Fluorite Compounds



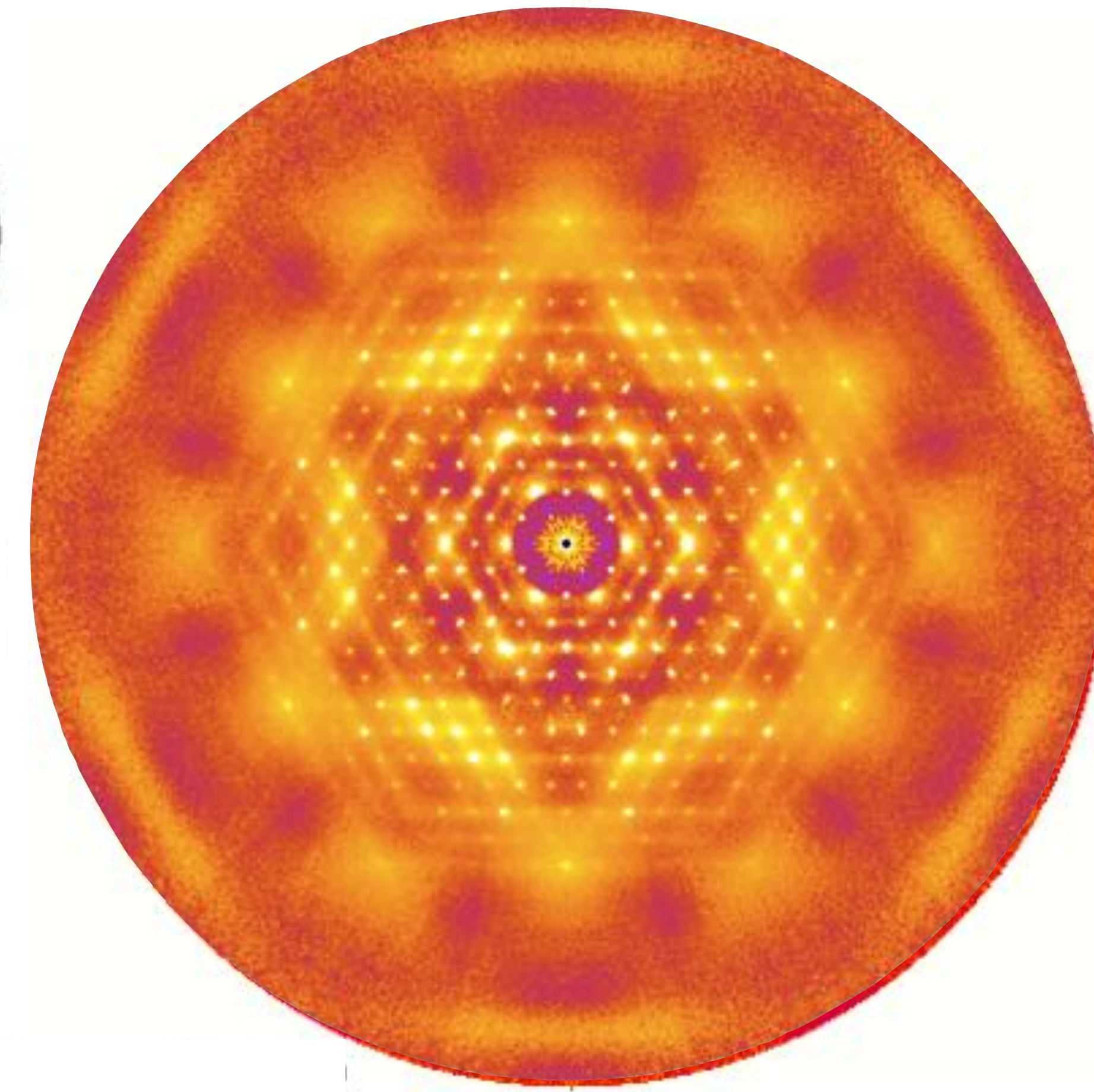
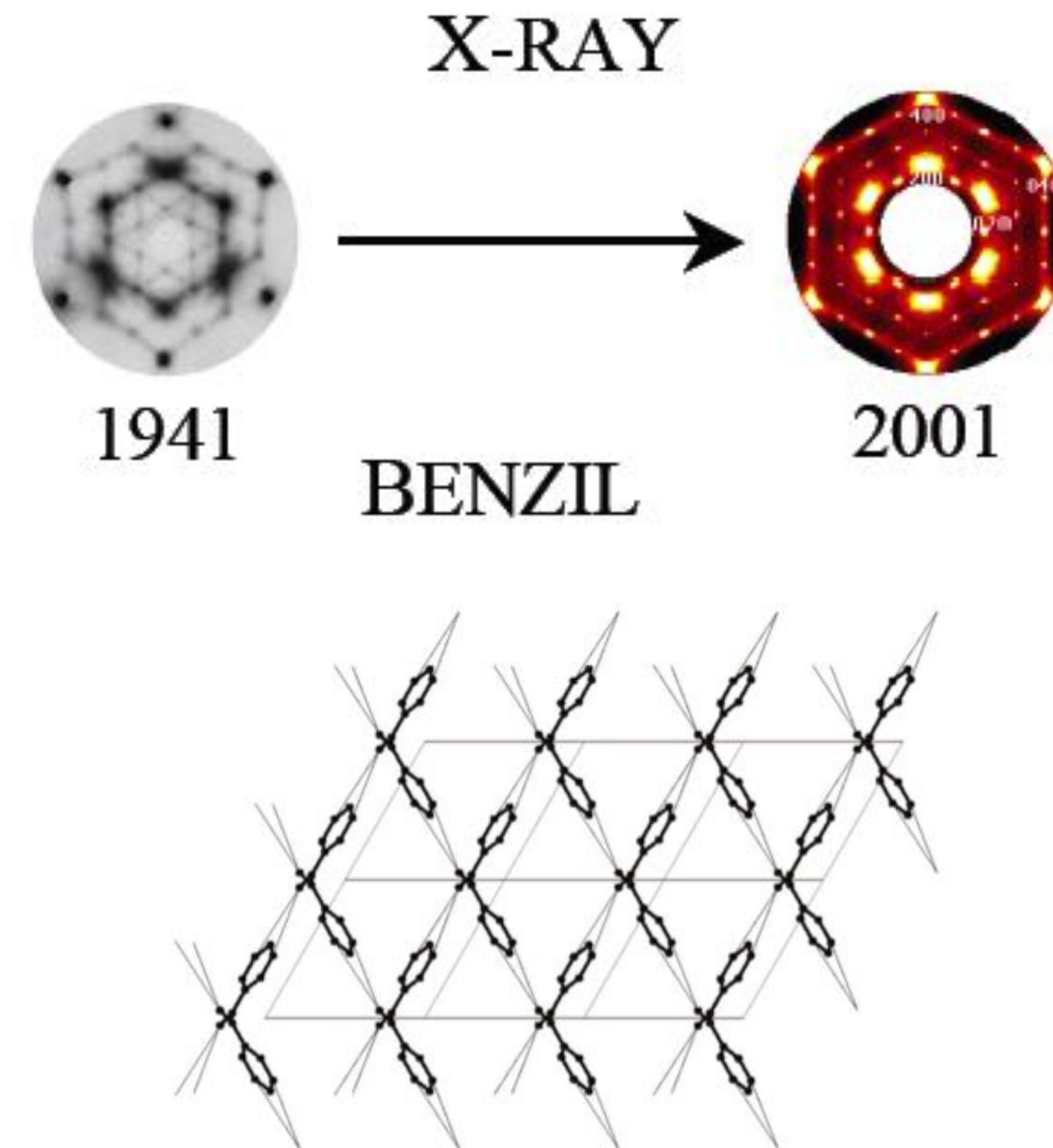
CaF_2

M. T. Hutchings et al
J. Phys. C 17, 3903 (1984)



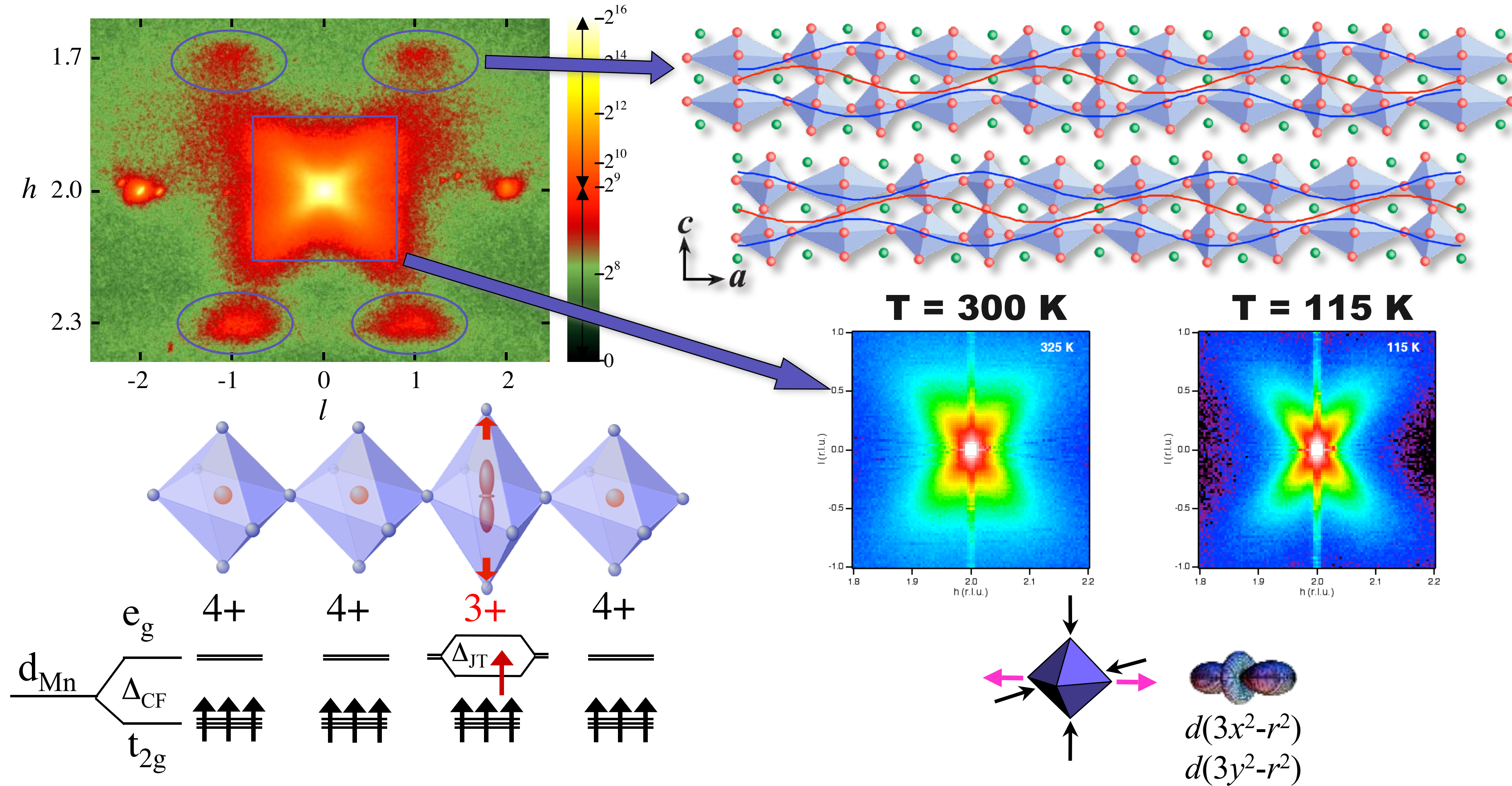
DIFFUSE SCATTERING FROM MOLECULAR SOLIDS

Molecular Flexibility in Benzil



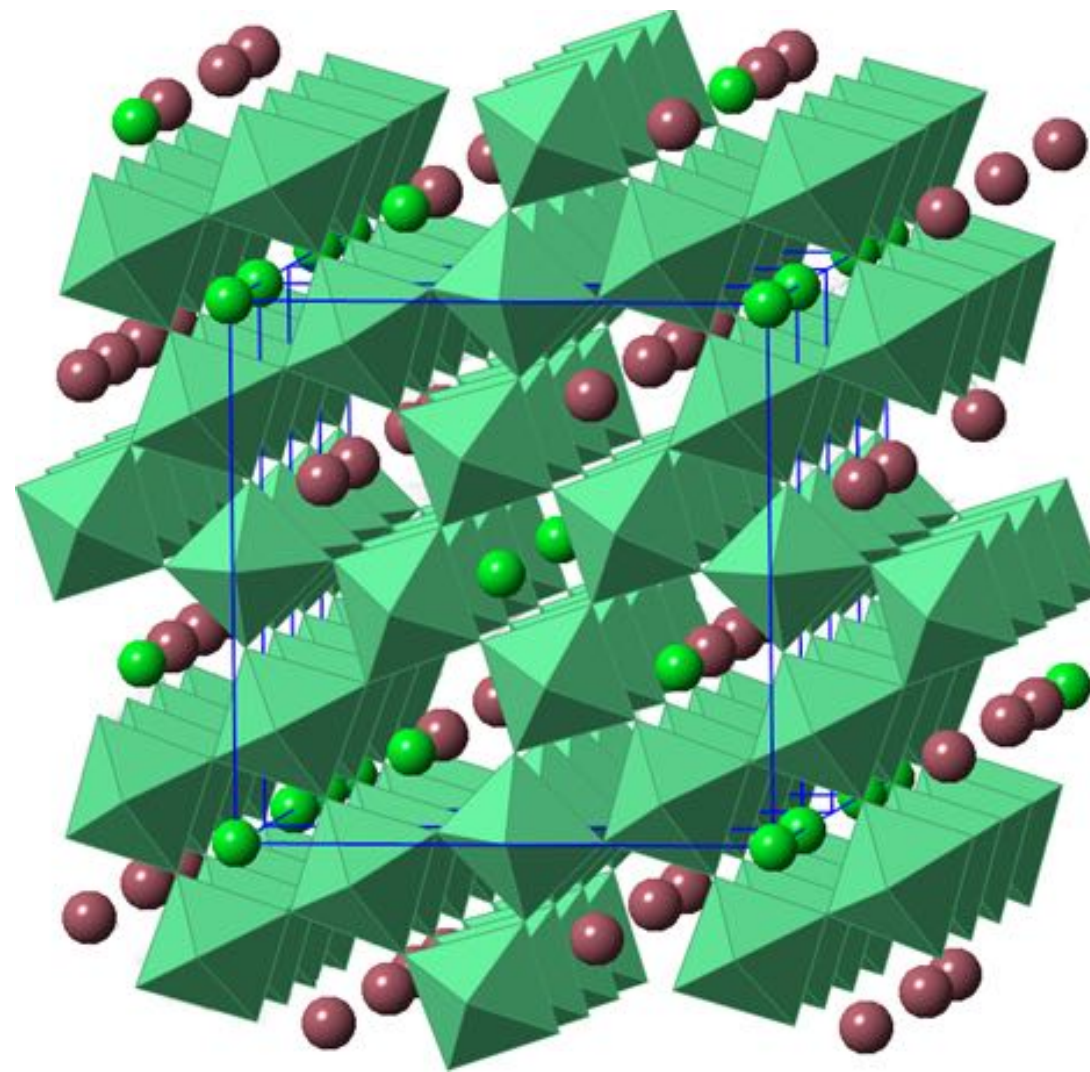
T. R. Welberry *et al* J. Appl. Cryst. 36, 1400 (2003)

DIFFUSE SCATTERING FROM JAHN-TELLER POLARONS

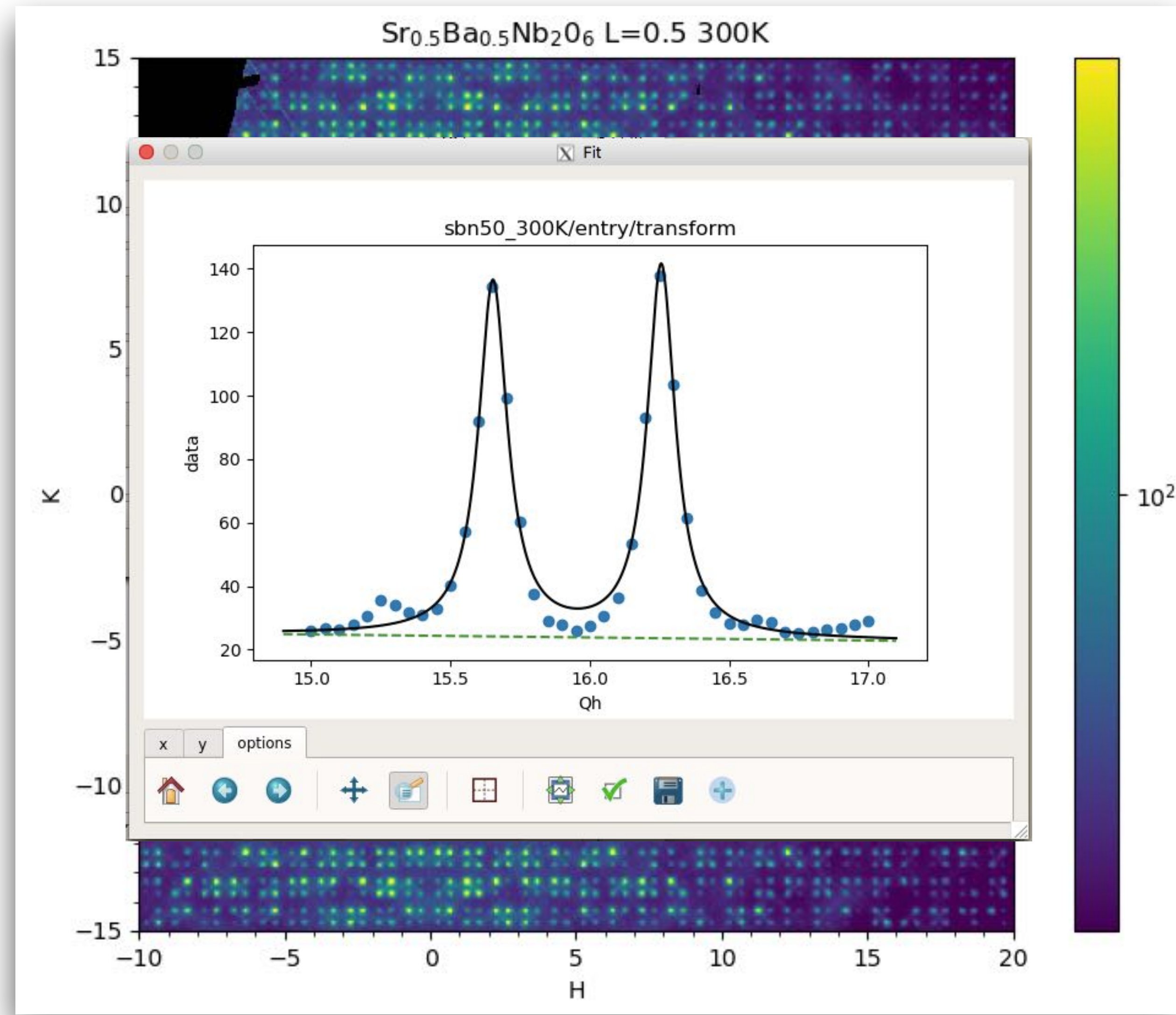


B. J. Campbell, et al., Phys Rev B 65, 014427 (2002).

INCOMMENSURATE MODULATIONS IN $\text{Sr}_{0.5}\text{Ba}_{0.5}\text{NbO}_6$

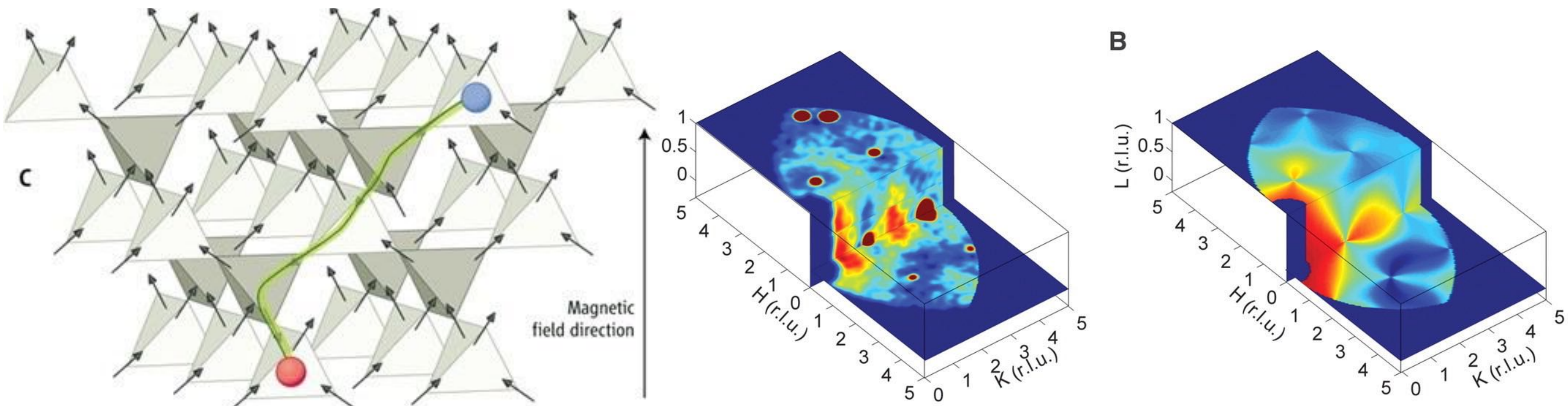


Acknowledgements:
Bixia Wang and Daniel Phelan



MAGNETIC MONOPOLES IN SPIN ICE

Diffuse Magnetic Scattering in $\text{Dy}_2\text{Ti}_2\text{O}_7$



D. J. P. Morris, et al., Science 326, 411 (2009).

HOW DO I MODEL IT?



U.S. DEPARTMENT OF
ENERGY
Argonne National Laboratory is a
U.S. Department of Energy laboratory
managed by UChicago Argonne, LLC.



DIFFUSE SCATTERING THEORY

A Few Equations $I = \sum_i \sum_j b_i b_j \exp(i\mathbf{Q} \cdot \mathbf{r}_{ij})$

- **Laue Monotonic Diffuse Scattering**

$$I = \bar{b}^2 \sum_{ij} \exp(i\mathbf{Q} \cdot \mathbf{r}_{ij}) + N(\bar{b}^2 - \bar{b}^2); \quad \bar{b}^2 = (c_A b_A + c_B b_B)^2; \quad \bar{b}^2 = c_A c_B (b_B - b_A)^2$$

- **Cowley Short-Range Order**

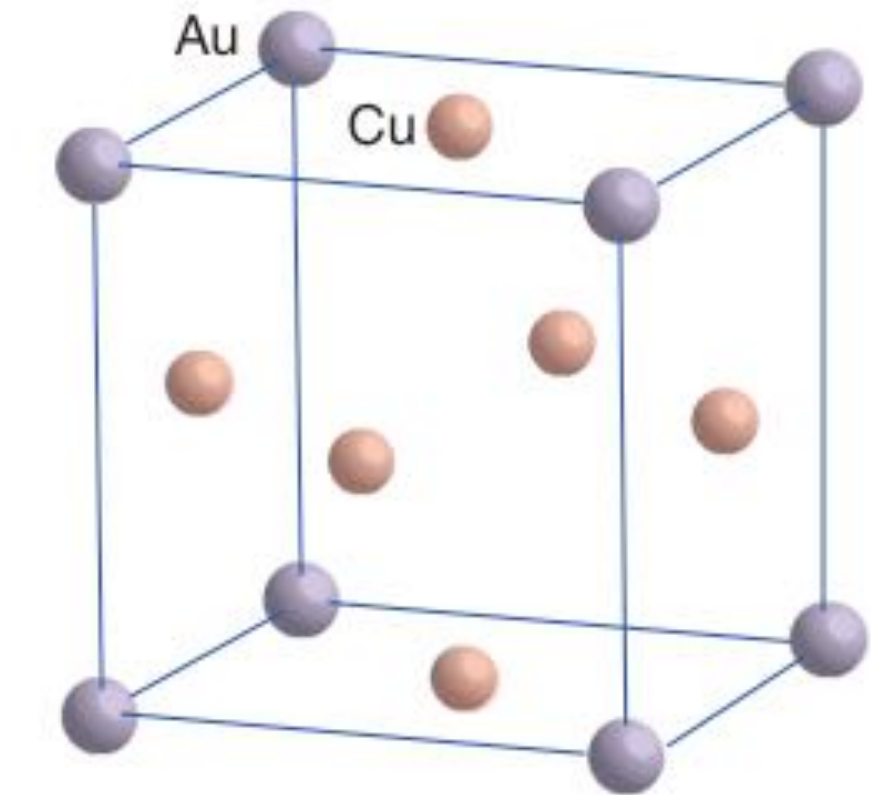
$$I_{diffuse} = N c_A c_B (b_B - b_A)^2 + \sum_{ij} \alpha_{ij} c_B c_A (b_B - b_A)^2 \exp(i\mathbf{Q} \cdot \mathbf{r}_{ij}); \quad \alpha_{ij} = \left(1 - \frac{P_{ij}}{c_j}\right)$$

- **Warren Size Effect**

$$I_{diffuse} = N c_A c_B (b_B - b_A)^2 \left(1 + \sum_{ij} \alpha_{ij} \exp(i\mathbf{Q} \cdot \mathbf{r}_{ij}) + \beta_{ij} \exp(i\mathbf{Q} \cdot \mathbf{r}_{ij}) \right); \quad \beta_{ij} = f(\epsilon_{AA}^{ij}, \epsilon_{BB}^{ij})$$

- **Borie and Sparks Correlations**

$$I = \sum_i \sum_j b_i b_j \exp(i\mathbf{Q} \cdot (\mathbf{R}_i - \mathbf{R}_j)) \left[1 + i\mathbf{Q} \cdot (\mathbf{u}_i - \mathbf{u}_j) - \frac{1}{2} (\mathbf{Q} \cdot (\mathbf{u}_i - \mathbf{u}_j))^2 + \dots \right]$$



J. M. Cowley, J. Appl. Phys. **21**, 24 (1950)

V. M. Nield and D. A. Keen *Diffuse Neutron Scattering From Crystalline Materials* (2001)

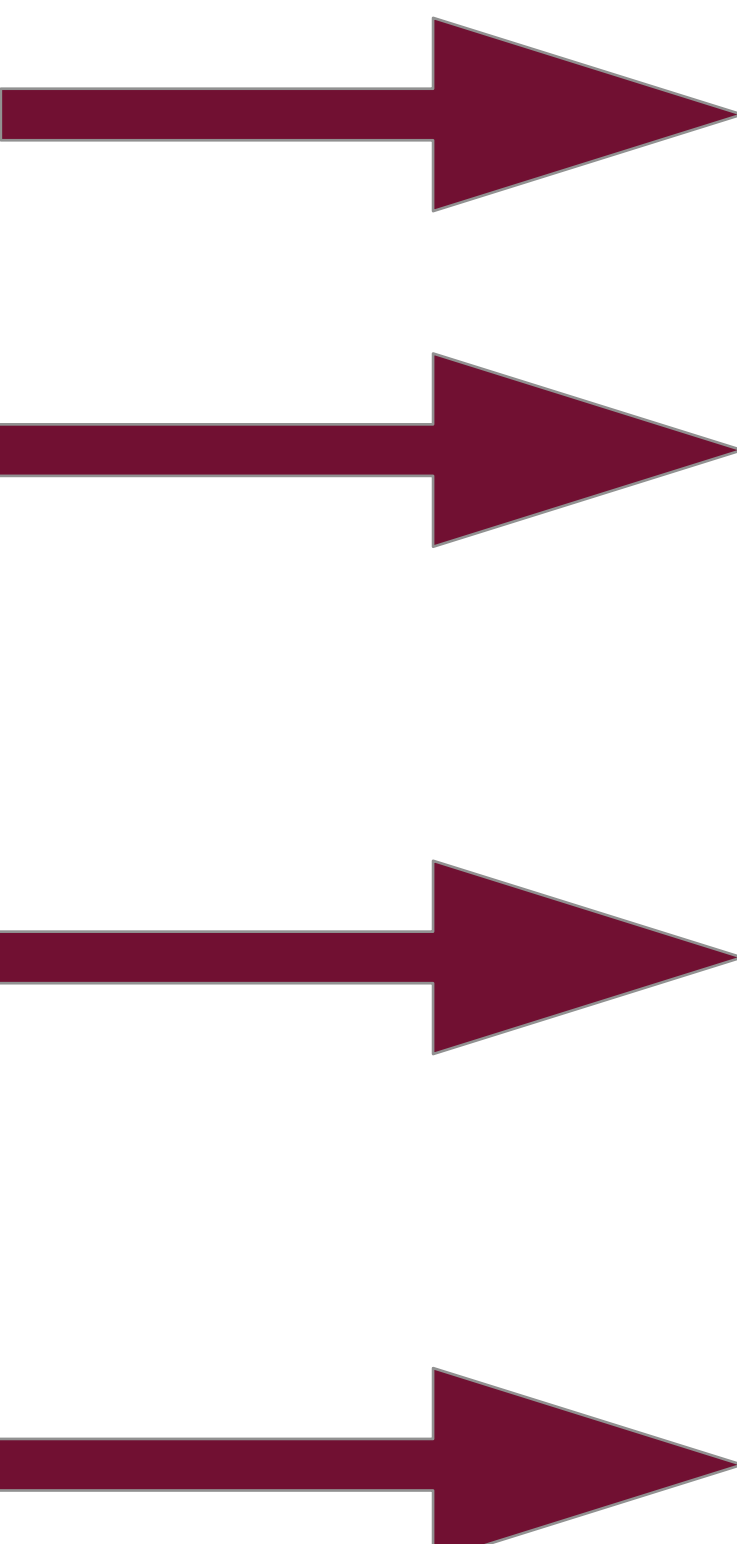
T. R. Welberry *Diffuse X-ray Scattering and Models of Disorder* (2022)

SOME RULES OF THUMB

Acknowledgment: Hans Beat Bürgi

Reciprocal space

- Sharp Bragg reflections
 - no defects
- Sharp diffuse rods
 - no defects
- Sharp diffuse planes
 - no defects
- Diffuse clouds
 - no defects



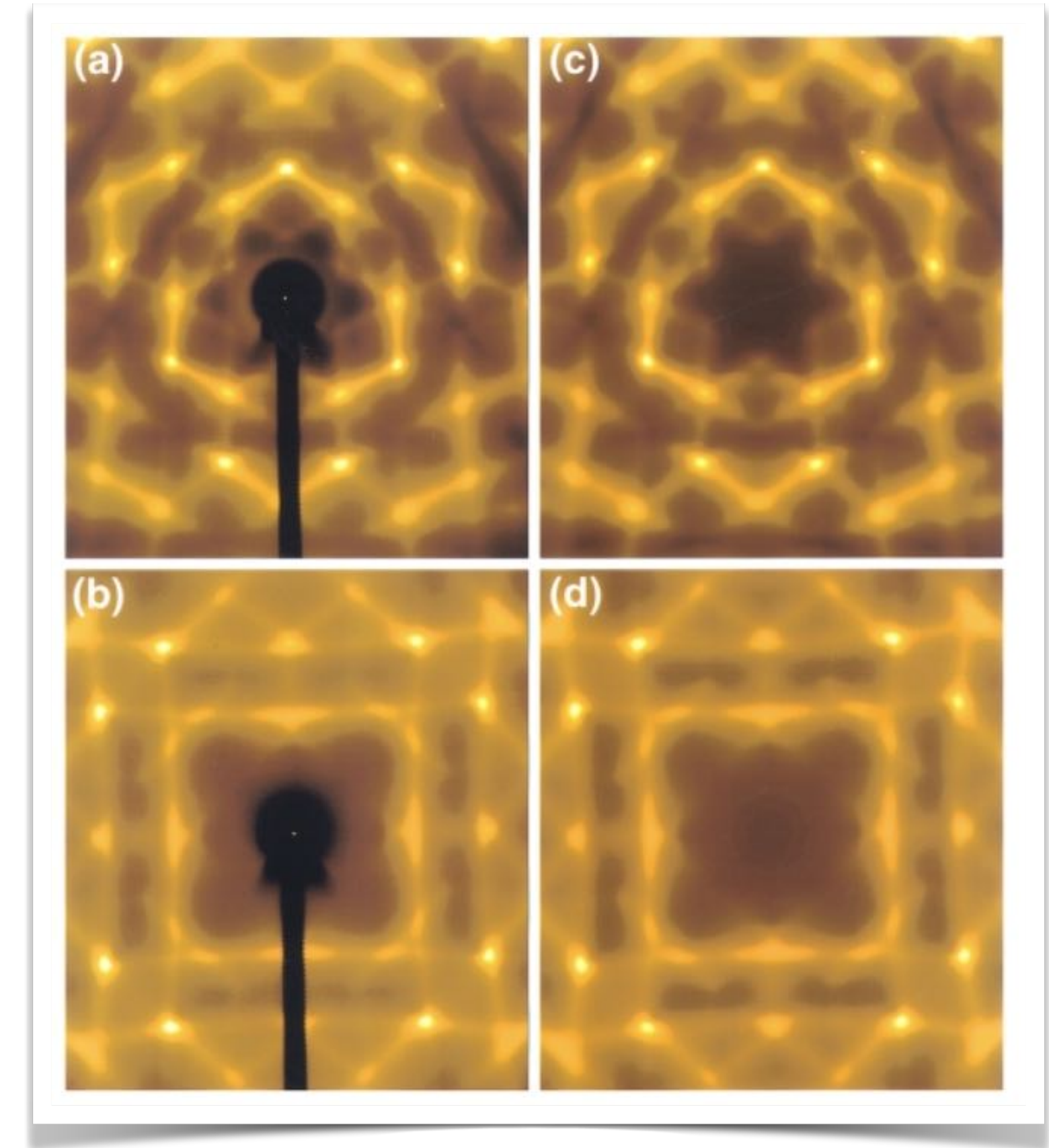
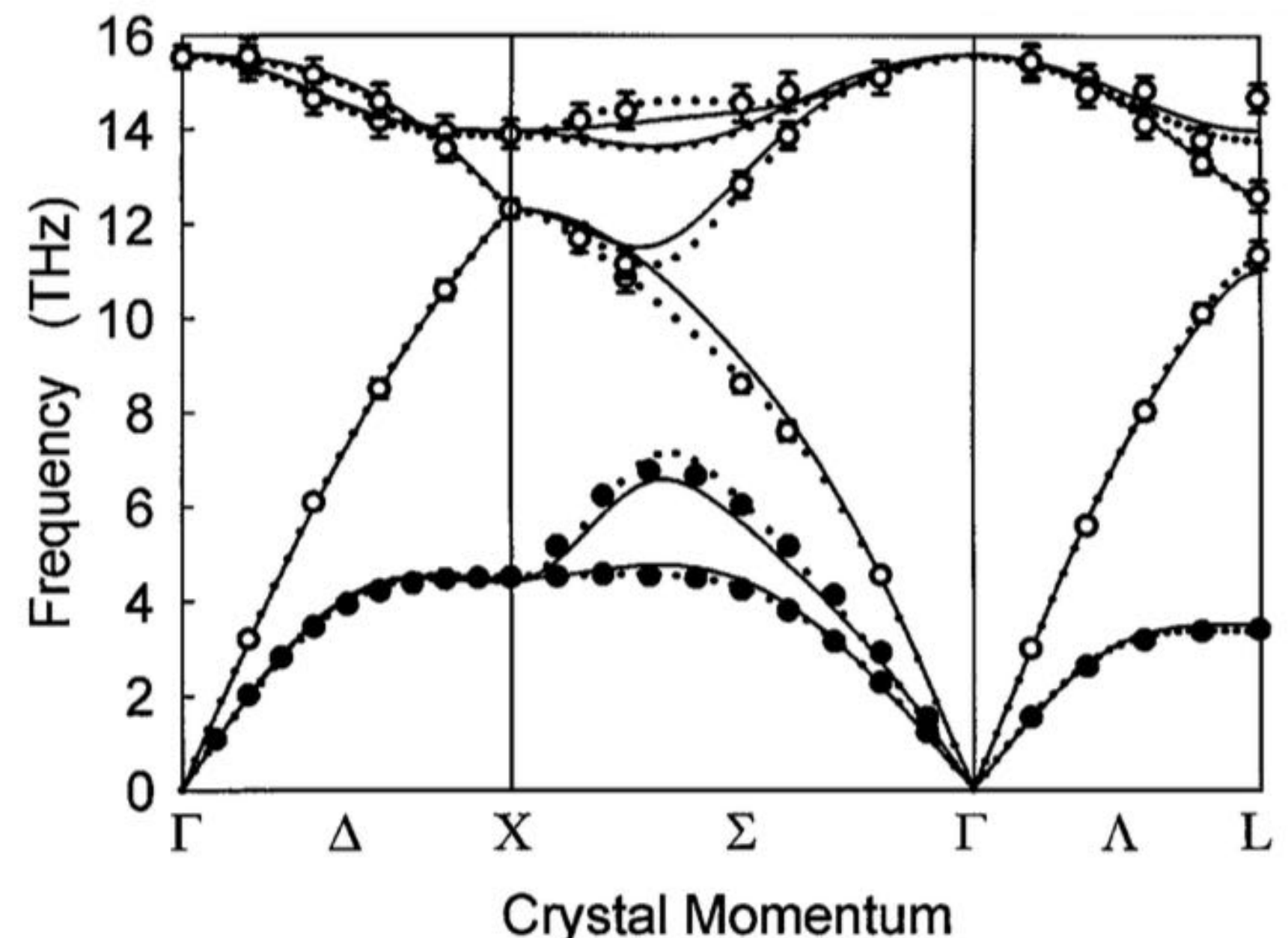
Direct space

- 3D-periodic structure
 - no defects
- 2D-periodic structure
 - perpendicular to the streaks
 - disordered in streak directions
- 1D-periodic structure
 - perpendicular to the planes
 - disordered within the plane
- 0D-periodic structure
 - no fully ordered direction

THERMAL DIFFUSE SCATTERING

M. Holt, et al, Phys Rev Lett 83, 3317 (1999).

- Lattice vibrations produce deviations from the average structure even in perfect crystals
- X-ray scattering intensity is given by the integral over all the phonon branches at each Q



$$I_0 \propto f^2 e^{-2M} \sum_{j=1}^6 \frac{|\mathbf{q} \cdot \hat{\mathbf{e}}_j|^2}{\omega_j} \coth\left(\frac{\hbar\omega_j}{2k_B T}\right).$$

HOW DO I MEASURE IT?



U.S. DEPARTMENT OF
ENERGY
Argonne National Laboratory is a
U.S. Department of Energy laboratory
managed by UChicago Argonne, LLC.

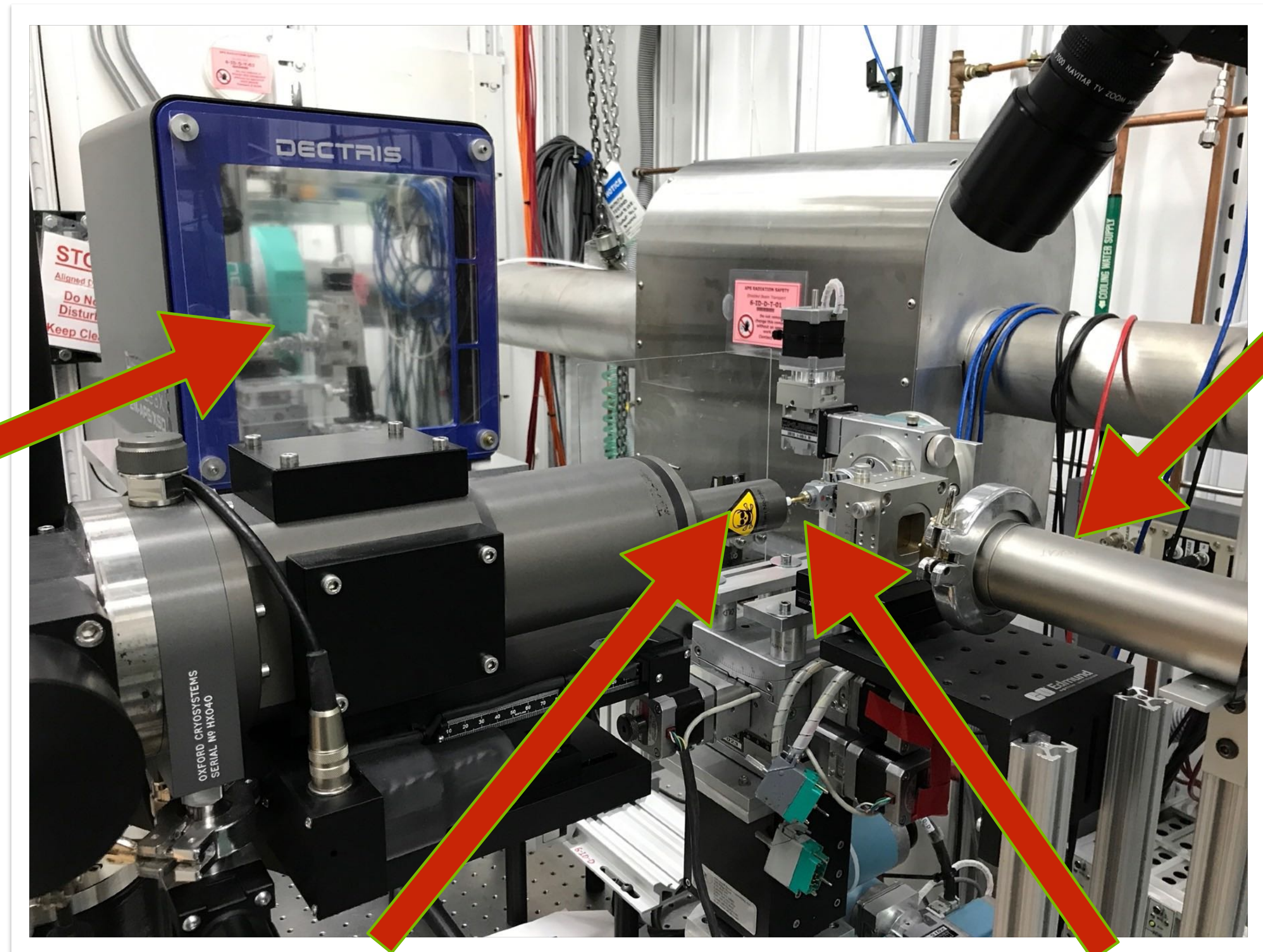


MEASURING X-RAY DIFFUSE SCATTERING

Continuous Rotation Method

Sector 6 - APS

Detector

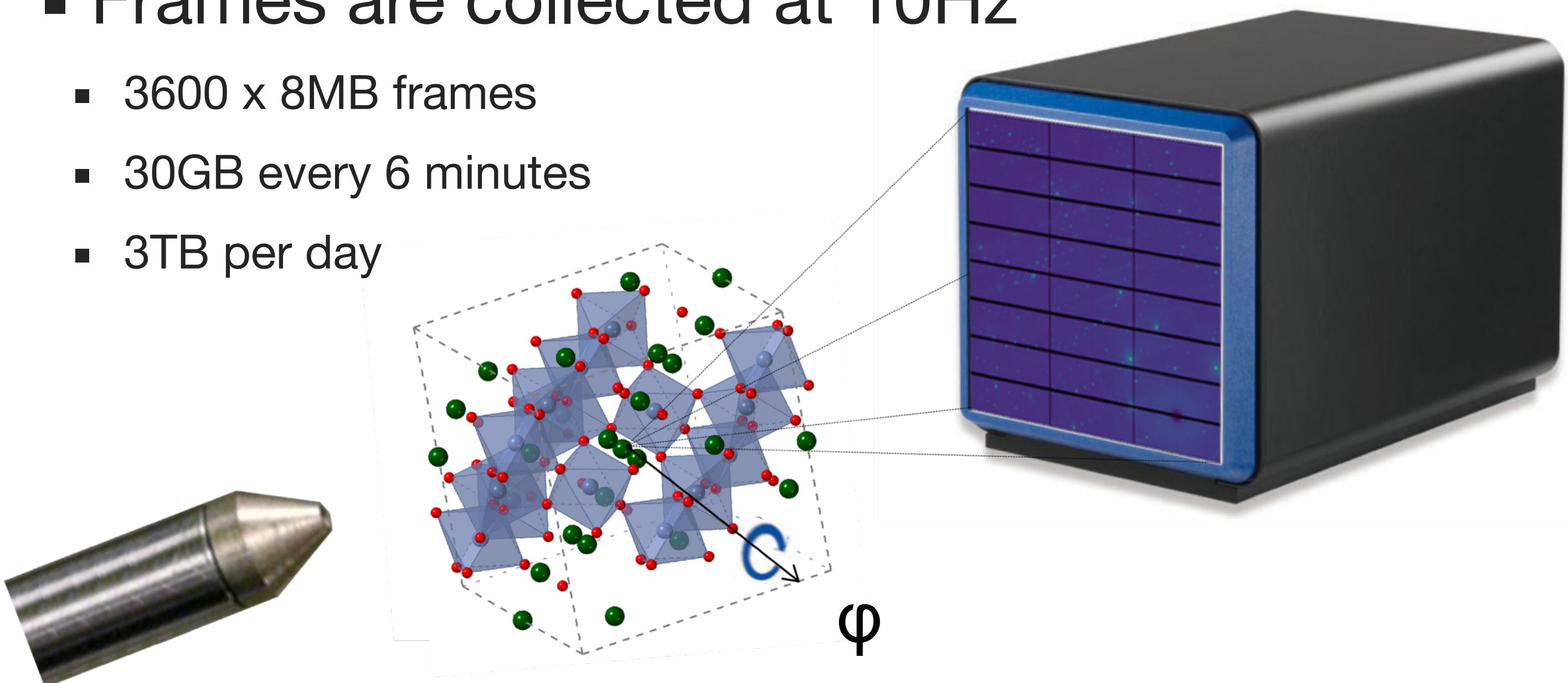


Sample

X-RAY SCATTERING GEOMETRY

Continuous Rotation Method

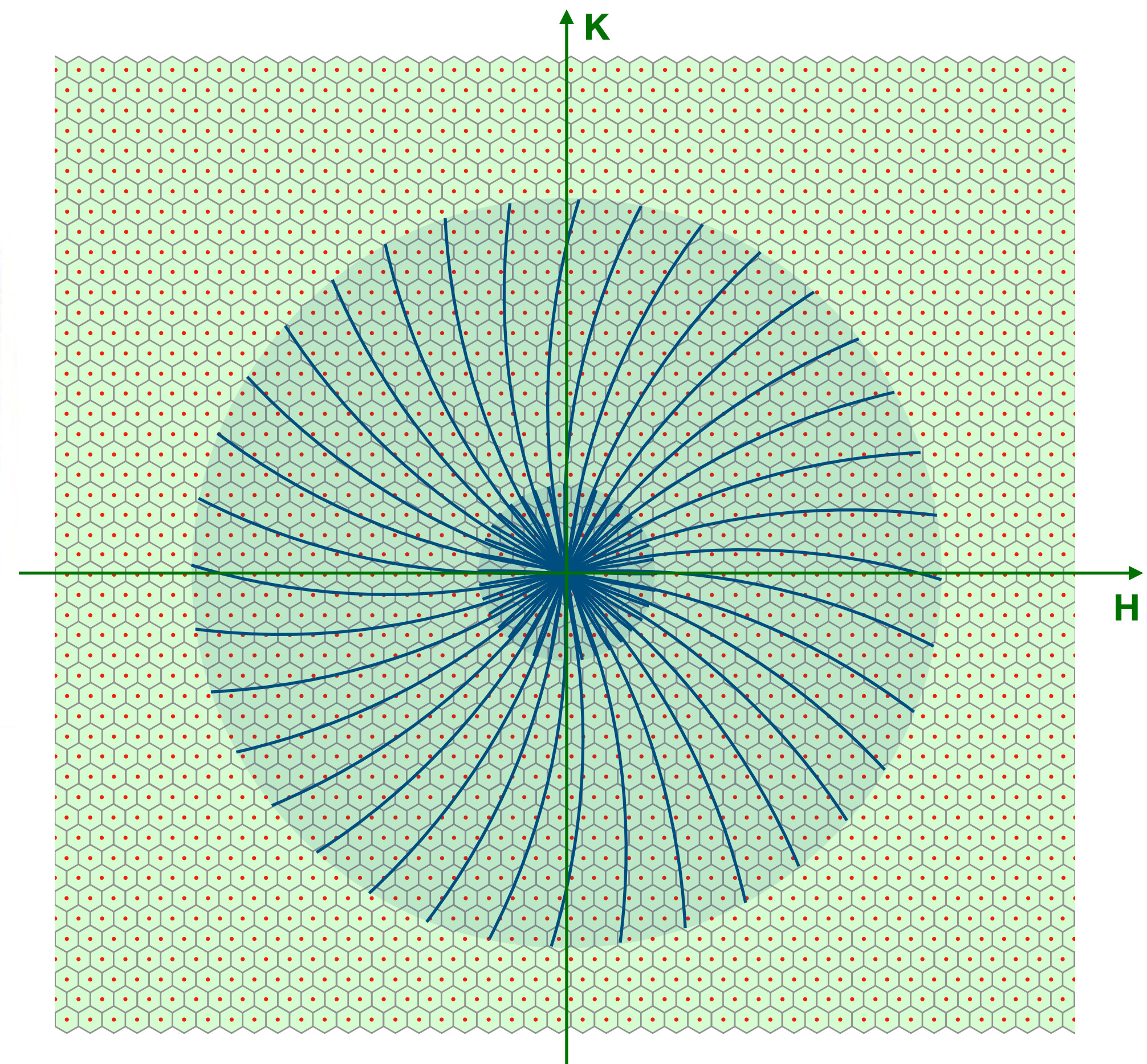
- The sample is continuously rotated at 1°s^{-1}
- Frames are collected at 10Hz
 - $3600 \times 8\text{MB}$ frames
 - 30GB every 6 minutes
 - 3TB per day



Incident
Beam

Sample

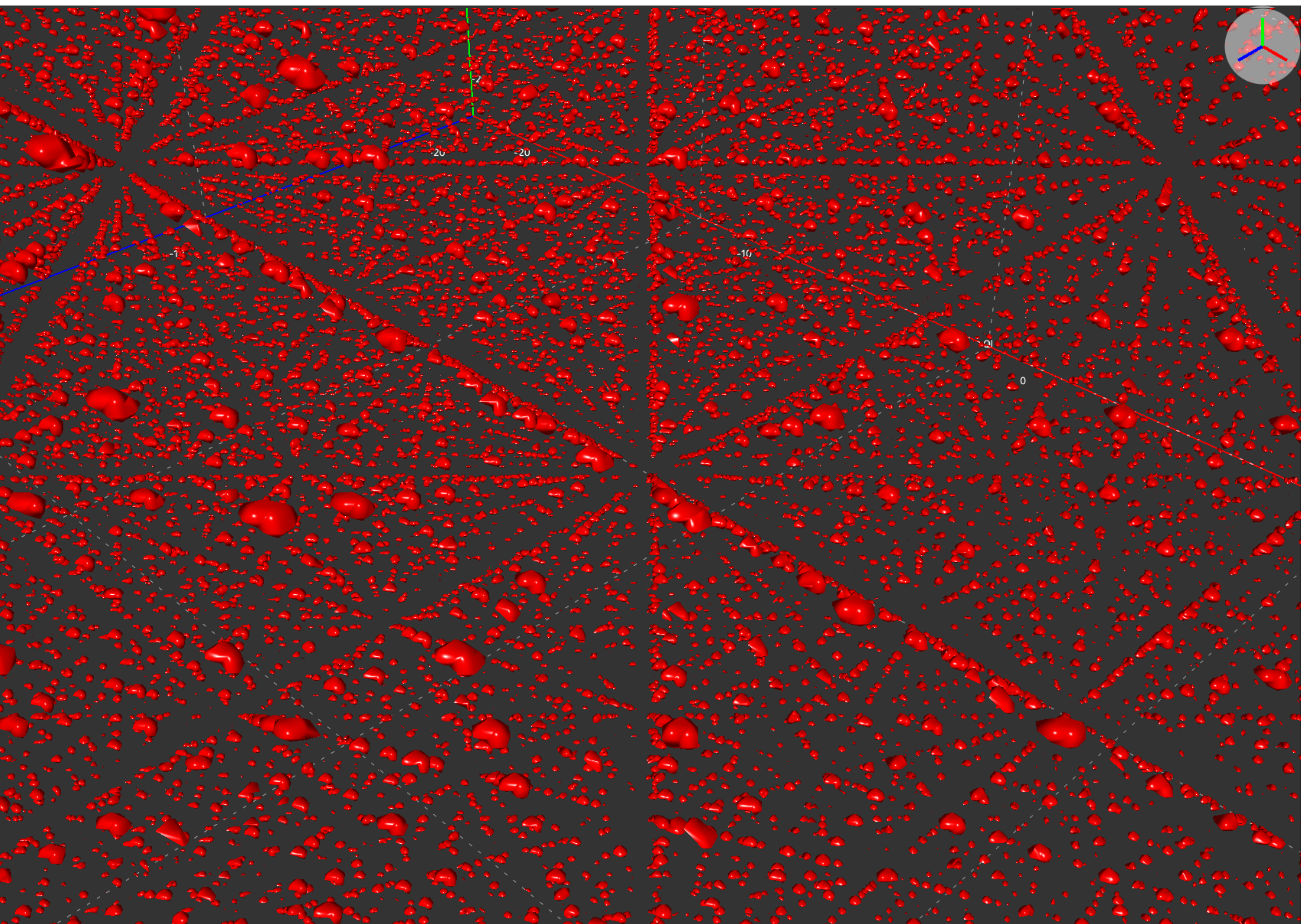
Pilatus 2M CdTe
Detector



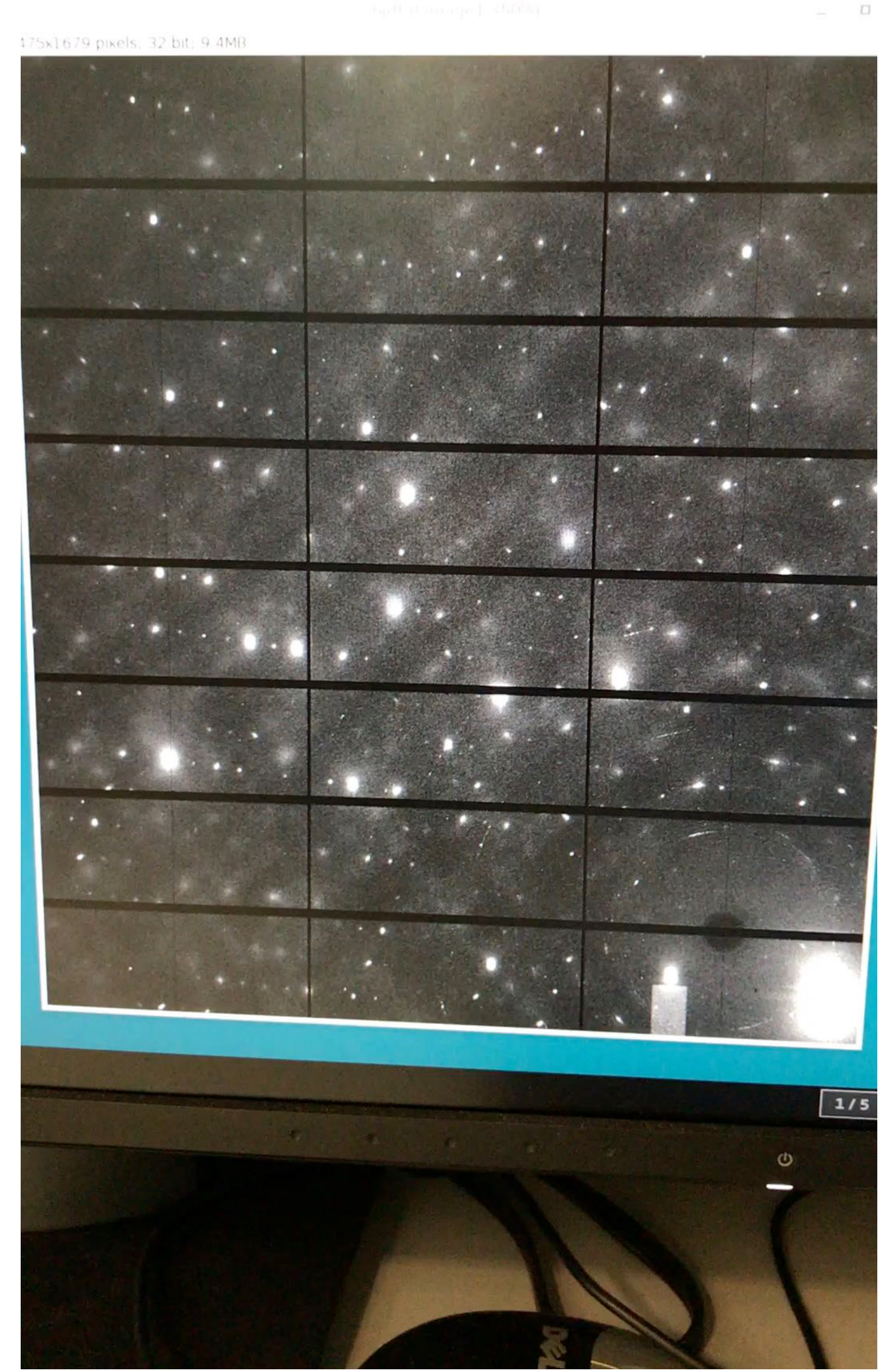
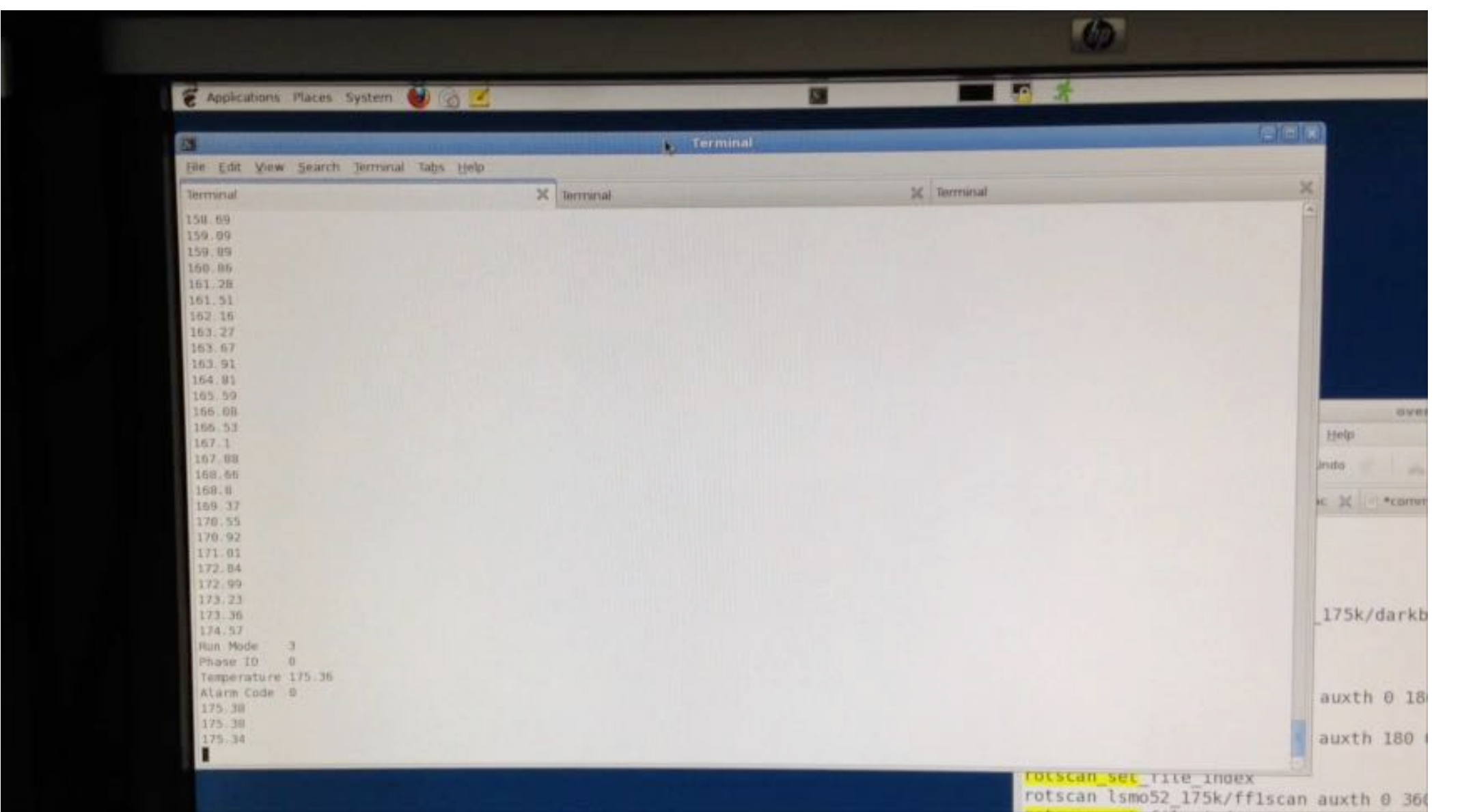
Reciprocal Space

Q-RANGE IN ROTATION METHOD ON SECTOR 6

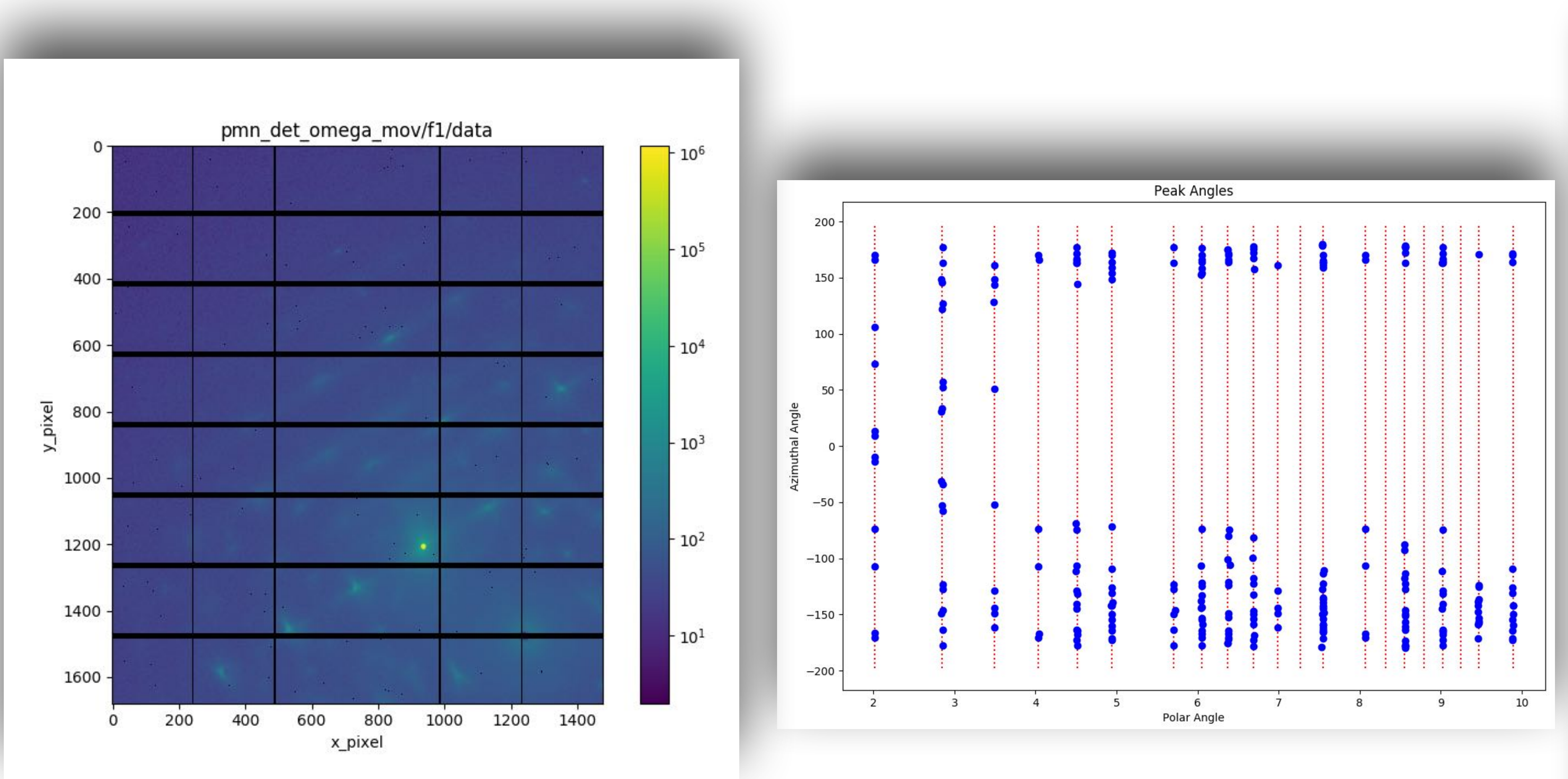
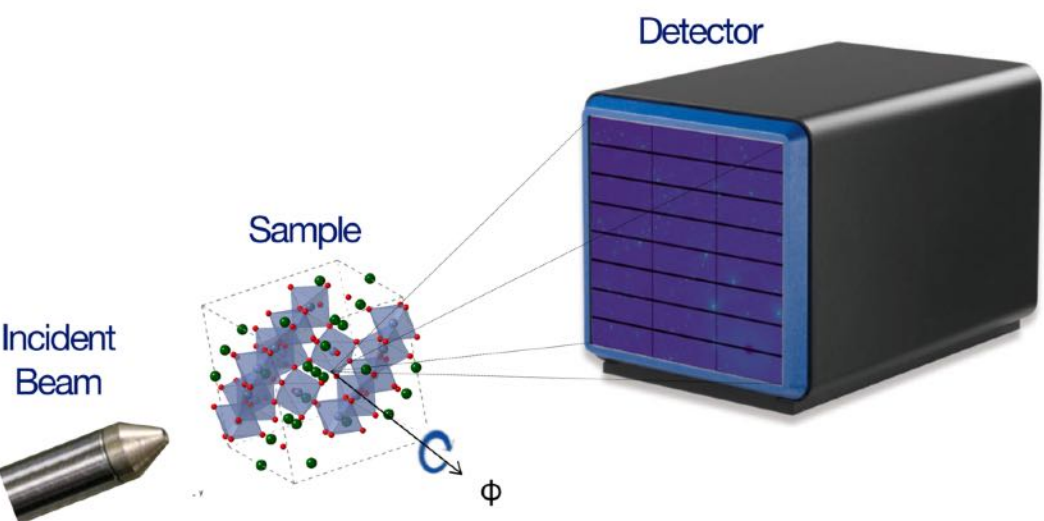
- With the following parameters,
we cover $-15\text{\AA}^{-1} < \mathbf{Q} < 15\text{\AA}^{-1}$
 - $E_i \sim 87 \text{ keV}$
 - $\lambda \sim 0.14 \text{ \AA}$
 - Detector distance $\sim 650 \text{ mm}$
 - Pilatus 2M CdTe: 1679×1475 pixels
 - Pixel size $\sim 170 \mu\text{m}$
- This Q-range includes thousands
of Brillouin zones.
 - e.g., for $a \sim 10 \text{ \AA}$, $\sim 60,000$ Bragg peaks



MANAGING THE FLOOD

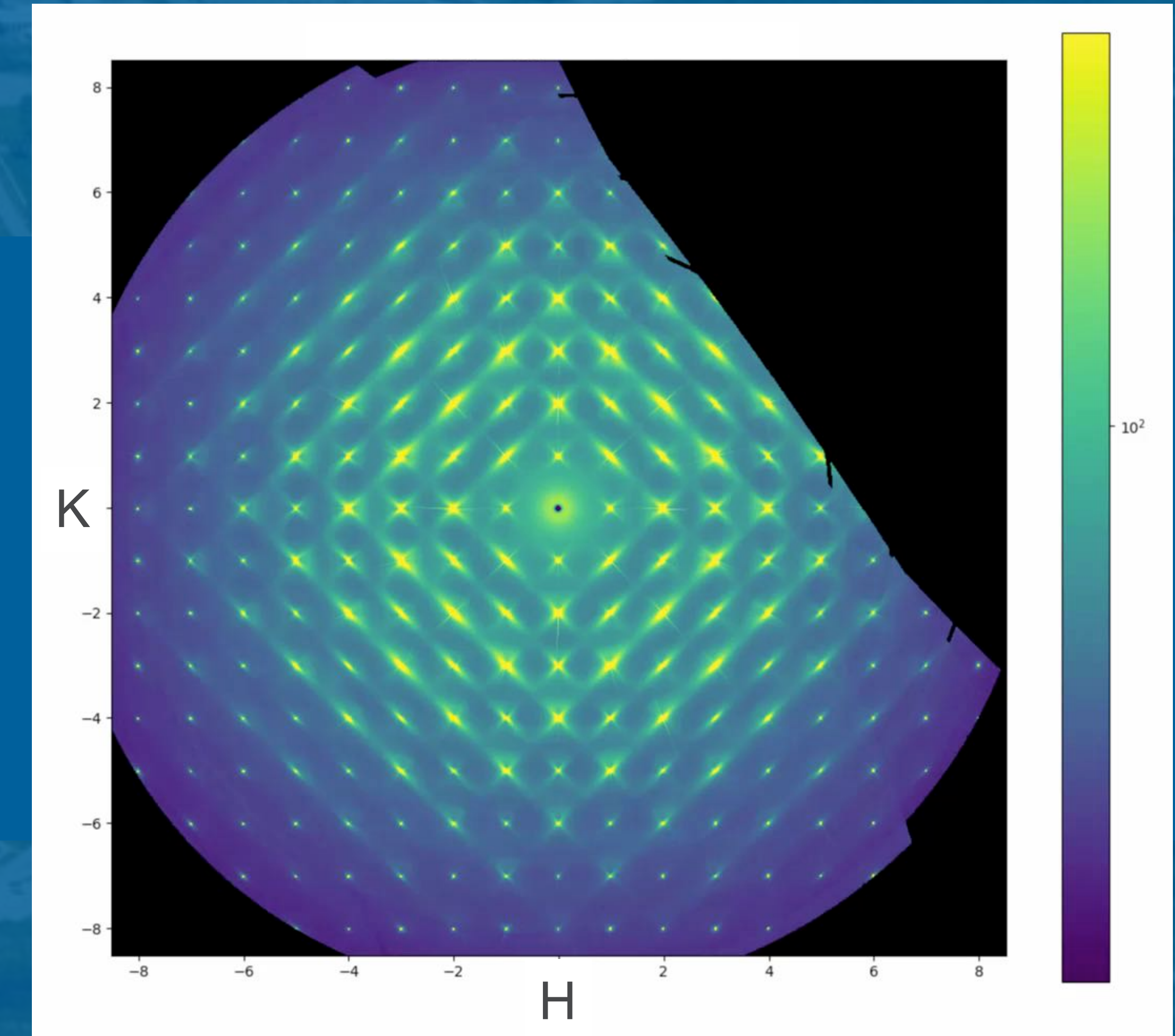


EXPERIMENT WORKFLOW



DIFFUSE SCATTERING IN 3D THE RELAXOR $\text{PbMg}_{1/3}\text{Nb}_{2/3}\text{O}_3$

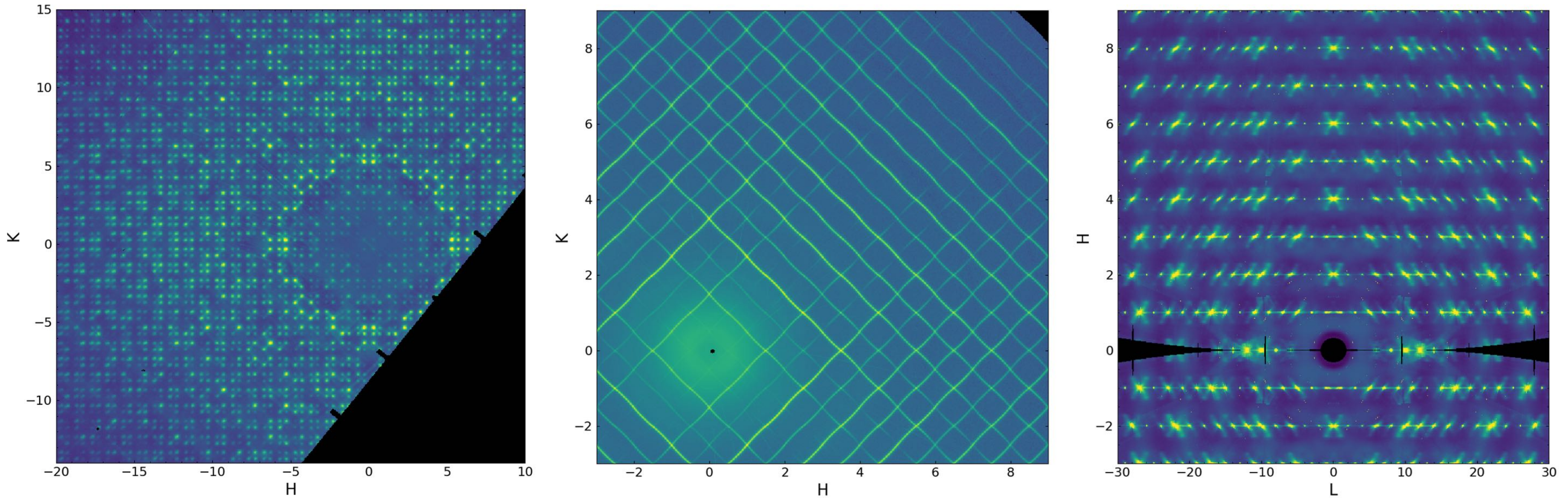
M. J. Krogstad, *et al*, Nature Materials 48, 1 (2018).



U.S. DEPARTMENT OF
ENERGY
Argonne National Laboratory is a
U.S. Department of Energy laboratory
managed by UChicago Argonne, LLC.



DIFFUSE GALLERY



CASE STUDY 1: MULLITE



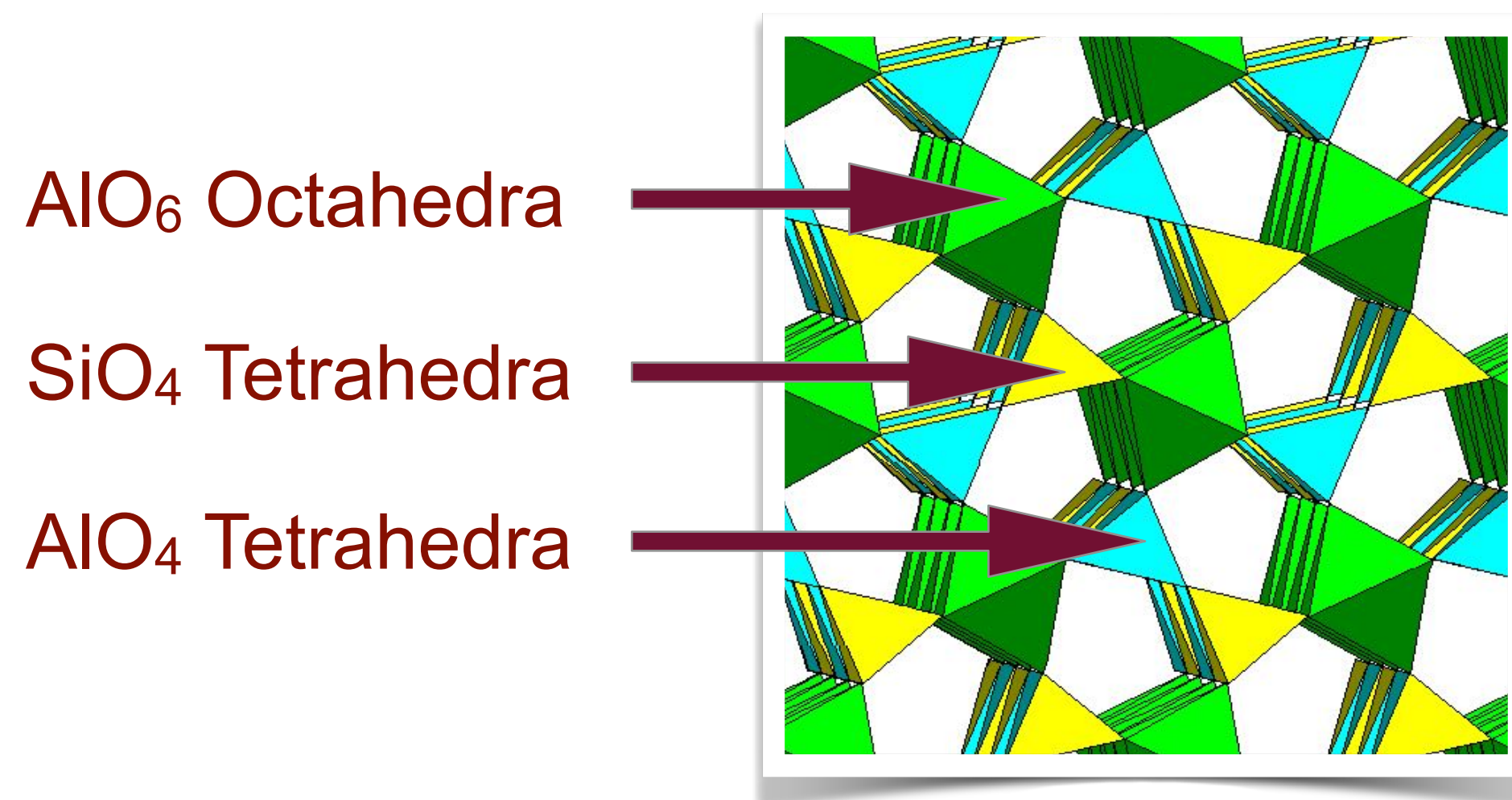
Argonne National Laboratory is a
U.S. Department of Energy laboratory
managed by UChicago Argonne, LLC.



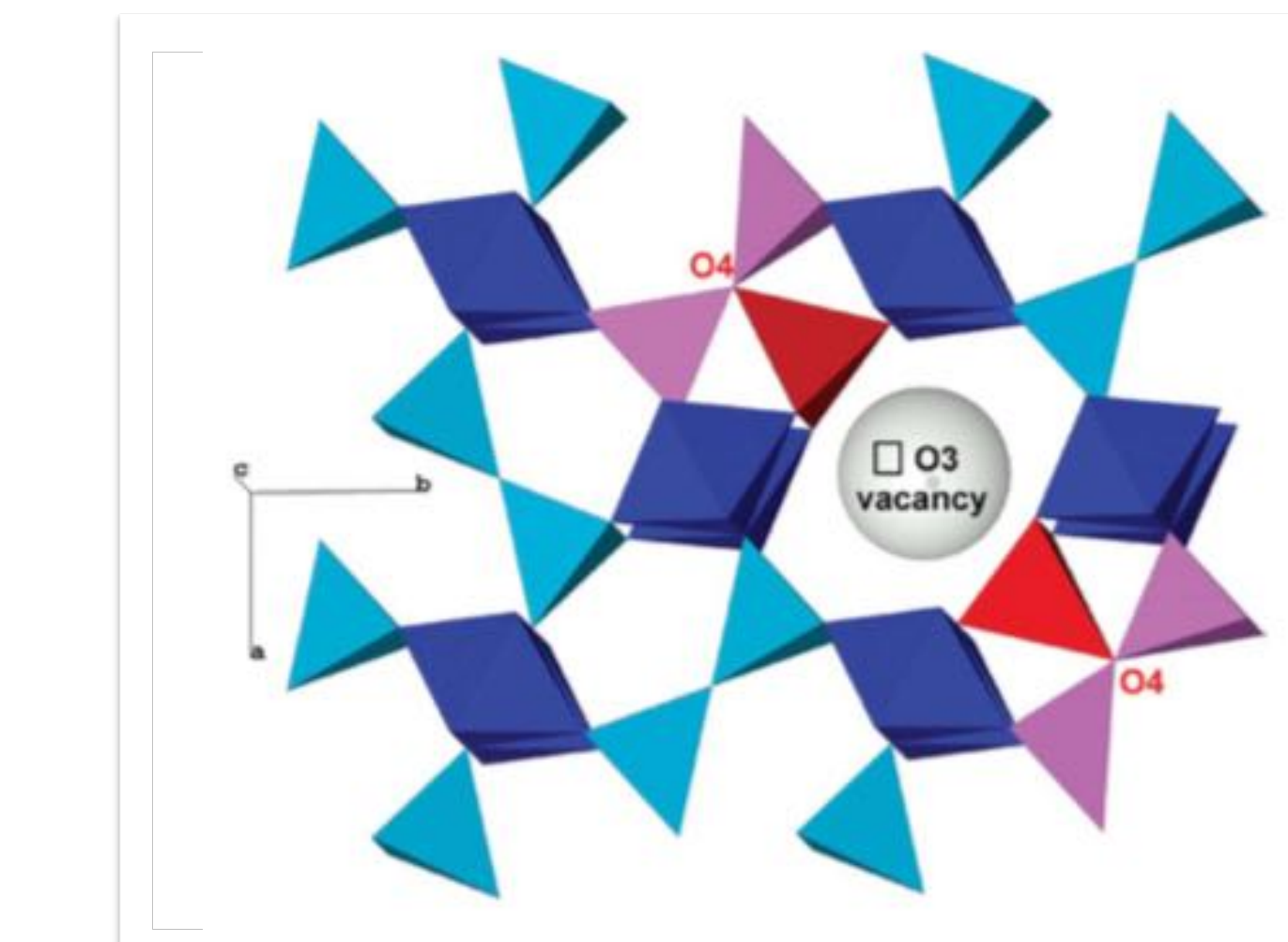
MULLITE - A CASE STUDY

B. D. Butler, T. R. Welberry, & R. L. Withers, Phys Chem Minerals **20**, 323 (1993)

- Mullite is a ceramic that is formed by adding O²⁺ vacancies to Sillimanite
 - Sillimanite has alternating AlO₄ and SiO₄ tetrahedra
 - Mullite has excess Al³⁺ occupying Si²⁺ sites for charge balance
- This results in strong vacancy-vacancy correlations



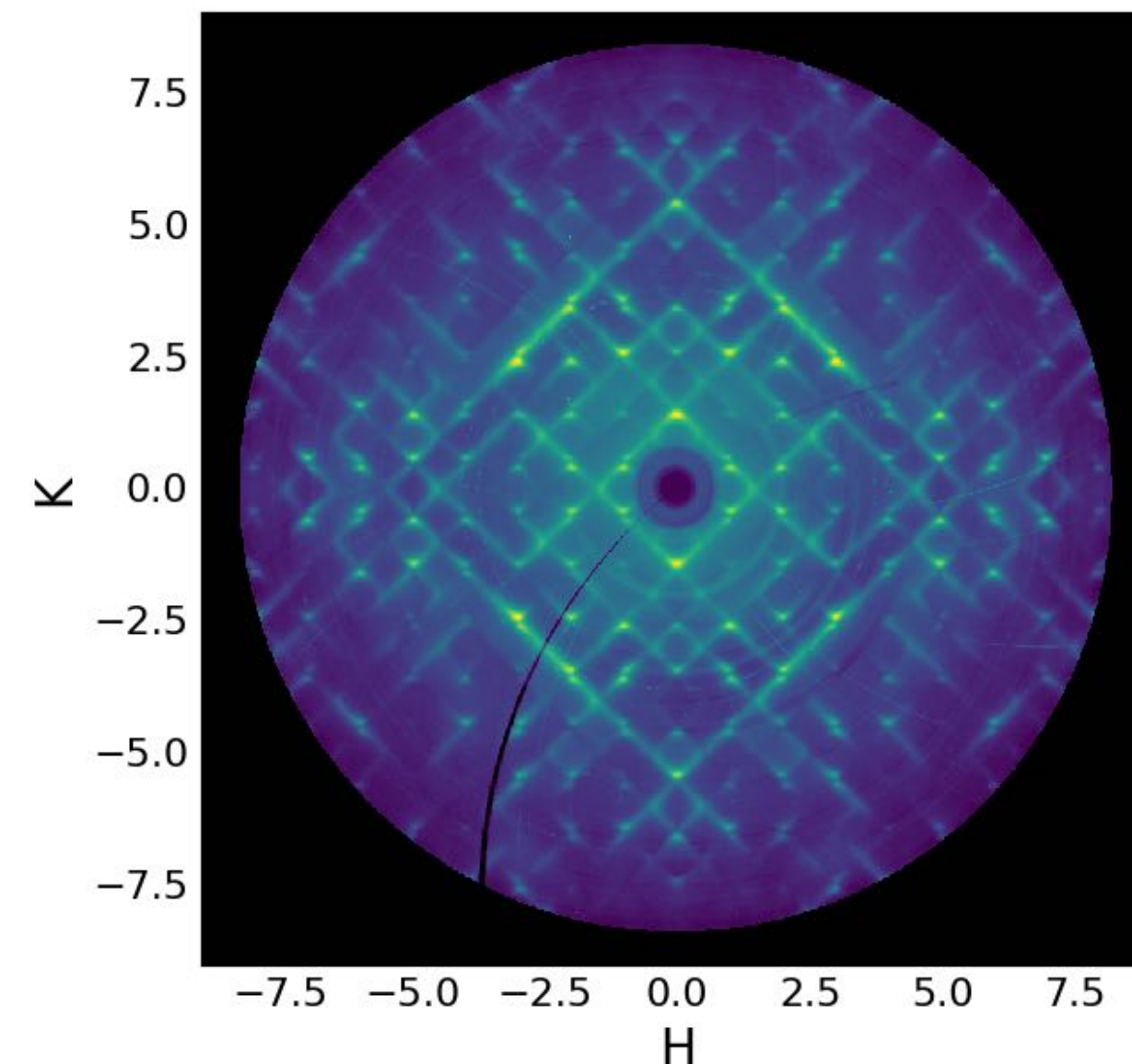
Sillimanite: Al₂SiO₅



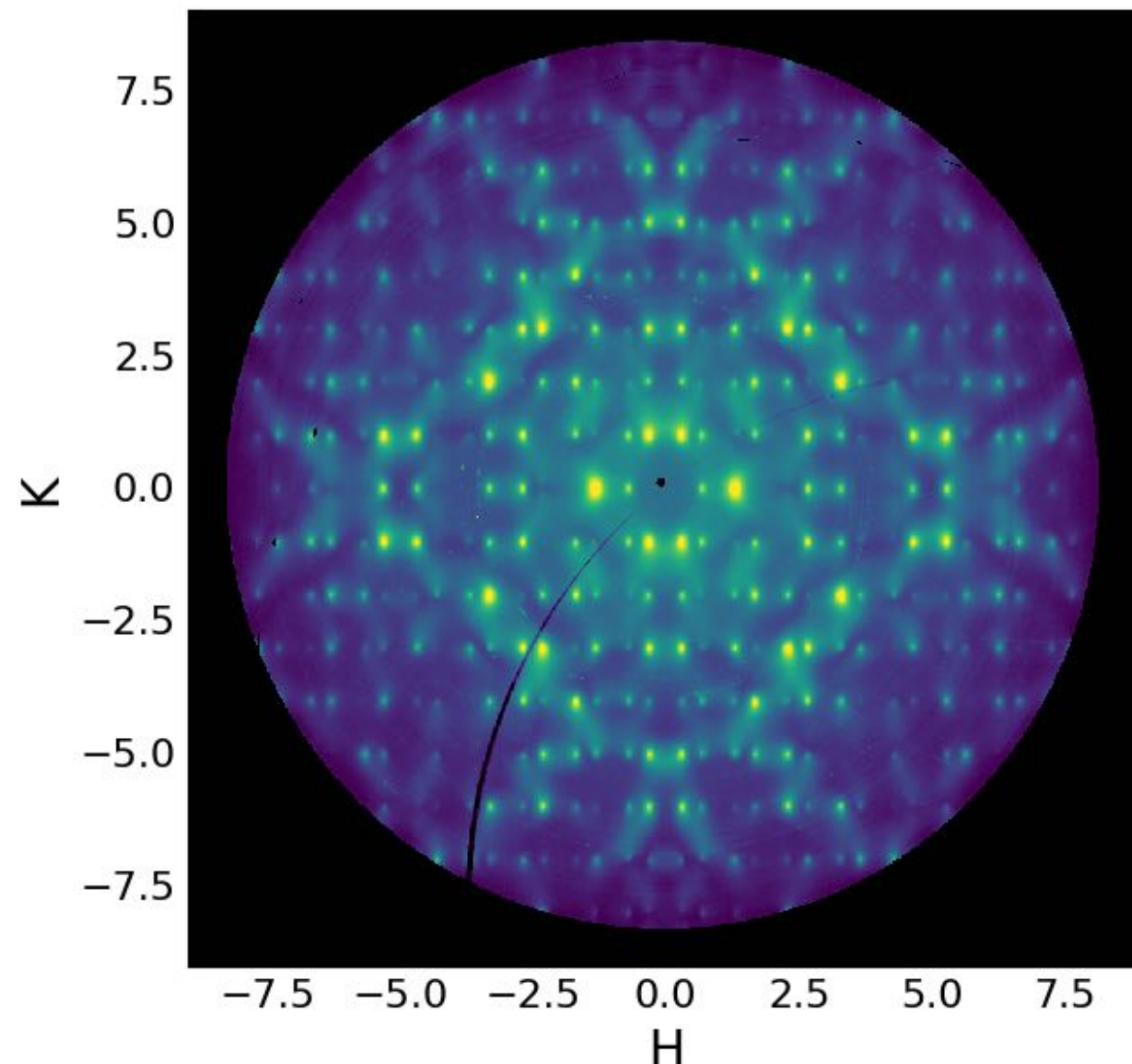
Mullite: Al₂(Al_{2+2x}Si_{2-2x})O_{10-x}

3D DIFFUSE SCATTERING IN MULLITE

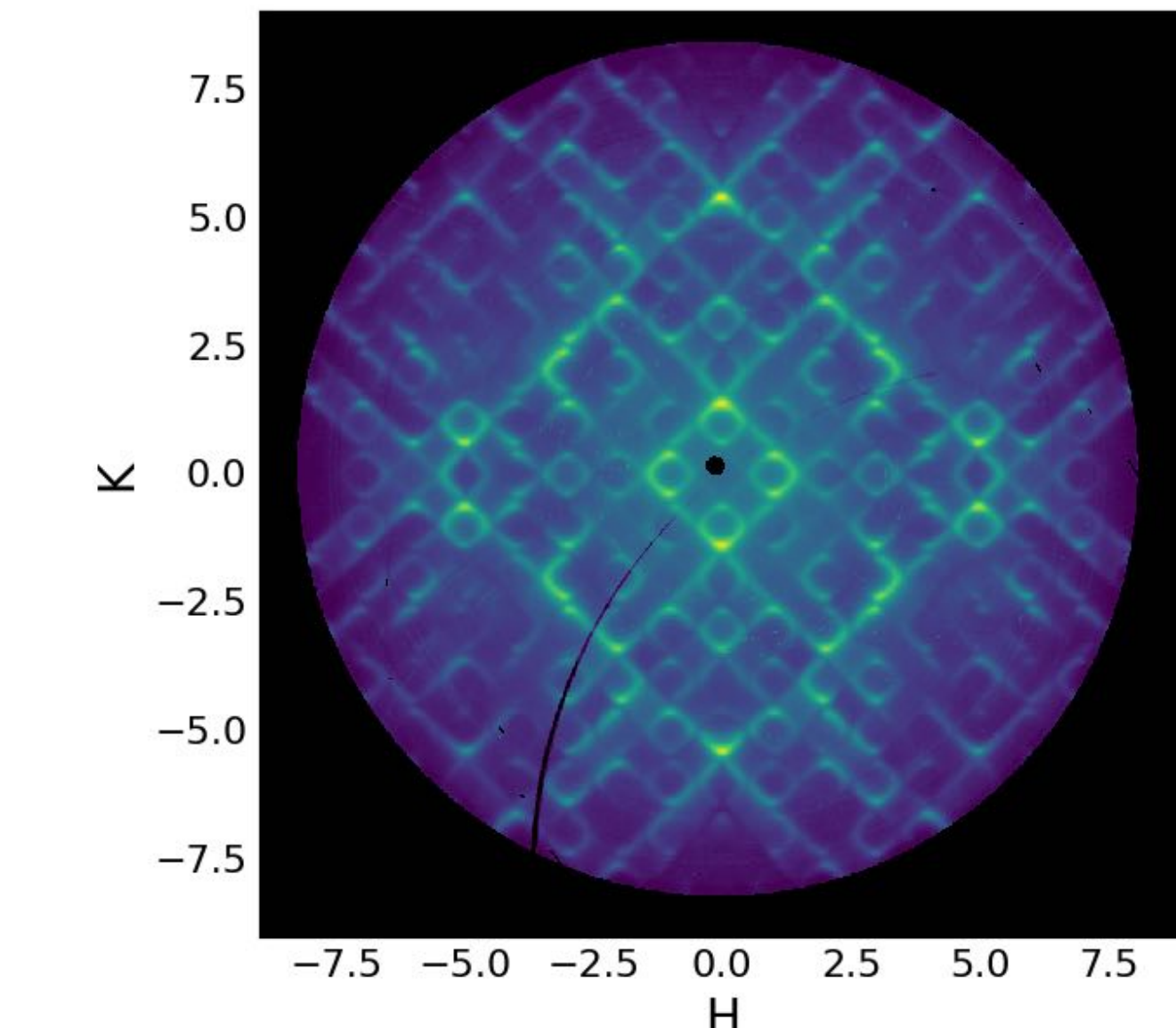
- There is strong diffuse scattering throughout reciprocal space
- The shape of the diffuse scattering is strongly dependent on the value of L



$L=0.16$



$L=0.5$

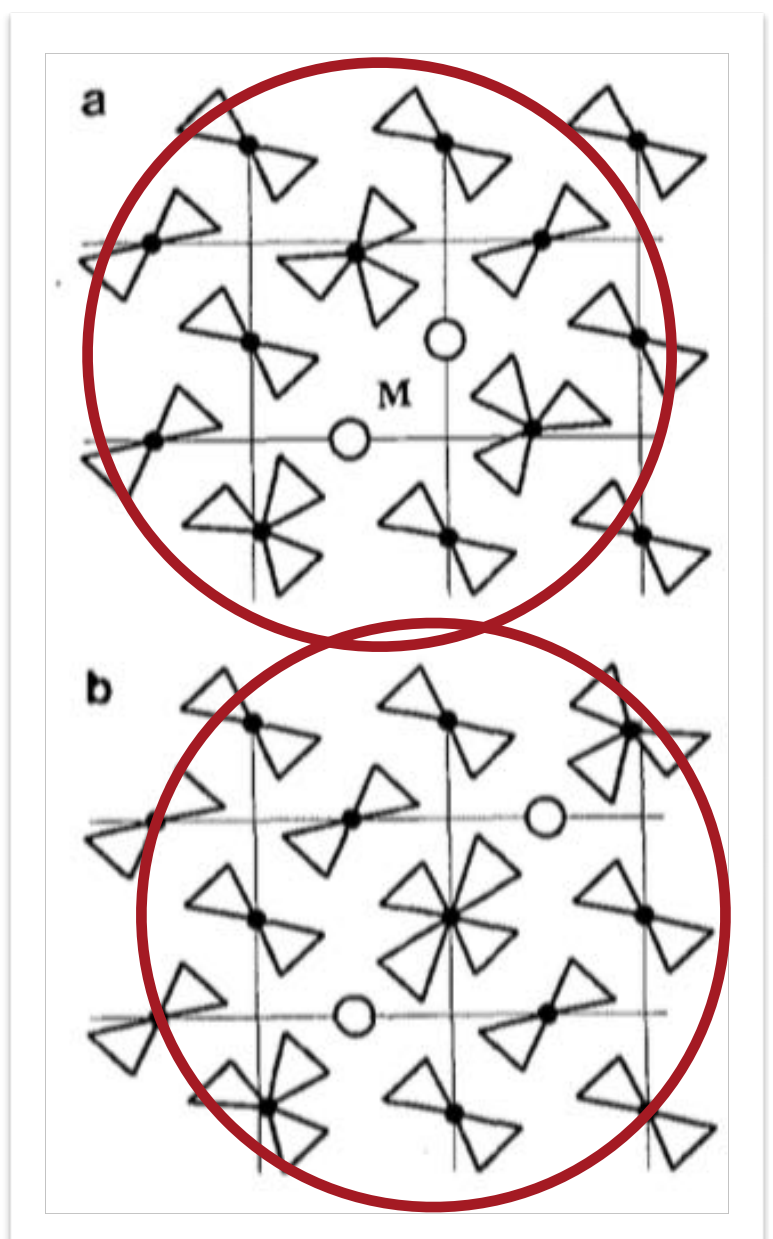
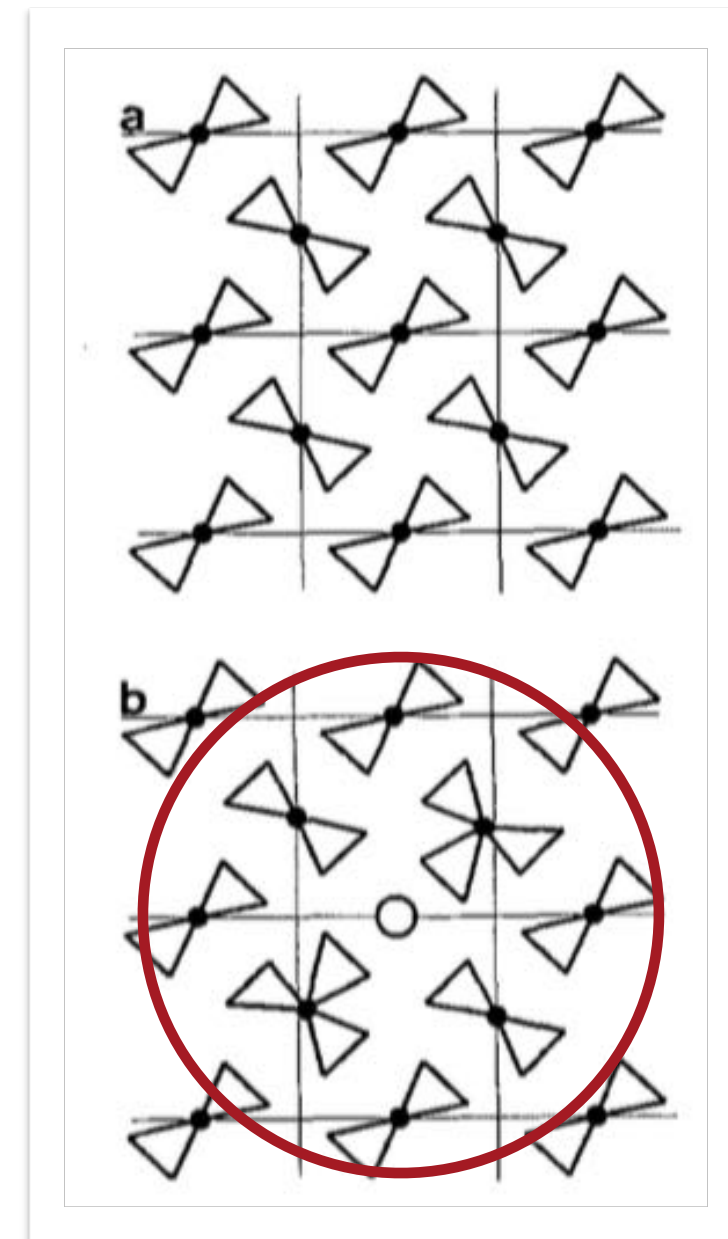


$L=0.75$

MONTE CARLO ANALYSIS

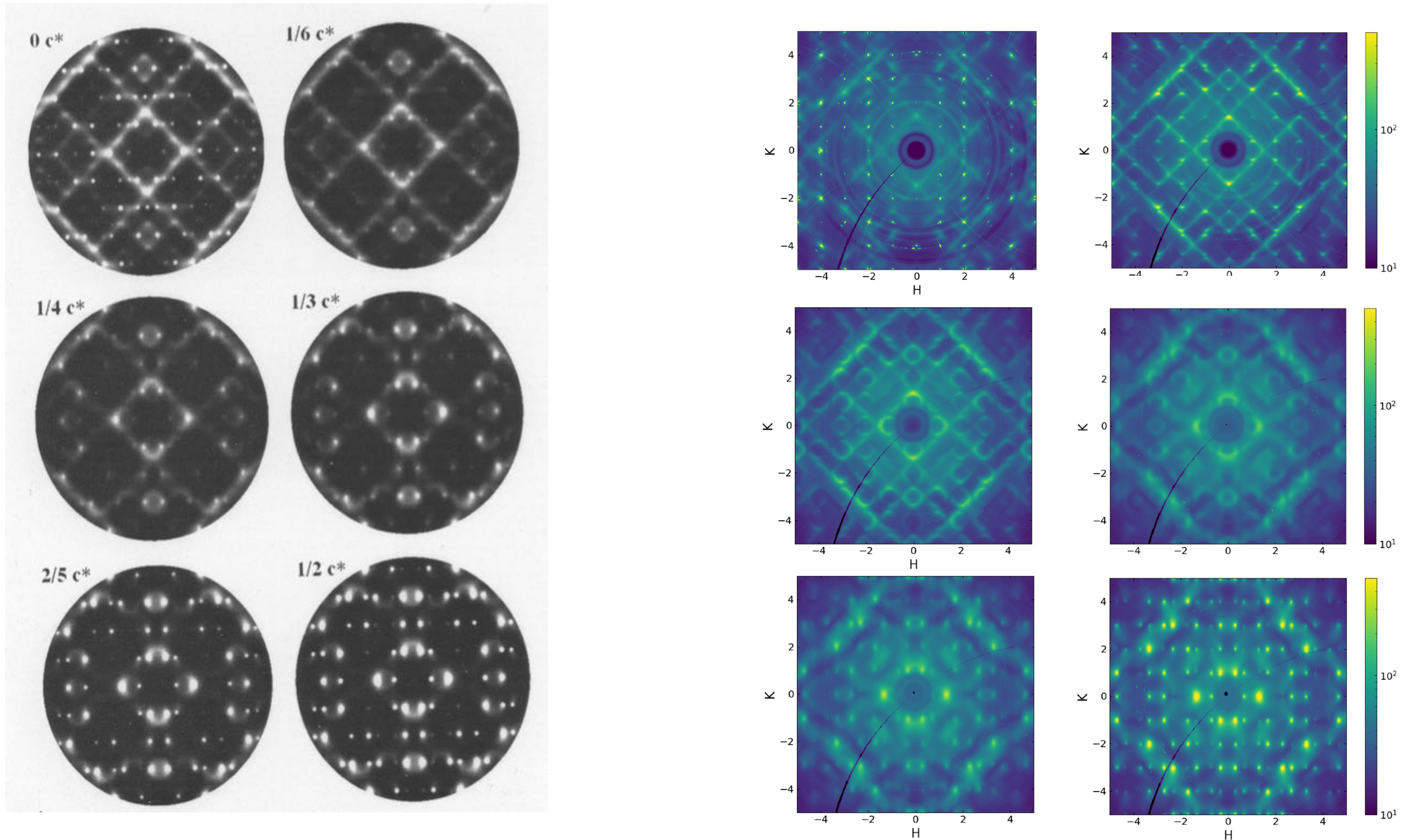
B. D. Butler, T. R. Welberry, & R. L. Withers,
Phys Chem Minerals 20, 323 (1993)

- In a classic analysis, Richard Welberry and colleagues developed a set of interaction energies to model mullite disorder
- Interaction energies were initialized:
 - insights from chemical intuition
 - insights from the measured diffuse scattering
- The diffuse scattering was calculated using a Monte Carlo algorithm to generate vacancy distributions first in 2D slices and then in 3D

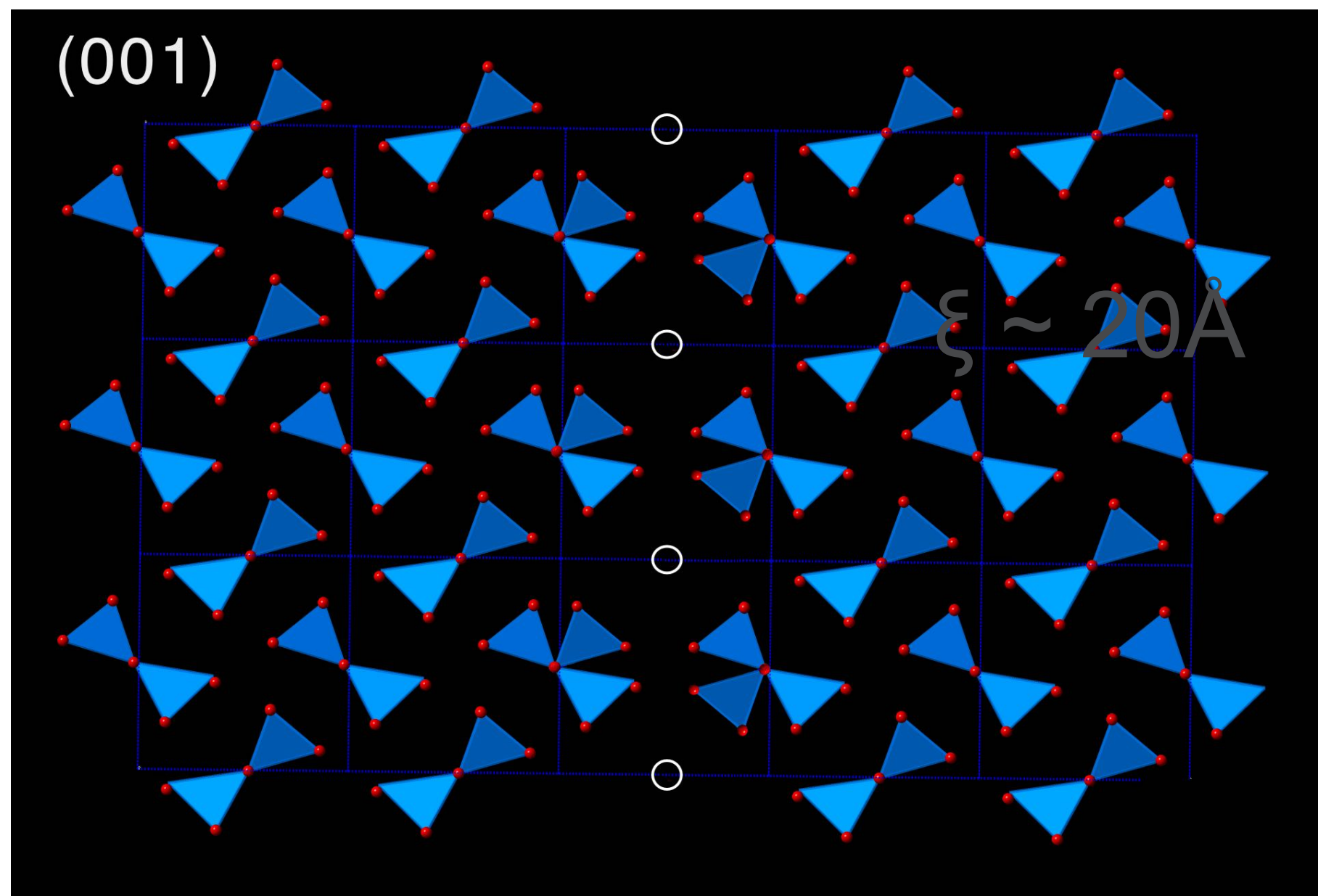
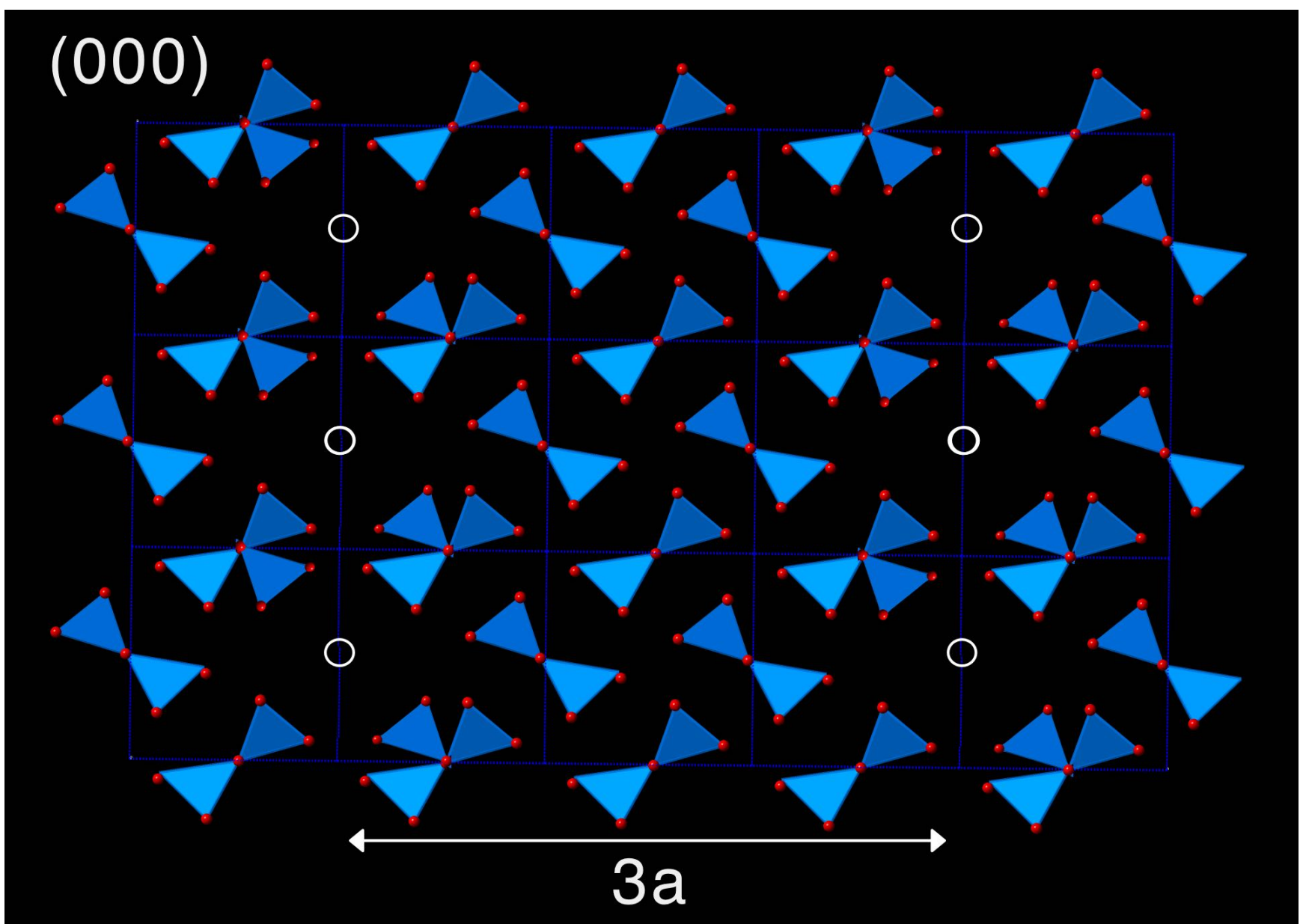


Interatomic vector	α_{lmn}	Interatomic vector	α_{lmn}
$\frac{1}{2}\langle 1\ 1\ 0 \rangle$	-0.24	$\langle 0\ 2\ 0 \rangle$	+0.13
$[1\ 1\ 0]$	-0.23	$\frac{1}{2}\langle 3\ 1\ 0 \rangle$	+0.22
$[1\ -1\ 0]$	-0.05	$\frac{1}{2}\langle 1\ 3\ 0 \rangle$	-0.01
$\langle 1\ 0\ 0 \rangle$	-0.06	$\langle 1\ 0\ 1 \rangle$	+0.07
$\langle 0\ 1\ 0 \rangle$	+0.22	$\langle 0\ 1\ 1 \rangle$	-0.12
$\langle 0\ 0\ 1 \rangle$	-0.03	$\frac{1}{2}\langle 3\ 3\ 0 \rangle$	+0.17
$\frac{1}{2}[1\ -1\ 2]$	+0.12	$\langle 1\ 1\ 1 \rangle$	-0.01
$\frac{1}{2}[1\ 1\ 2]$	+0.12	$\frac{1}{2}\langle 3\ 1\ 2 \rangle$	-0.11
$\langle 2\ 0\ 0 \rangle$	-0.12	$\frac{1}{2}\langle 3\ 3\ 2 \rangle$	-0.07

MONTE CARLO ANALYSIS RESULTS



VACANCY ORDERING IN MULLITE



$$c = 0$$

$$\mathbf{q} = \pm \frac{1}{2}\mathbf{c}^* \pm \frac{1}{3}\mathbf{a}^*$$

$$c = 1.0$$

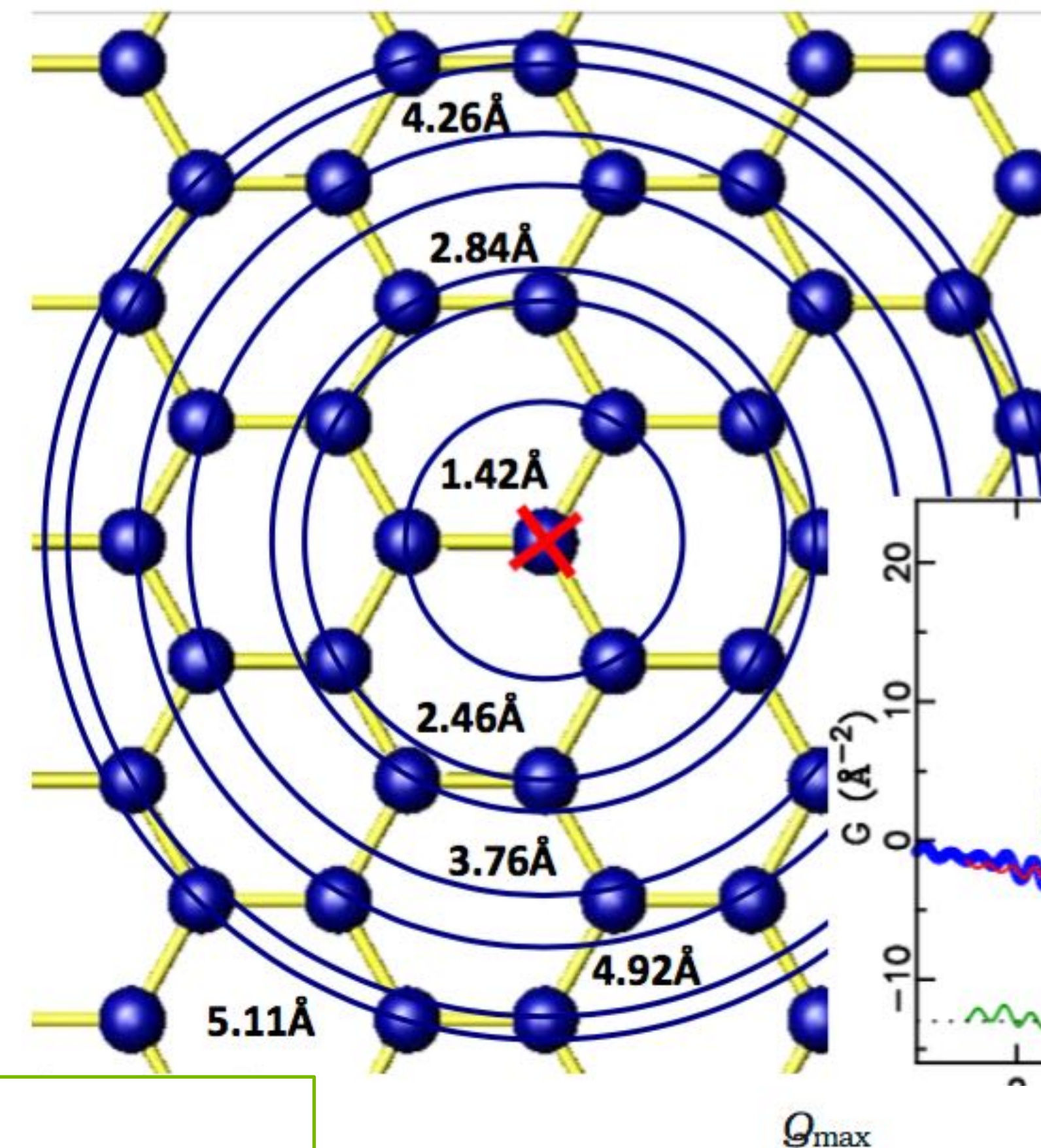
CASE STUDY 2: SODIUM-INTERCALATED V₂O₅ 3D-ΔPDF



U.S. DEPARTMENT OF
ENERGY
Argonne National Laboratory is a
U.S. Department of Energy laboratory
managed by UChicago Argonne, LLC.

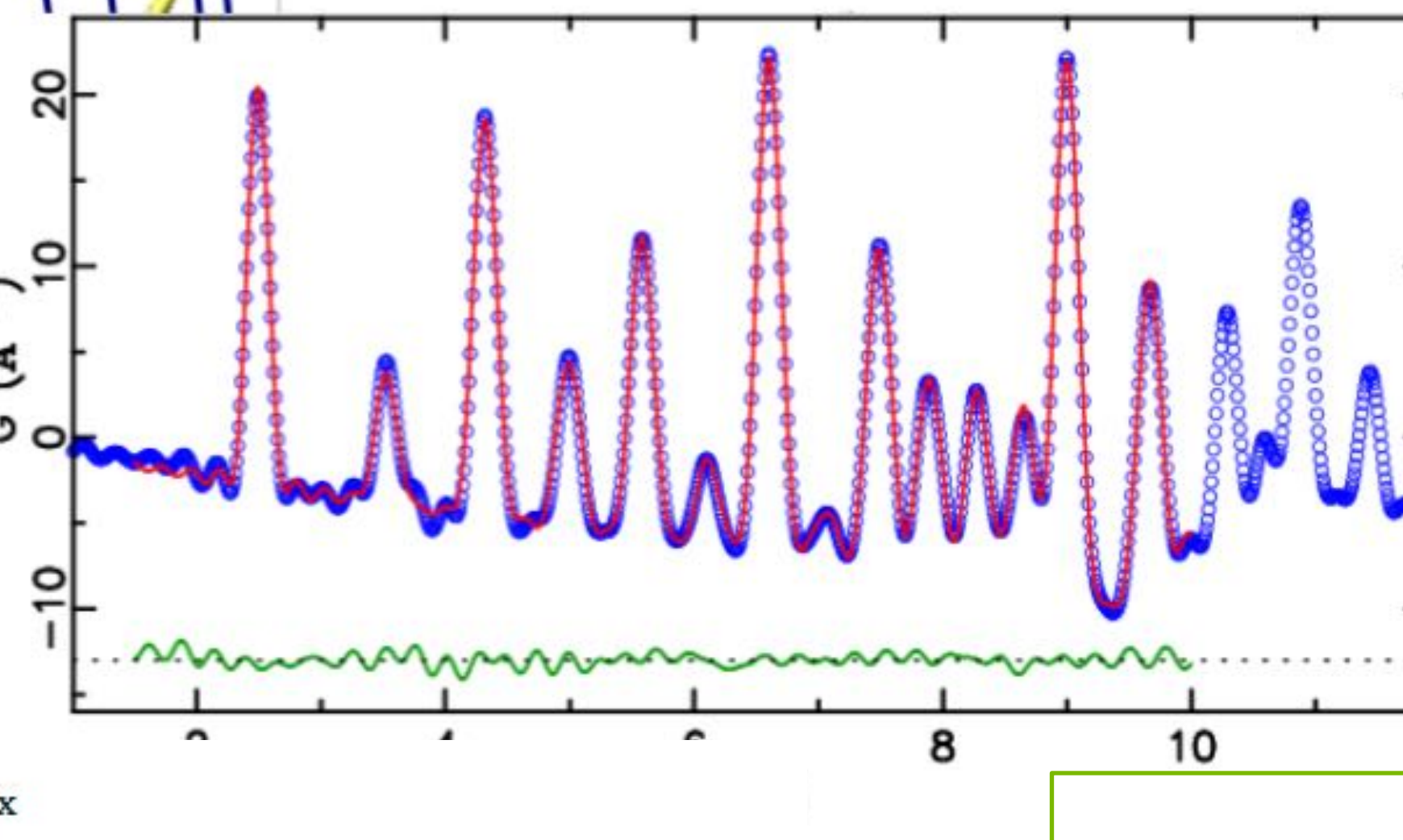


PAIR DISTRIBUTION FUNCTION ANALYSIS



$$G(r) = 4\pi r[\rho(r) - \rho_o] = (2/\pi) \int_{Q=Q_{\min}}^{Q_{\max}} Q[S(Q)-1]\sin(Qr)dQ$$

Radial atomic pair distribution function (PDF) gives the interatomic distance distribution, or “probability” of finding atomic pairs distance r apart



Emil Bozin (ADD 2013)

THREE-DIMENSIONAL PAIR DISTRIBUTION FUNCTIONS

238

Z. Kristallogr. 2012, 227, 238–247 / DOI 10.1524/zkri.2012.1504

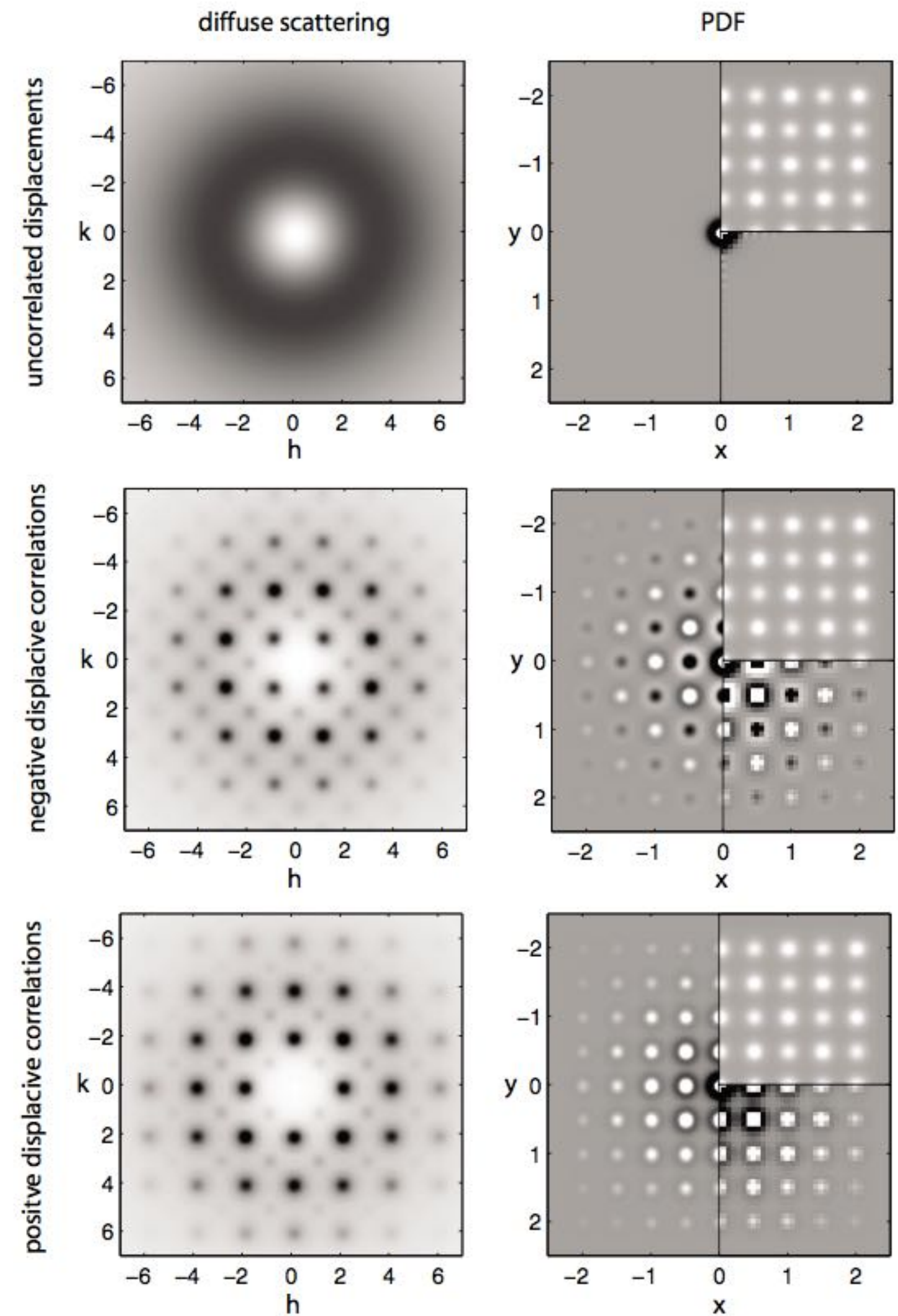
© by Oldenbourg Wissenschaftsverlag, München

The three-dimensional pair distribution function analysis of disordered single crystals: basic concepts

Thomas Weber* and Arkadiy Simonov

Laboratory of Crystallography, ETH Zurich Wolfgang-Pauli-Str. 10, 8093 Zurich, Switzerland

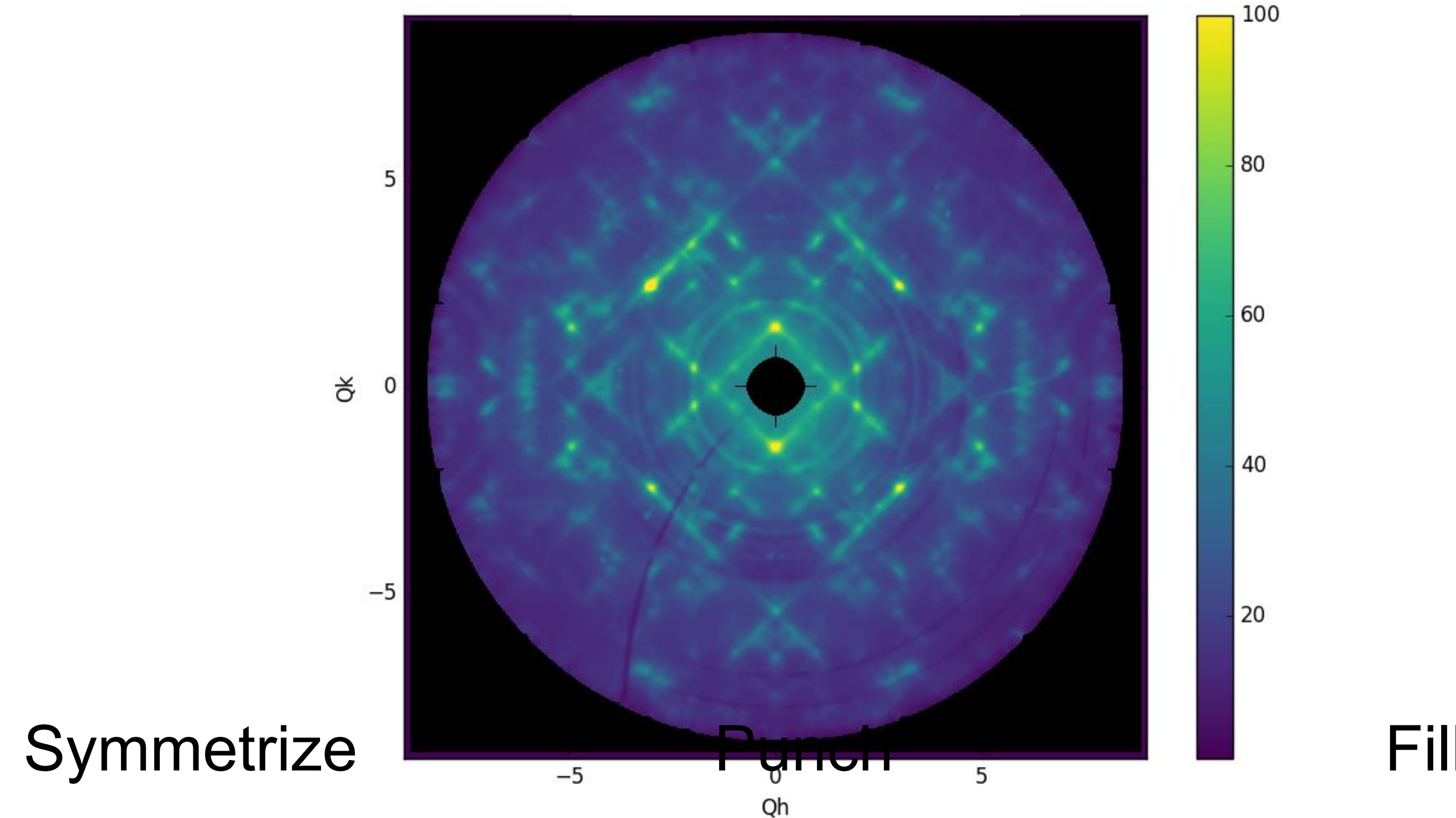
- The 3D PDF technique was pioneered by Thomas Weber and colleagues at ETH
 - Philippe Schaub, Walter Steurer, Arkadiy Simonov
 - See Yell - A. Simonov, et al, J Appl Cryst **47**, 1146 (2014).
- The ability to measure three-dimensional $S(\mathbf{Q})$ over a large volume of reciprocal space provides the 3D analog of PDF measurements.
 - Total PDFs if Bragg peaks and diffuse scattering can be measured simultaneously
 - Δ PDFs if the Bragg peaks are eliminated
- This allows a model-independent view of the measurements in real space.



“PUNCH AND FILL”

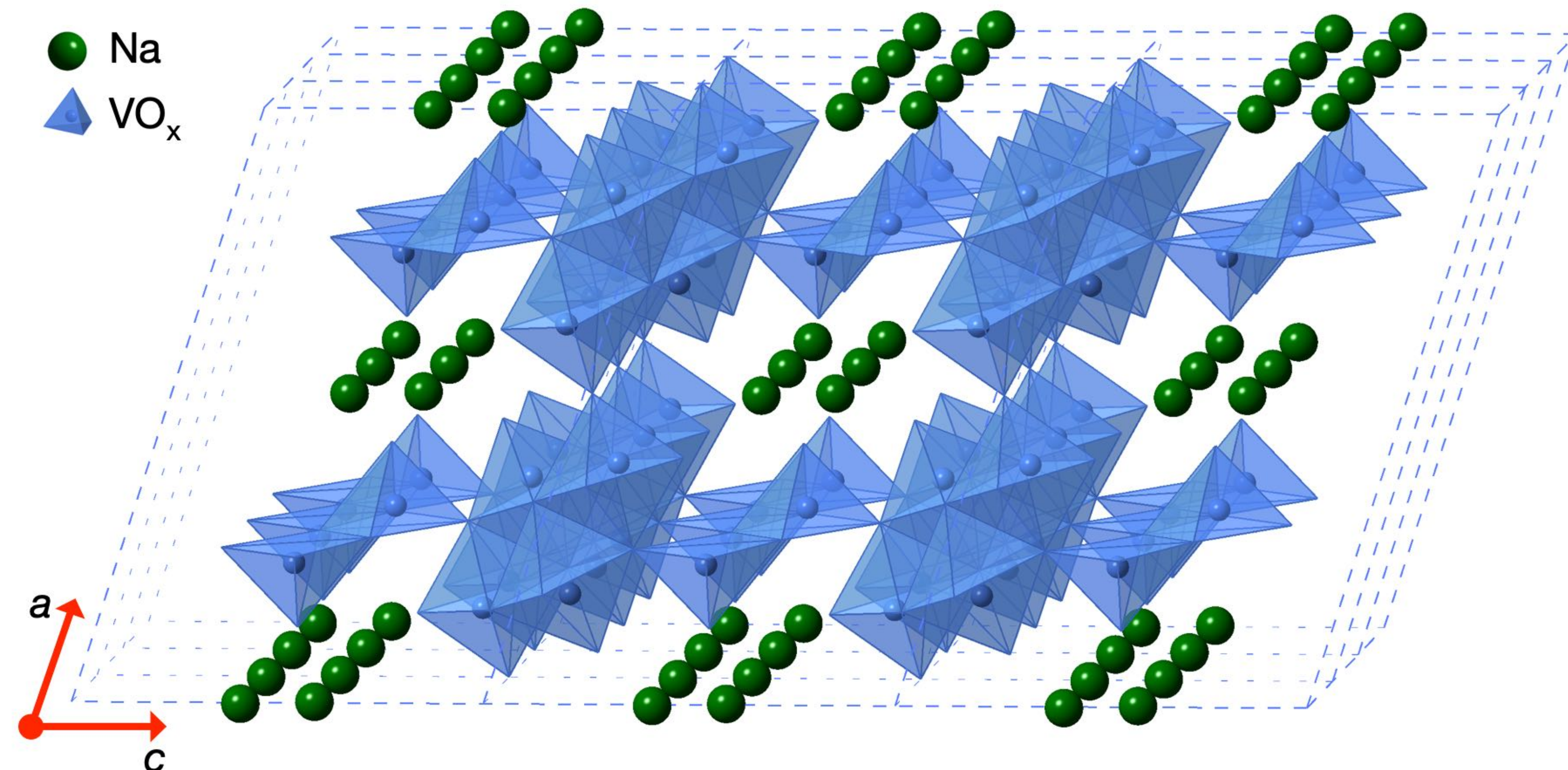
$$I = \sum_i \sum_j b_i b_j \exp(i\mathbf{Q} \cdot \mathbf{r}_{ij})$$

$$P_{tot}(\mathbf{r}) = FT[I(\mathbf{Q})] = FT[|\bar{F}(\mathbf{Q})|^2] + FT[|\Delta F(\mathbf{Q})|^2] = P_{hkl}(\mathbf{r}) + \Delta P(\mathbf{r})$$



A. Simonov, T. Weber, and W. Steurer, Journal of Applied Crystallography **47**, 1146 (2014).

SODIUM-INTERCALATED V_2O_5

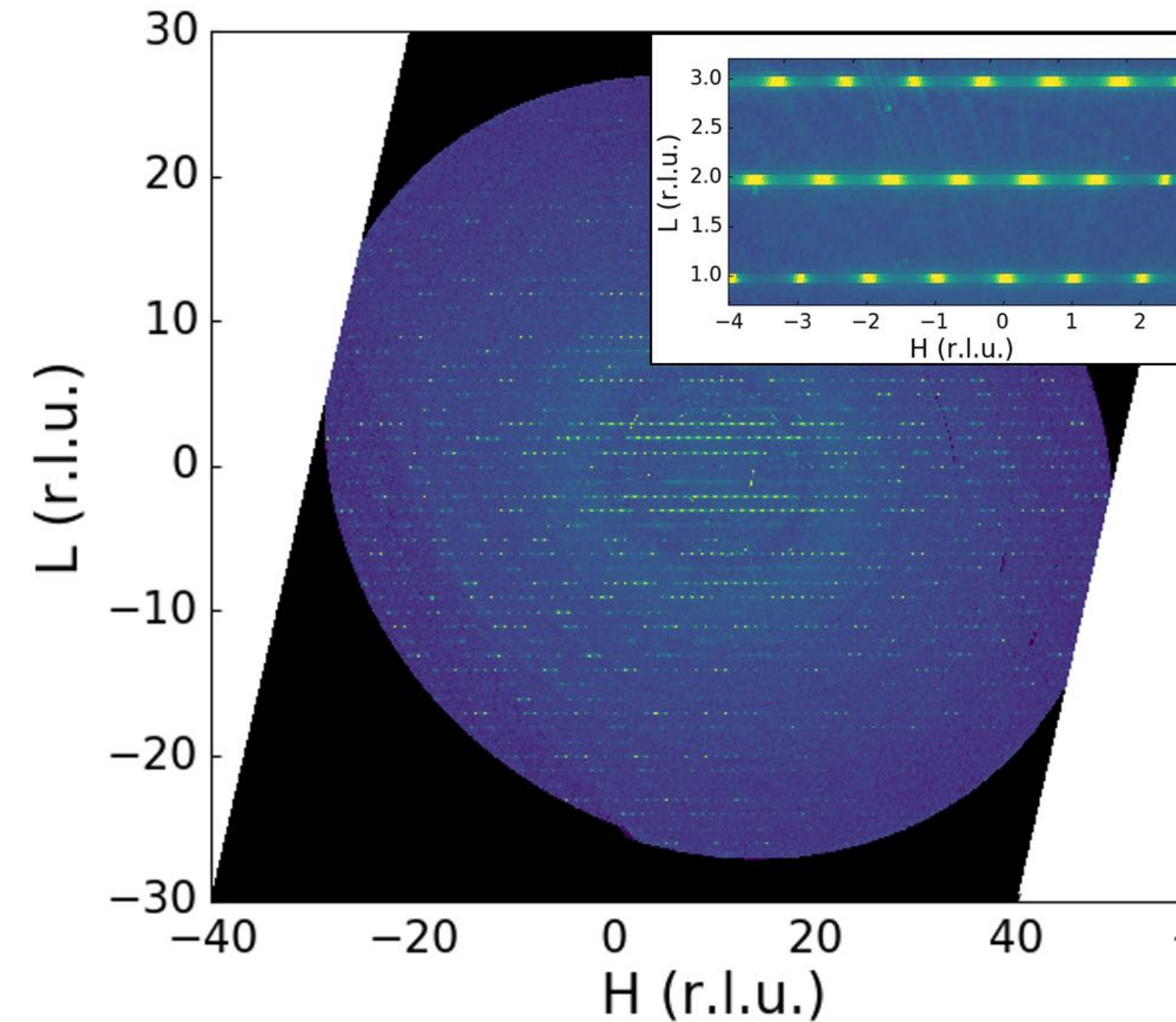


M. J. Krogstad, S. Rosenkranz, J. M. Wozniak, G. Jennings, J. P. C. Ruff, J. T. Vaughn, and R. Osborn
Nature Materials **19**, 63 (2020).

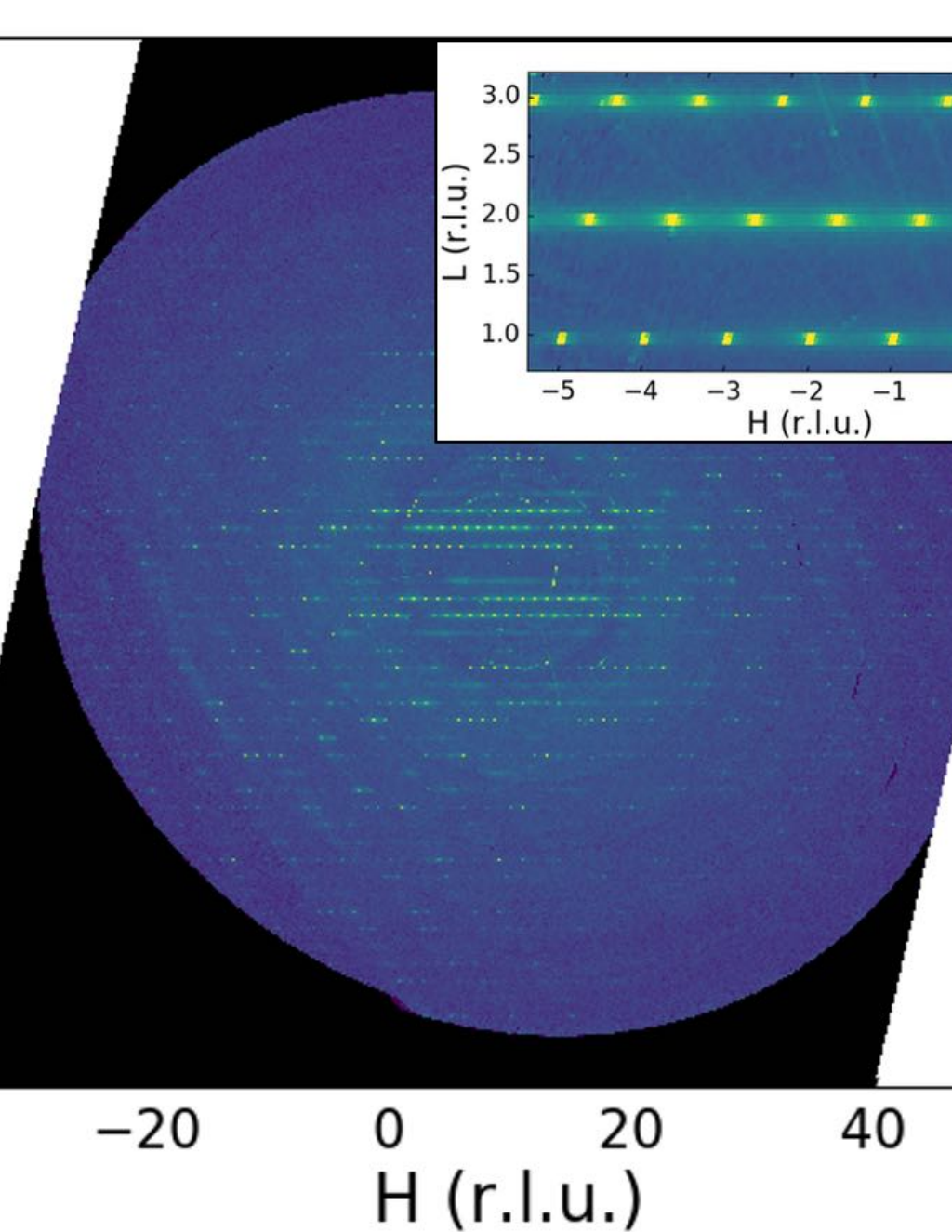
SUBLATTICE MELTING IN $\text{Na}_{0.45}\text{V}_2\text{O}_5$

Order-Disorder Transition in the Half-Filled Sodium Sublattice

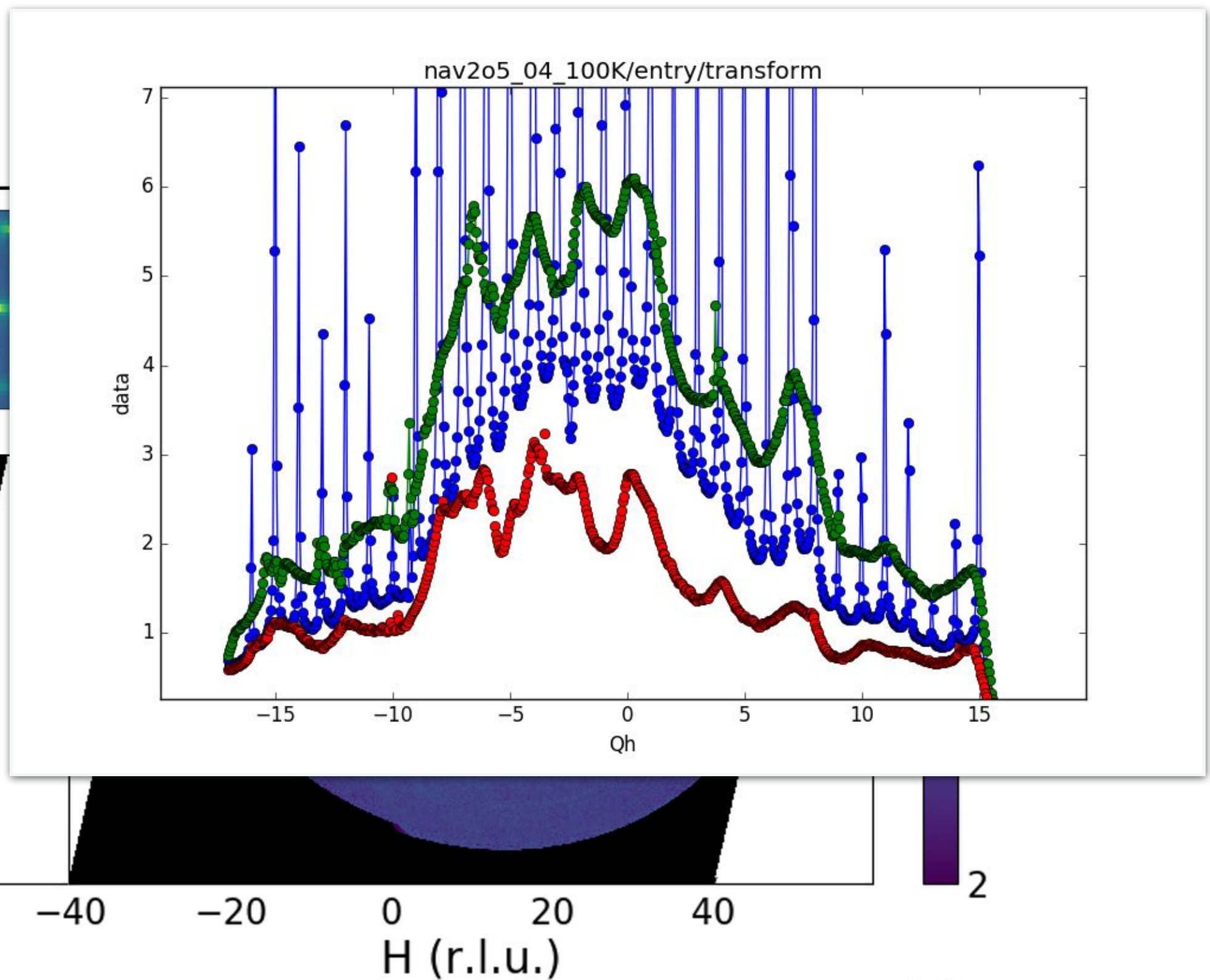
K=0.5



50K

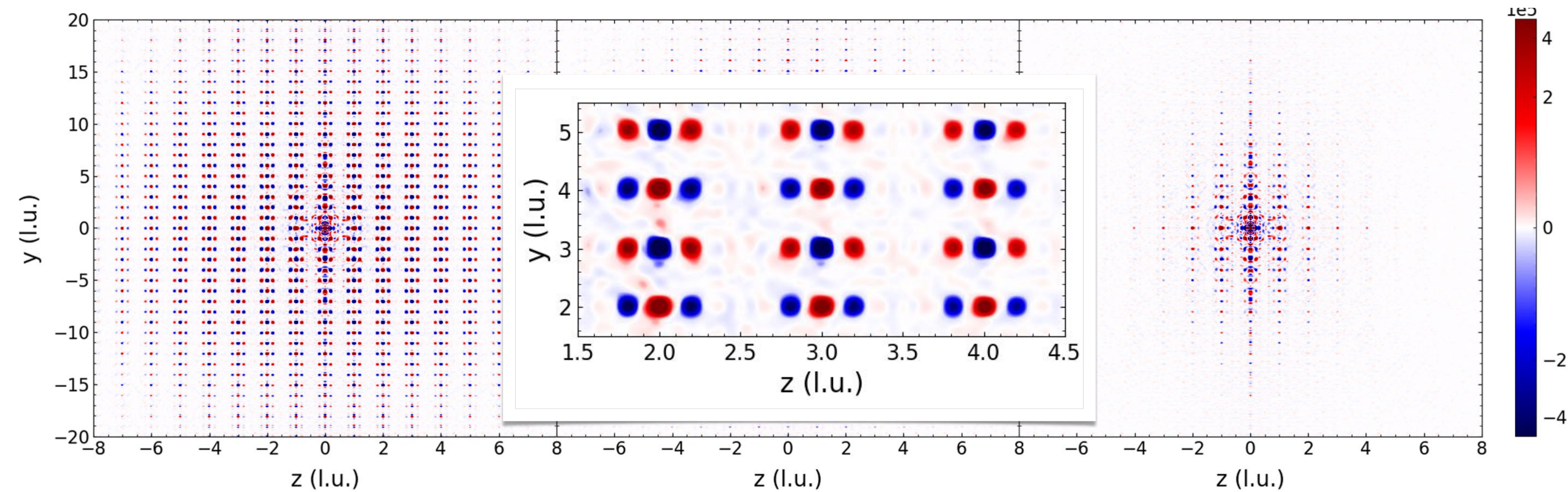


200K



250K

3D- Δ PDF ANALYSIS OF $\text{Na}_{0.45}\text{V}_2\text{O}_5$

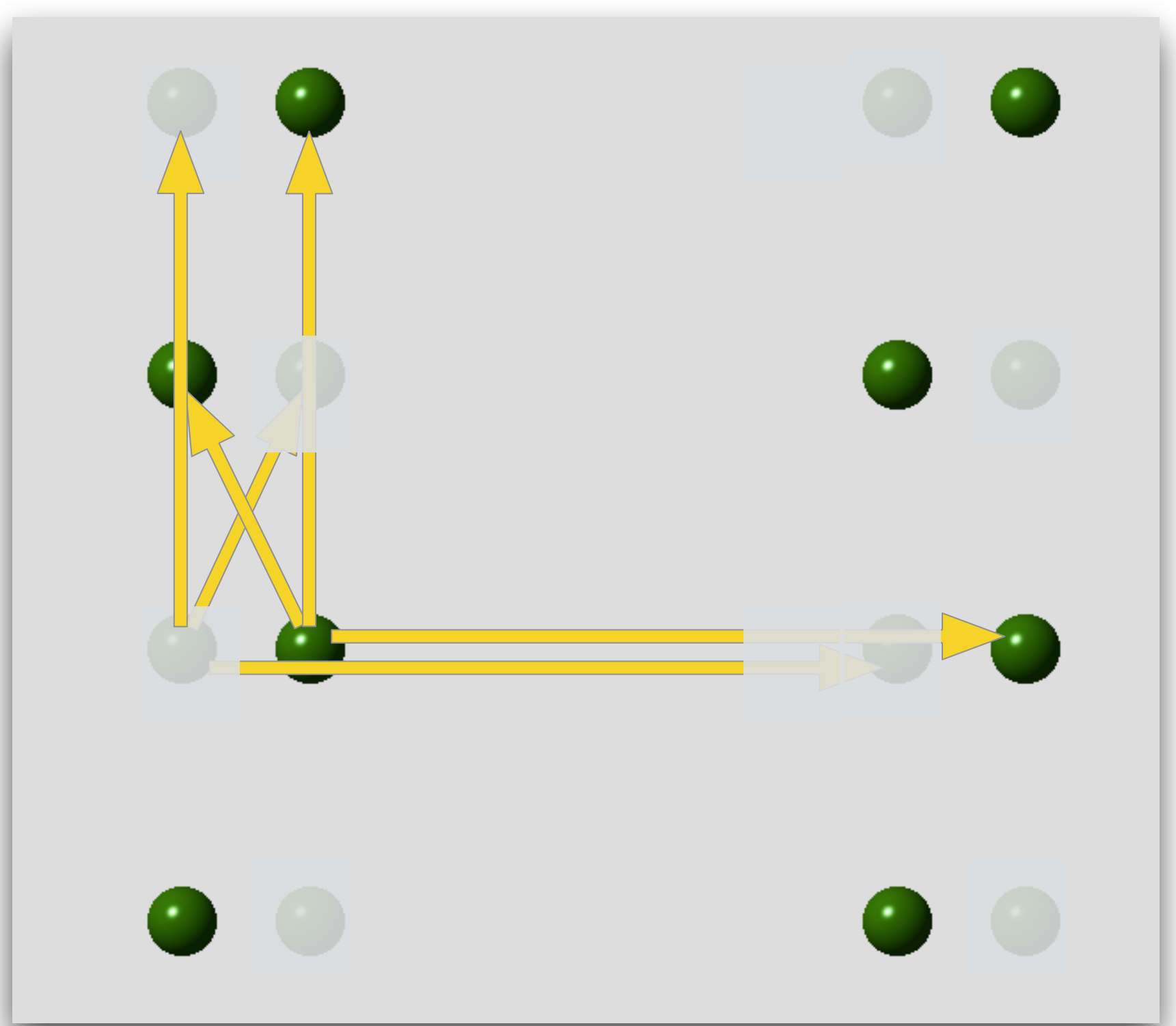
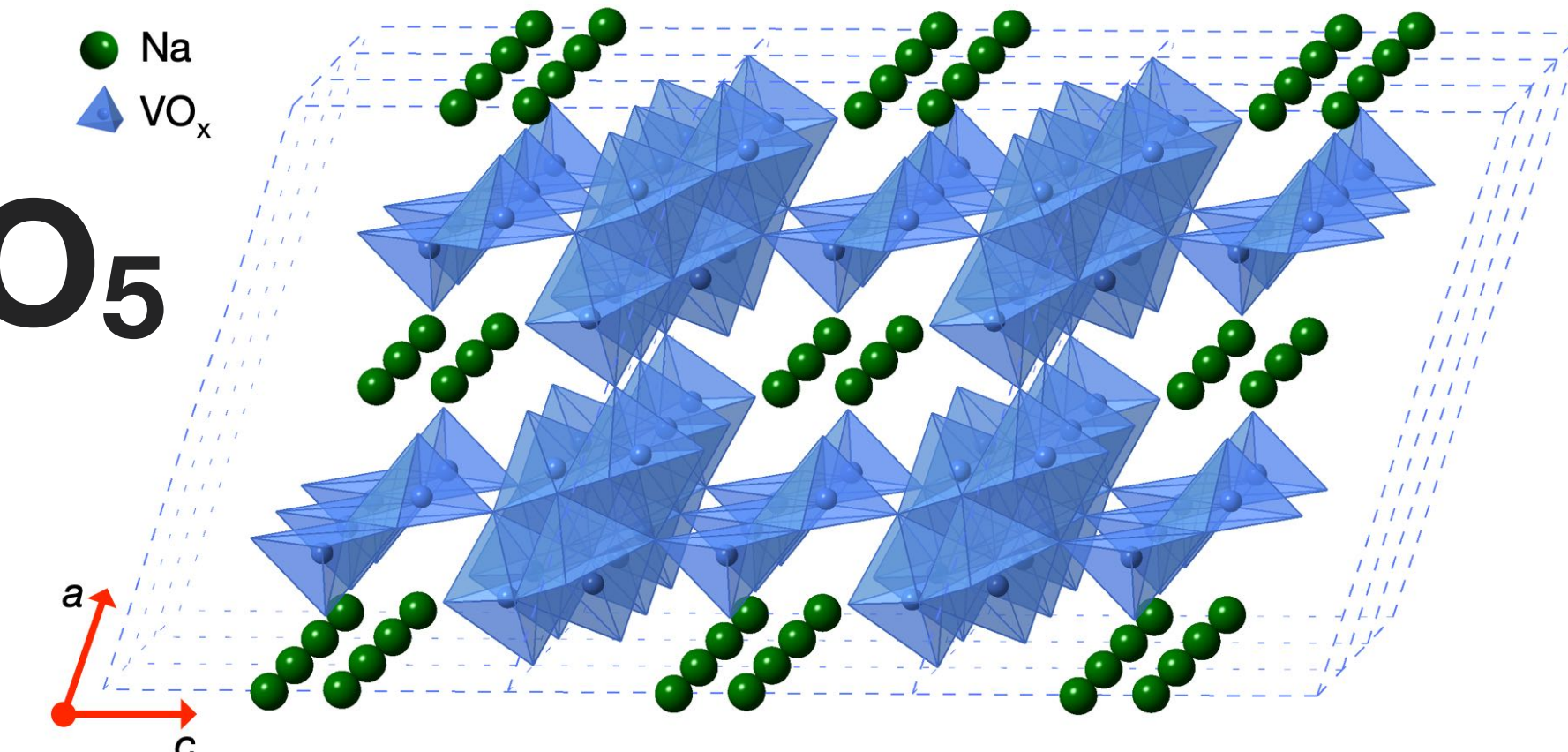
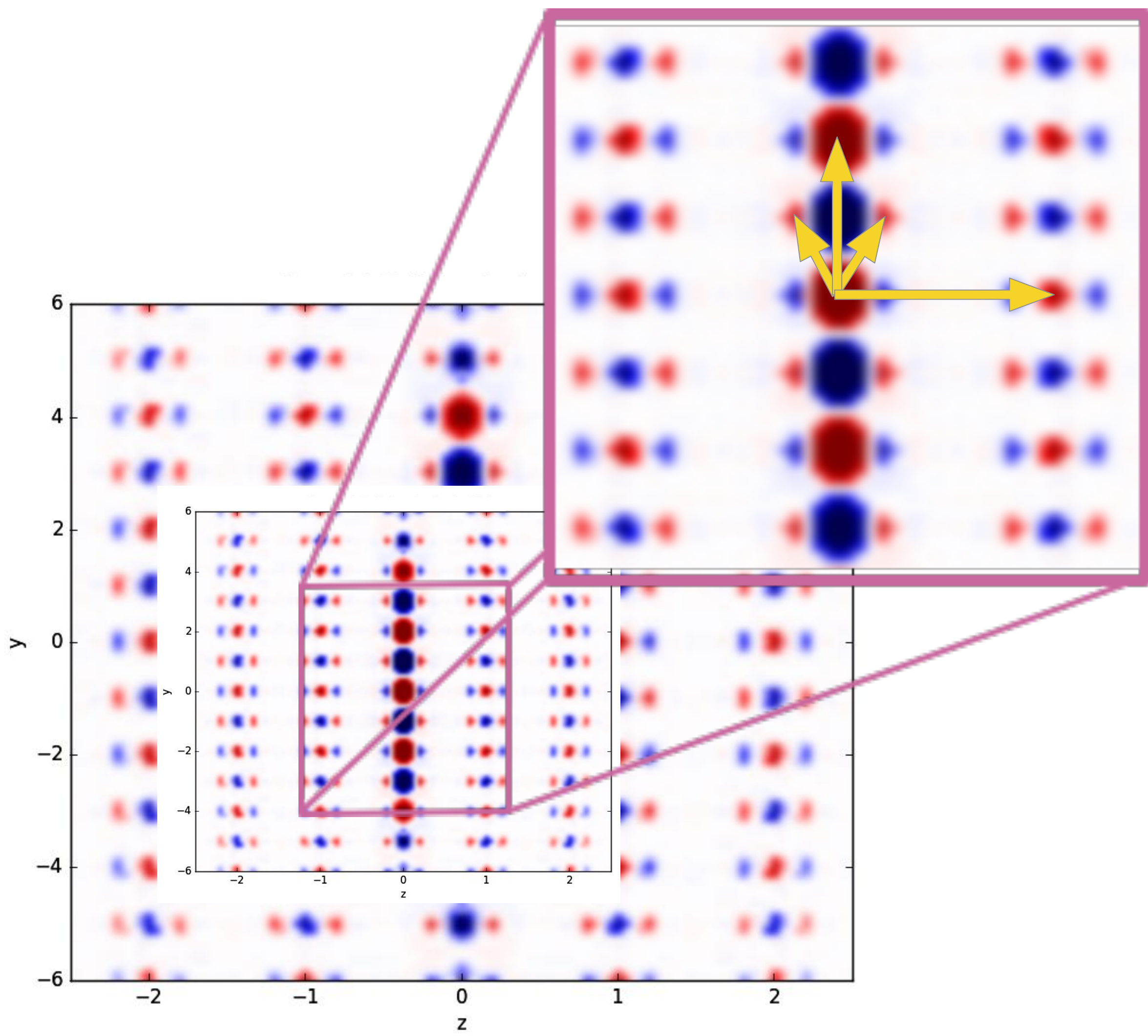


50K

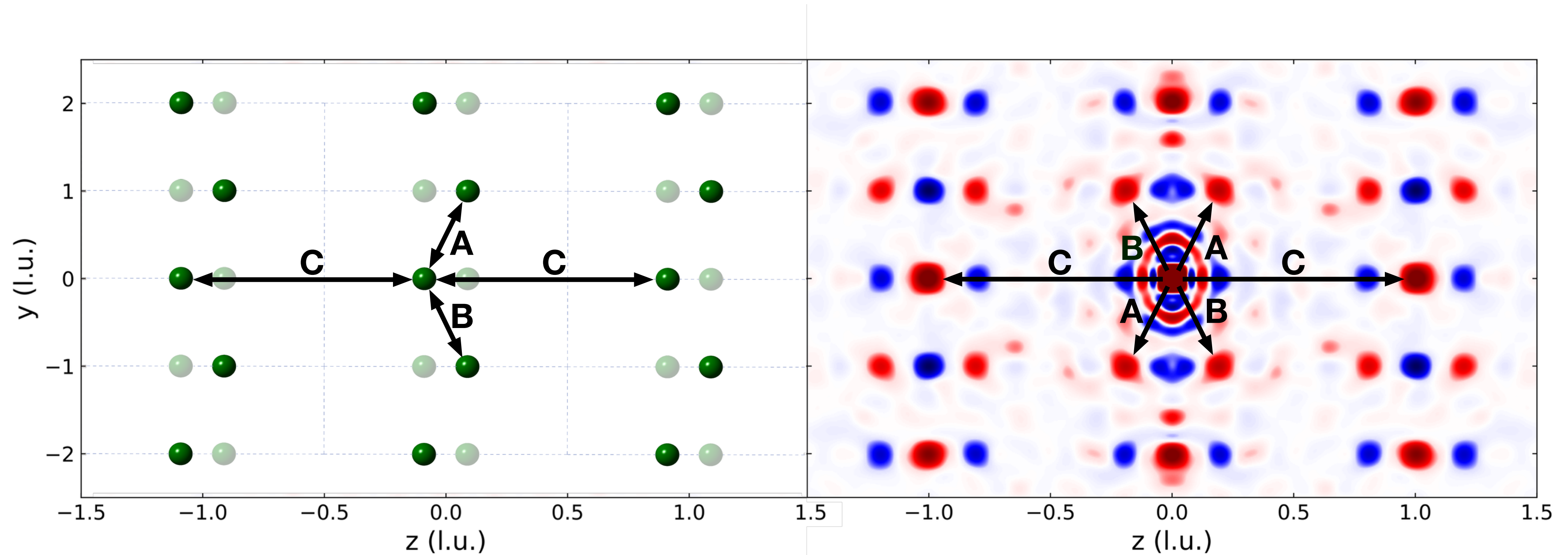
200K

250K

3D- Δ PDF ANALYSIS OF $\text{Na}_{0.45}\text{V}_2\text{O}_5$

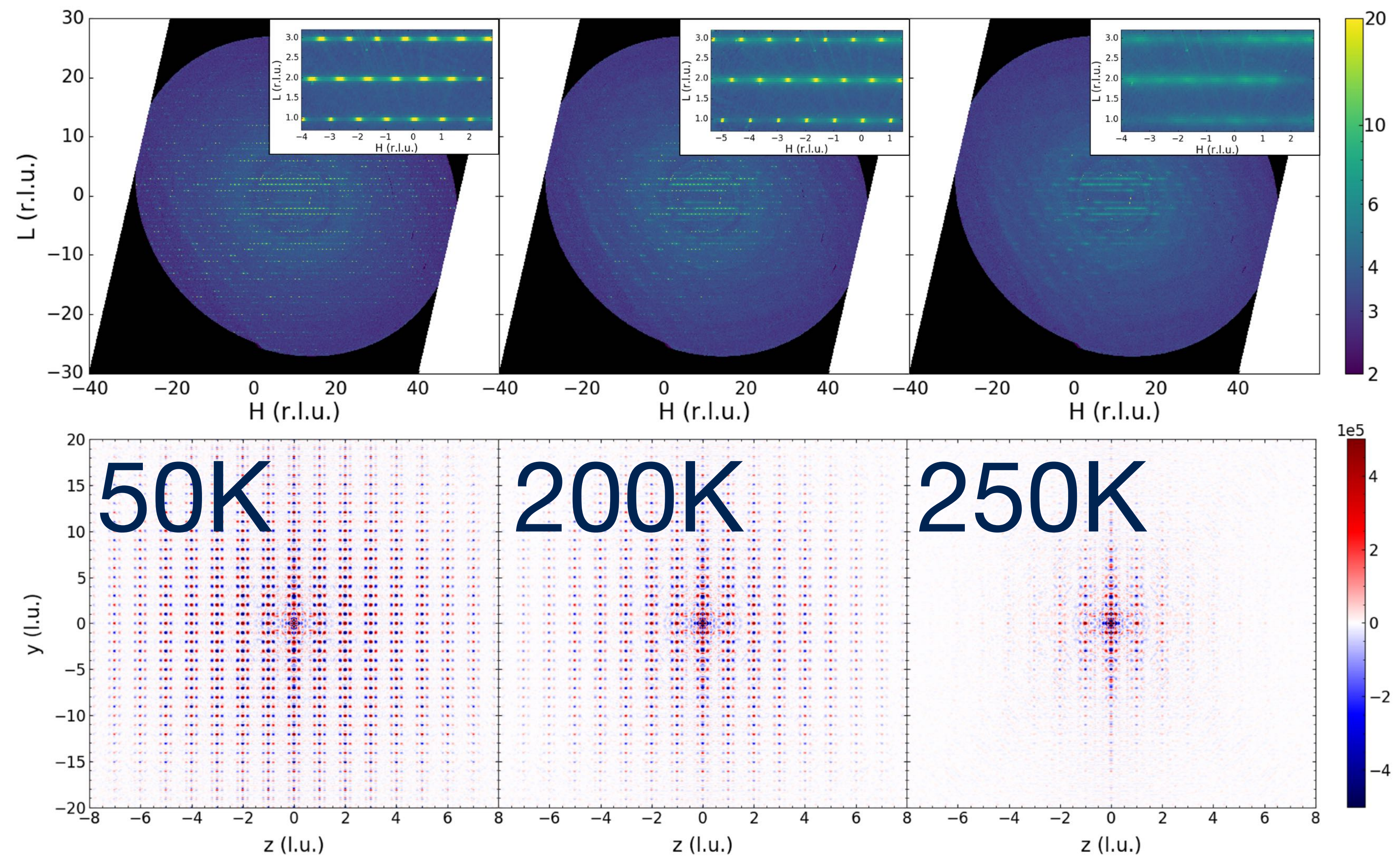


REAL SPACE vs 3D- Δ PDF



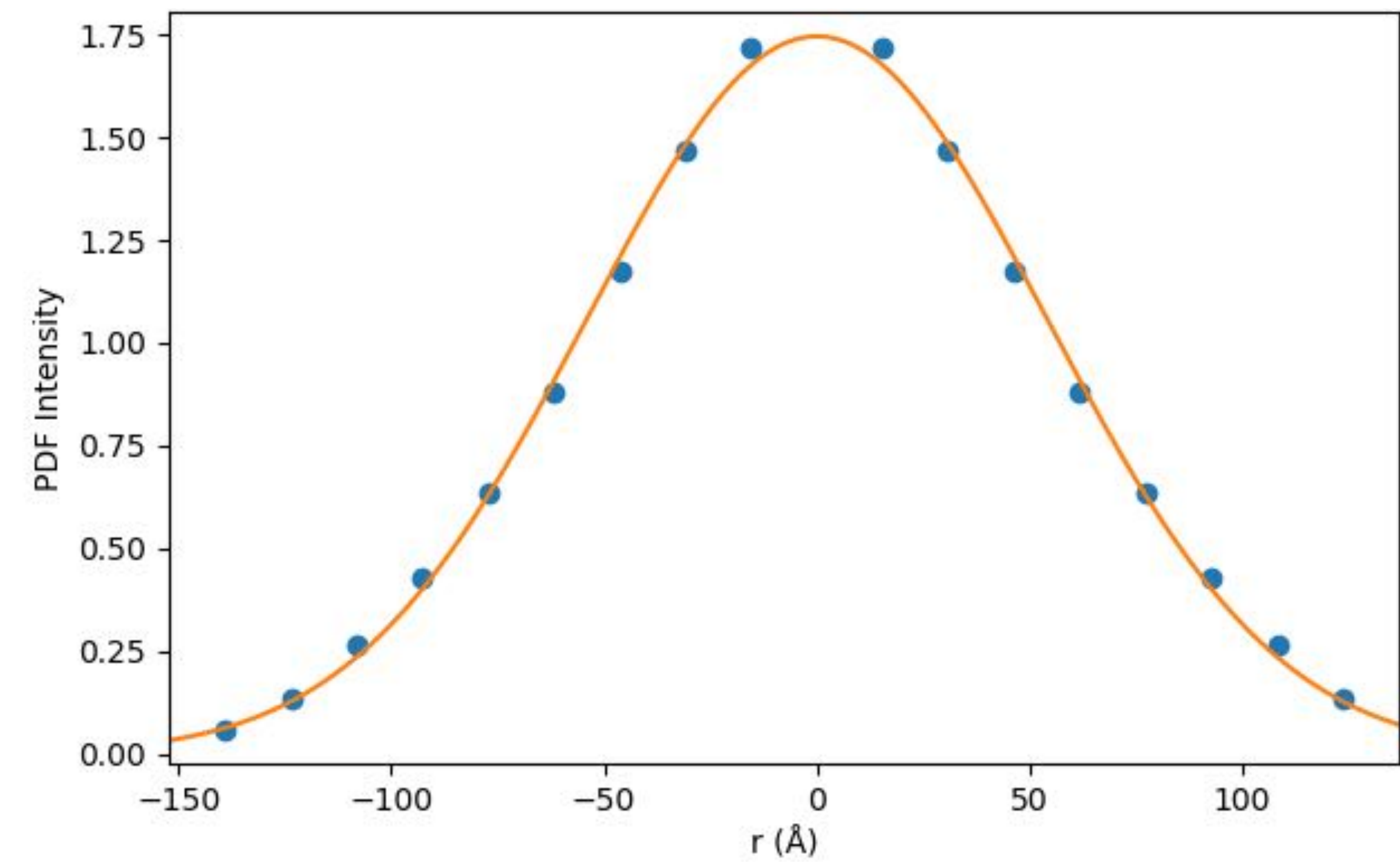
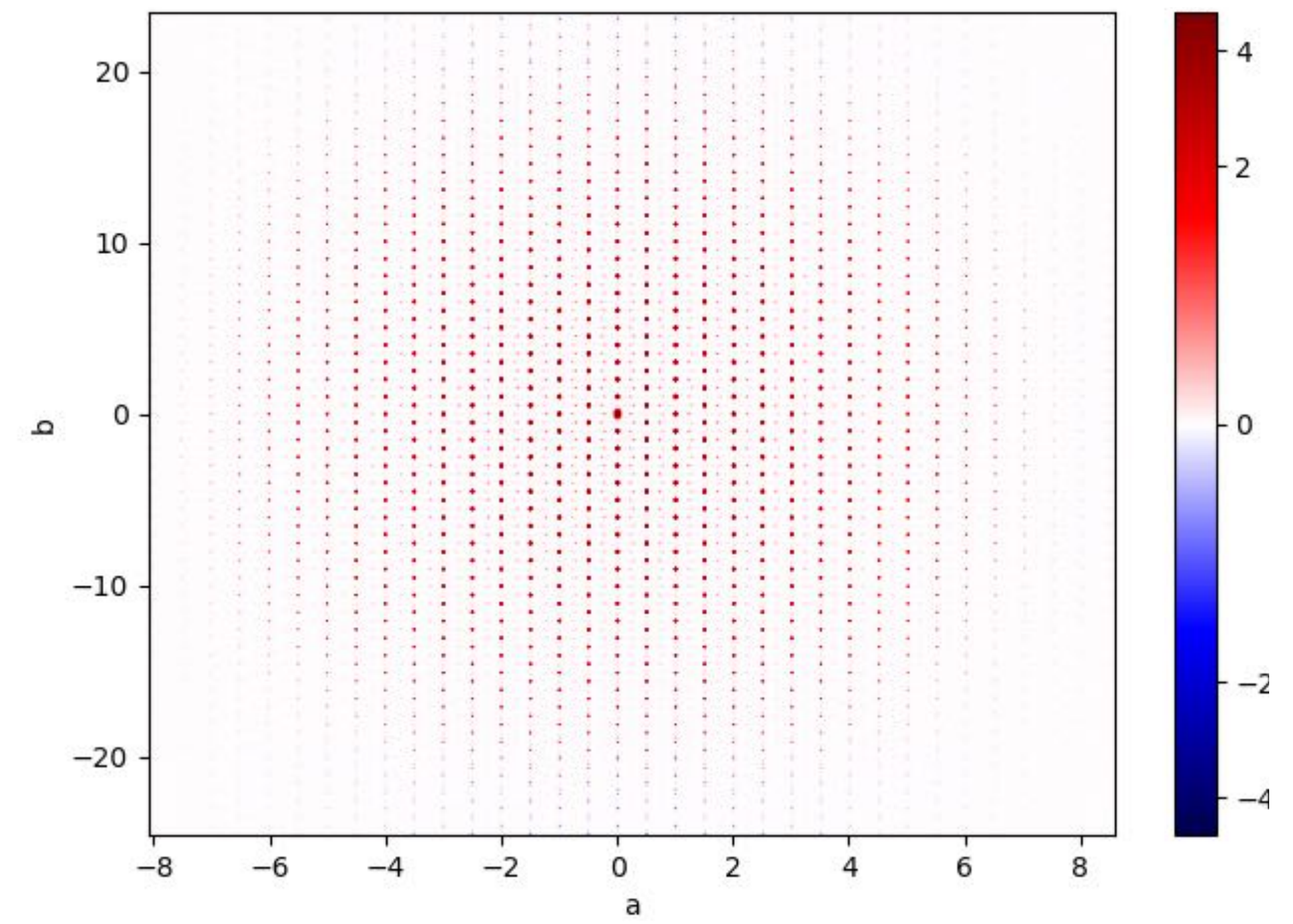
ORDER-DISORDER TRANSITION VIEWED IN REAL SPACE

Na_{0.45}V₂O₅

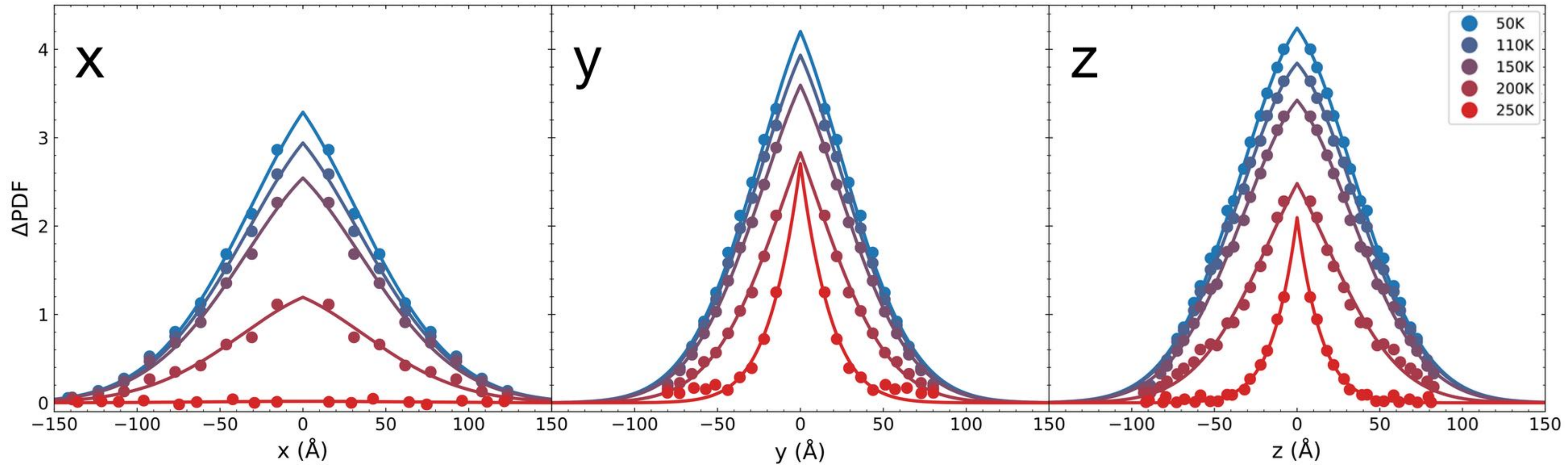


EFFECT OF Q-RESOLUTION

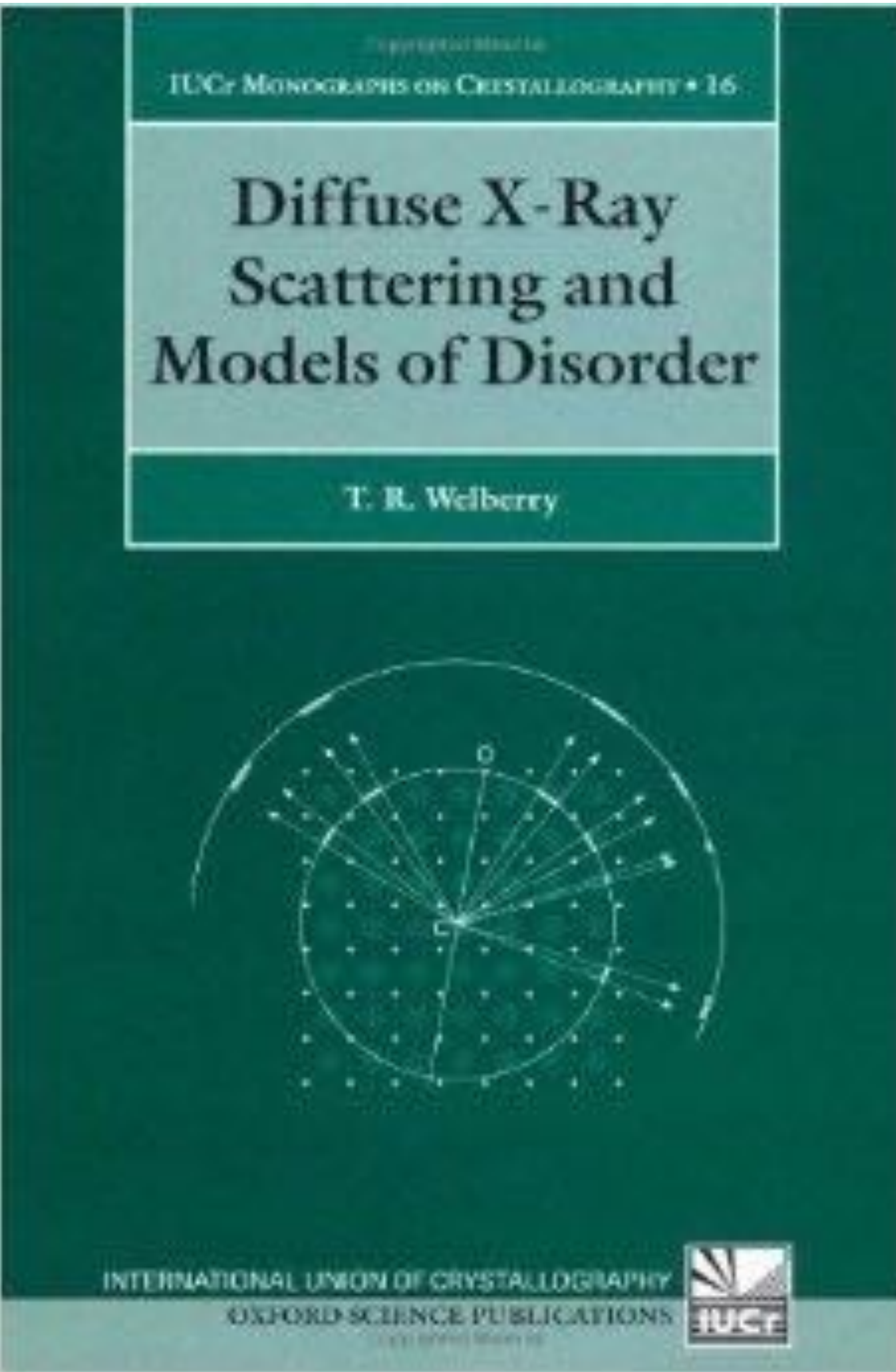
- Finite Q-resolution \rightarrow Gaussian envelope in real space.
- The width can be determined from the total PDF
 - *i.e.*, the transform of the long-range crystal structure.



FITTING CORRELATION LENGTHS IN REAL SPACE



$$f(\mathbf{r}) = A \times G(r) \times \exp(-|\mathbf{r}|/\xi)$$



24.3.3 Ordering of Na within the two-leg ladders.

Fig. 24.10(a) shows a small region near the origin of the $x = 0$ plane of the Δ PDF map obtained from the 50K X-ray data. The strong white origin peak indicates perfect positive correlation for an atom with itself. Other white peaks also indicate a positive correlation between an atom at the origin with another at a position given by the vectors A, B or C (and the reverse vectors $-A$, $-B$ and $-C$). Conversely the dark peaks indicate strong negative correlations. It is quite straightforward to deduce from the observed pattern of white and dark peaks that the local arrangement of the Na ions must follow a pattern like that shown in Fig. 24.10(b), where the occupancy of the two Na sites on each rung of the two-leg ladders tends to alternate between $(Na\Box^\dagger)$ and $(\Box Na)$ producing a zig-zag chain of occupied sites. Neighbouring ladders at $z = \pm 1.0$ have the same occupancy pattern which is in phase with the ladder at $z = 0$.

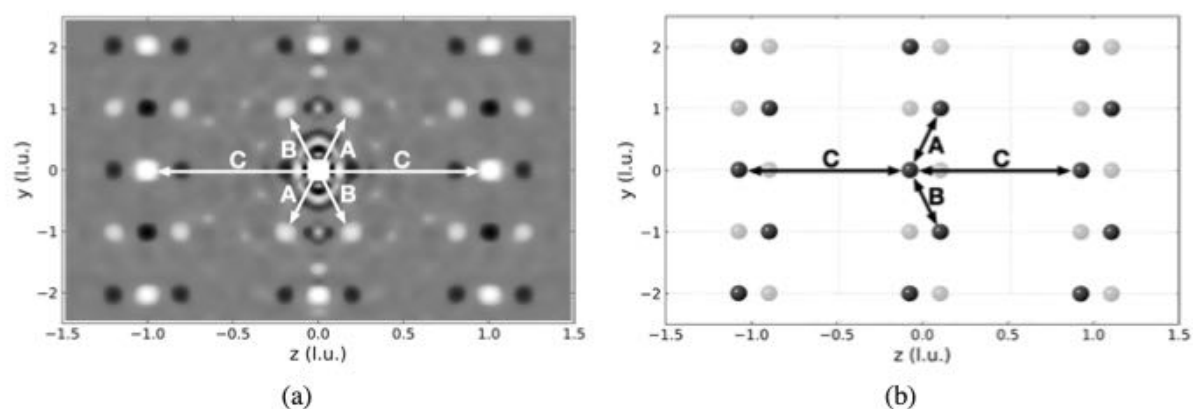


Fig. 24.10 A comparison of (a) the Δ PDF peak intensities at 50K in the $x = 0$ plane of $Na_{0.45}V_2O_5$ with (b) the derived real-space model of sodium ions. Data used in this figure are reproduced with kind permission of Dr Ray Osborn.

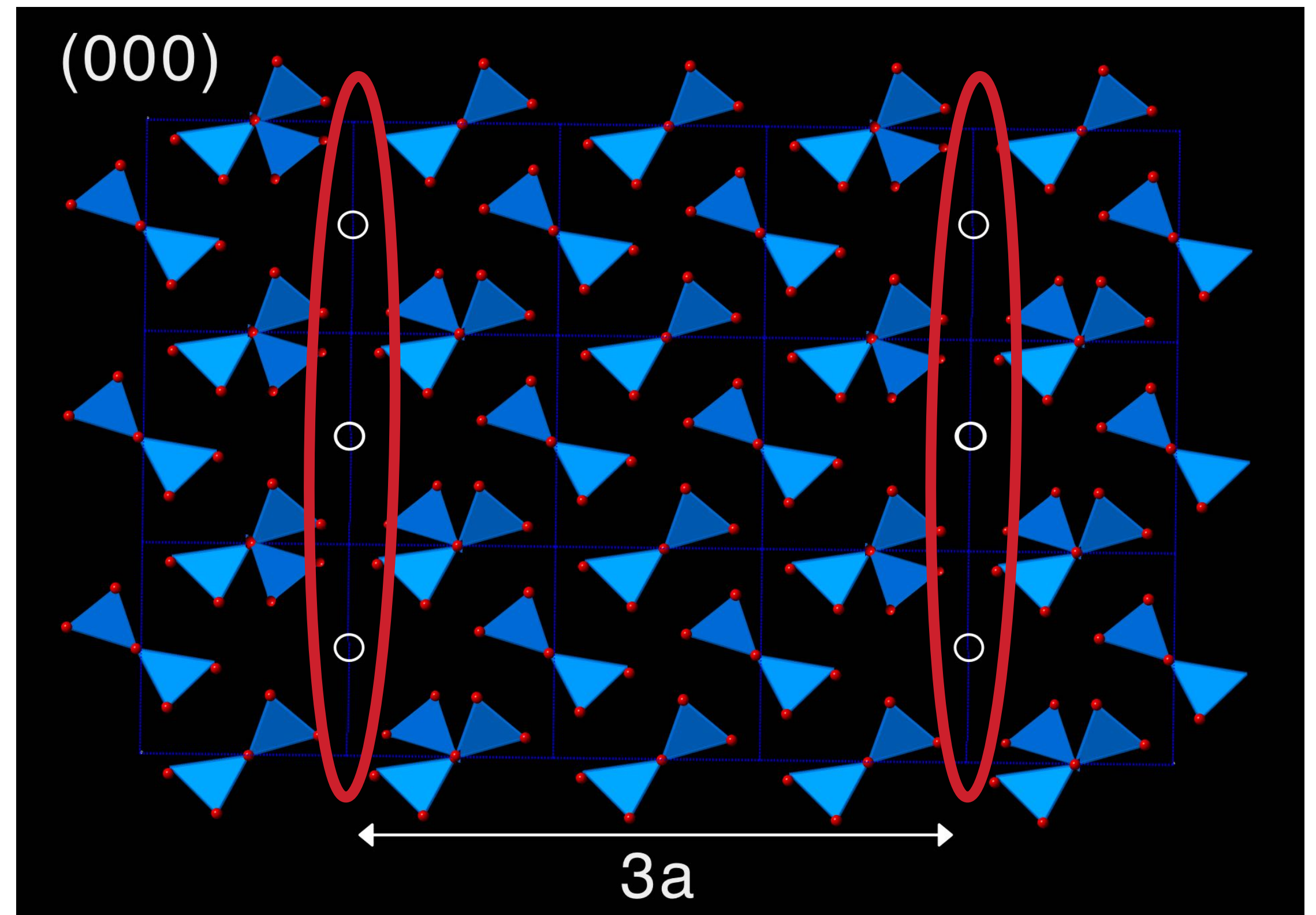
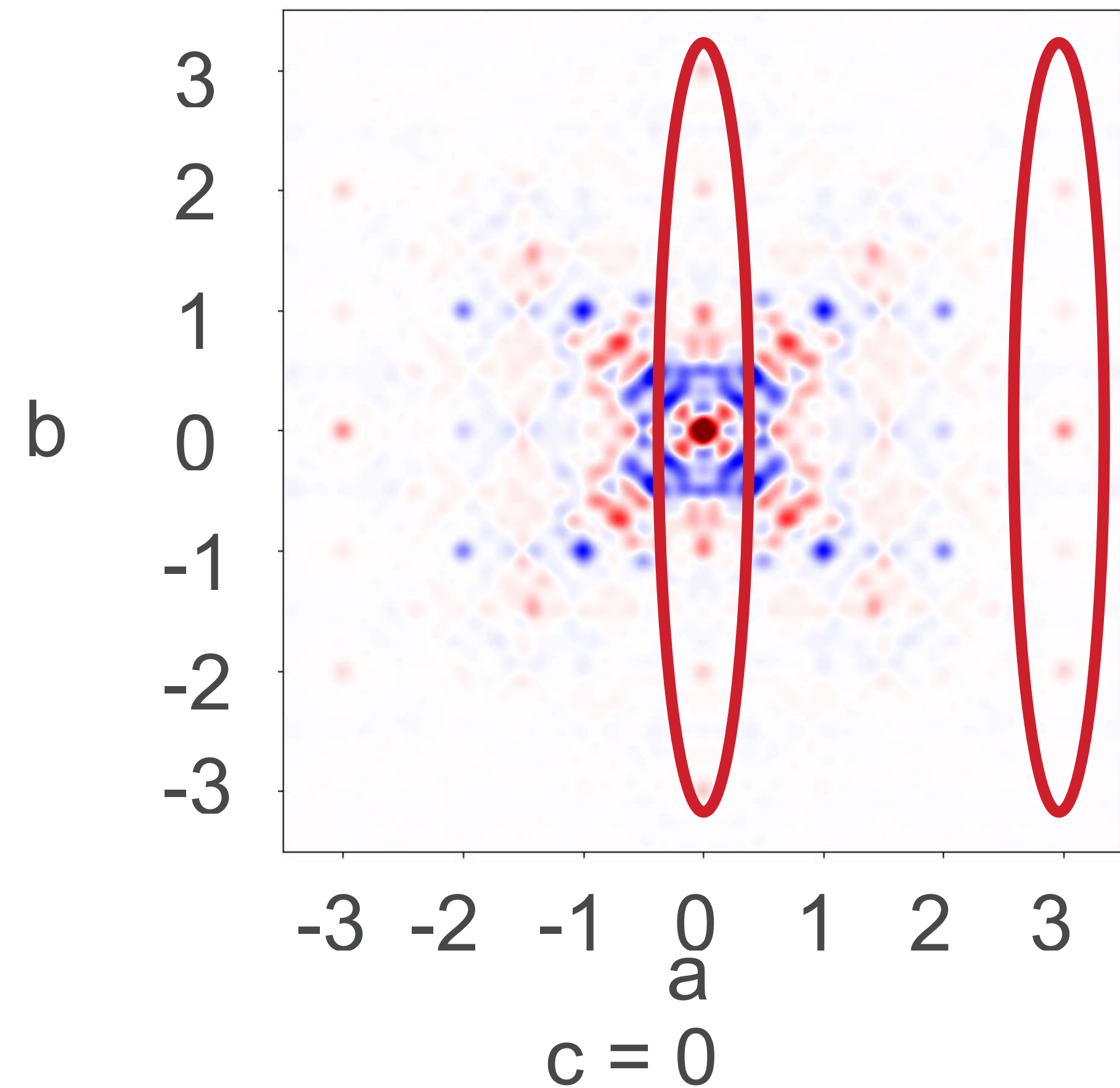
24.3.4 Δ PDF peak intensities in the $z = 0$ plane.

Fig. 24.12 shows the $z = 0$ plane of the Δ PDF map observed at three different temperatures. Fig. 24.11(b) shows an enlargement of part of Fig. 24.11(a) where white arrows (labelled A–F) have been used to identify different interatomic vectors. The same set of vectors is shown in Fig. 24.11(e) which is a plot of the $z = 0$ plane of the average structure. The maps are dominated by the same alternating correlations of Na occupancy along the ladder direction parallel to y . Similarly neighbouring chains at $x = \pm 1$ are instep with that at $x = 0$ for temperatures 50K and 150K but at 250K these correlations have been lost.

Although the maps are dominated by the correlations in the Na ladders there are numerous weaker peaks that correspond to correlations between the ladder Na_1 ions and the interstitial Na_2 ions. These correspond to vectors A, B, C and E in Fig. 24.11(e) and involve one Na_1 and one Na_2 ion. These peaks are clearly evident in the 50K map, somewhat less evident at 150K and even less evident at 250K. They are weak relative to those involving Na_1 ions alone simply because of the low occupancy of the Na_2 sites.

[†]here \Box is used to represent a vacant site

BACK TO MULLITE



HOW DO I LOOK AT STATIC DISORDER?



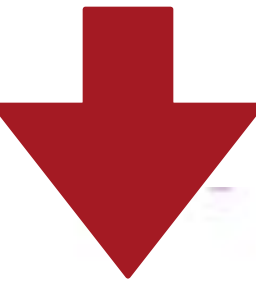
Argonne National Laboratory is a
U.S. Department of Energy laboratory
managed by UChicago Argonne, LLC.



COMPARISON OF ELASTIC SCATTERING AND THE STATIC APPROXIMATION

$$G(\mathbf{r}, t) = \frac{1}{N} \left\langle \sum_{i=1}^N \sum_{j=1}^N \delta(\mathbf{r} - \mathbf{r}_i(t) + \mathbf{r}_j(0)) \right\rangle$$

$$S(\mathbf{Q}, \omega) = \frac{1}{N} \frac{1}{2\pi\hbar} \int_{-\infty}^{\infty} e^{-i\omega t} dt \int G(\mathbf{r}, t) e^{-i\mathbf{Q} \cdot \mathbf{r}} d\mathbf{r} \quad \hbar\delta(t) = \frac{1}{2\pi} \int_{-\infty}^{\infty} e^{i\omega t} d(\hbar\omega)$$



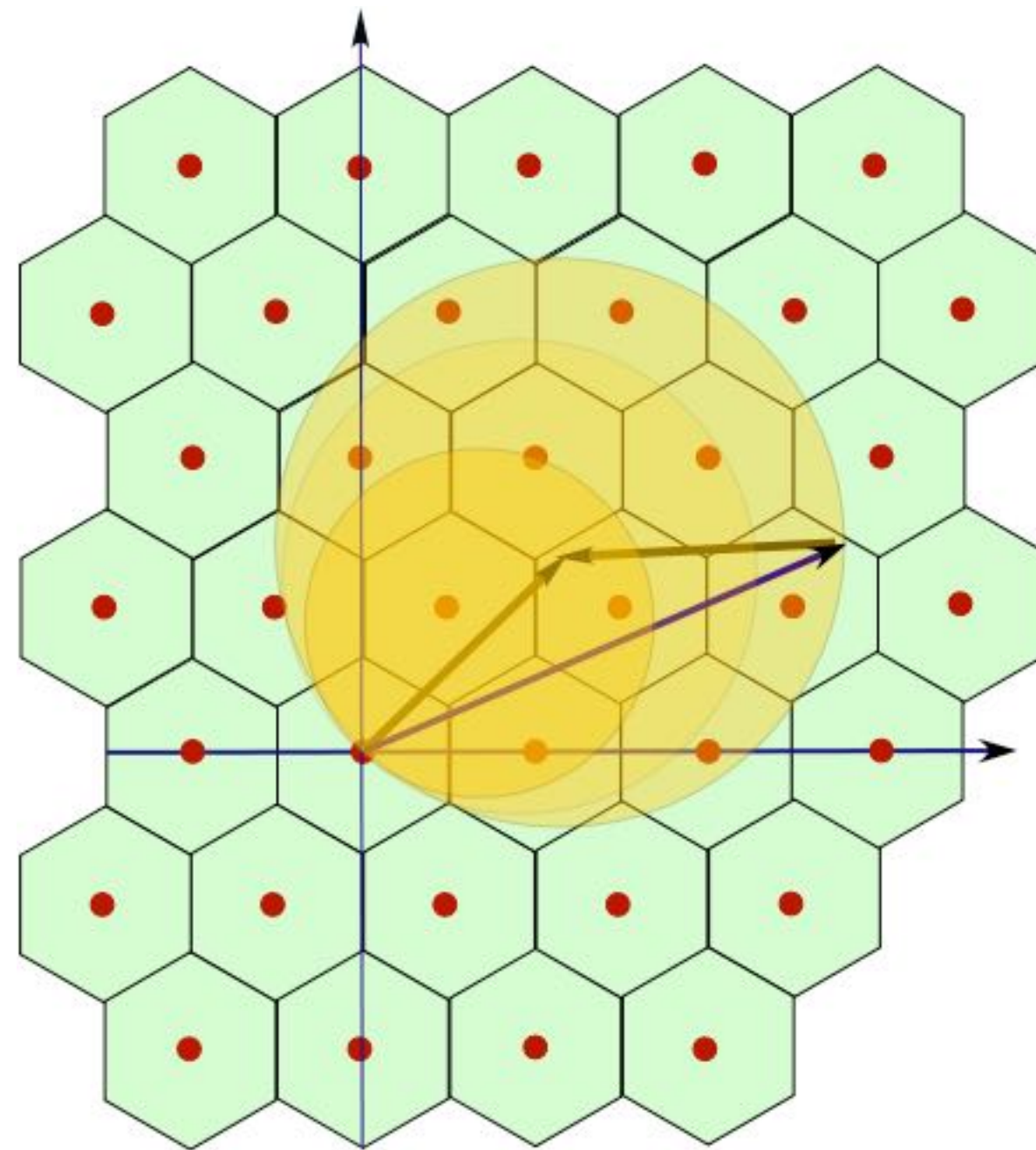
$$\left(\frac{d\sigma}{d\Omega} \right)_{coh}^{static} = b_{coh}^2 N \int G(\vec{r}, 0) e^{i\vec{Q} \cdot \vec{r}} d\vec{r}$$

$$\left(\frac{d\sigma}{d\Omega} \right)_{coh}^{elastic} = b_{coh}^2 N \int G(\vec{r}, \infty) e^{i\vec{Q} \cdot \vec{r}} d\vec{r}$$

MEASURING LARGE VOLUMES OF RECIPROCAL SPACE

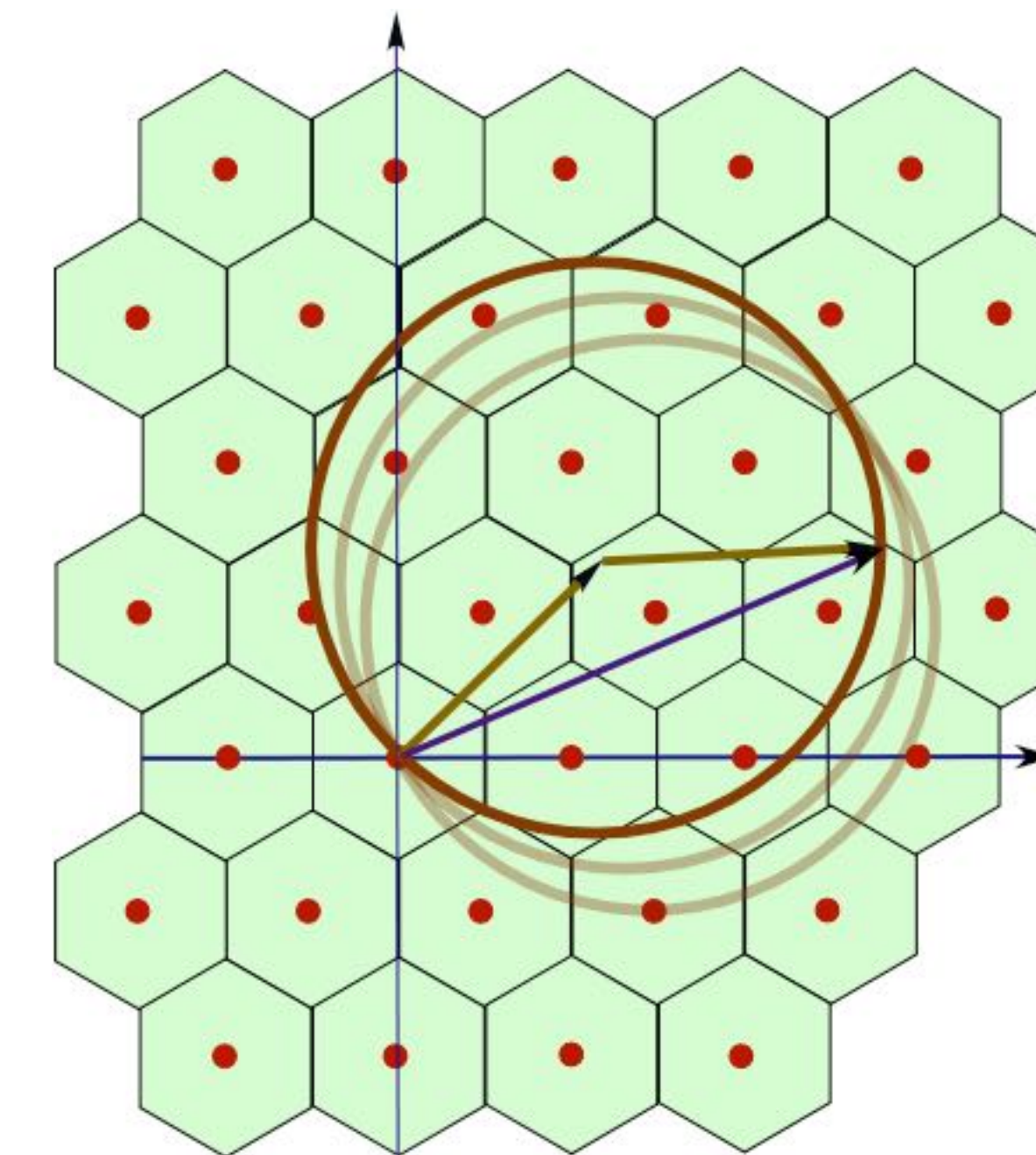
Conventional Time-of-Flight Neutron Methods

White Beam:
efficient



NO energy discrimination

Fixed k_i :
energy resolved



NOT efficient

CROSS CORRELATION CHOPPER

S. Rosenkranz and R. Osborn, PRAMANA- Journal of Physics, 71, 705 (2008).

TOF Laue Diffractometer

- highly efficient data collection
- wide dynamic range in Q

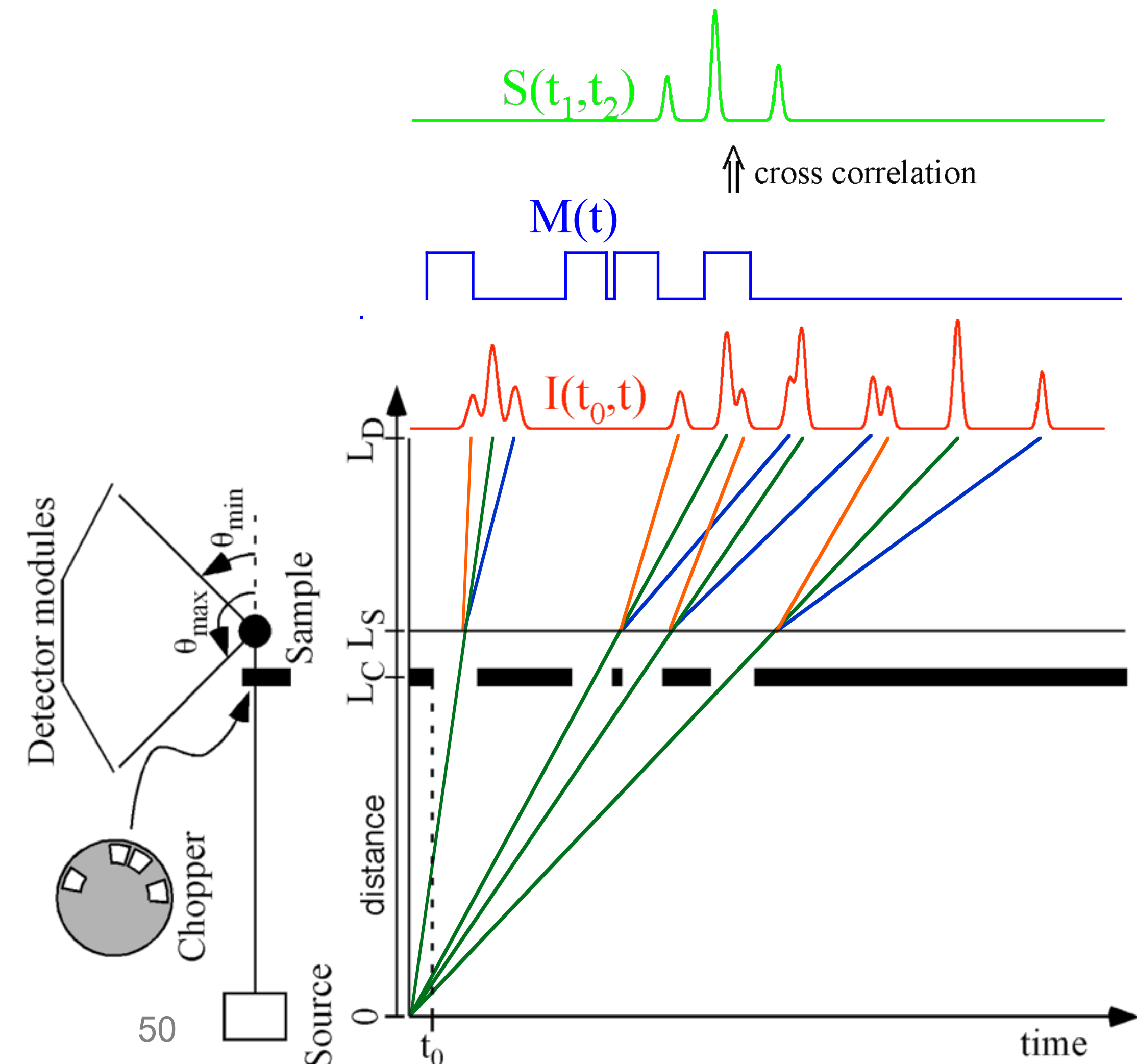
Statistical Chopper

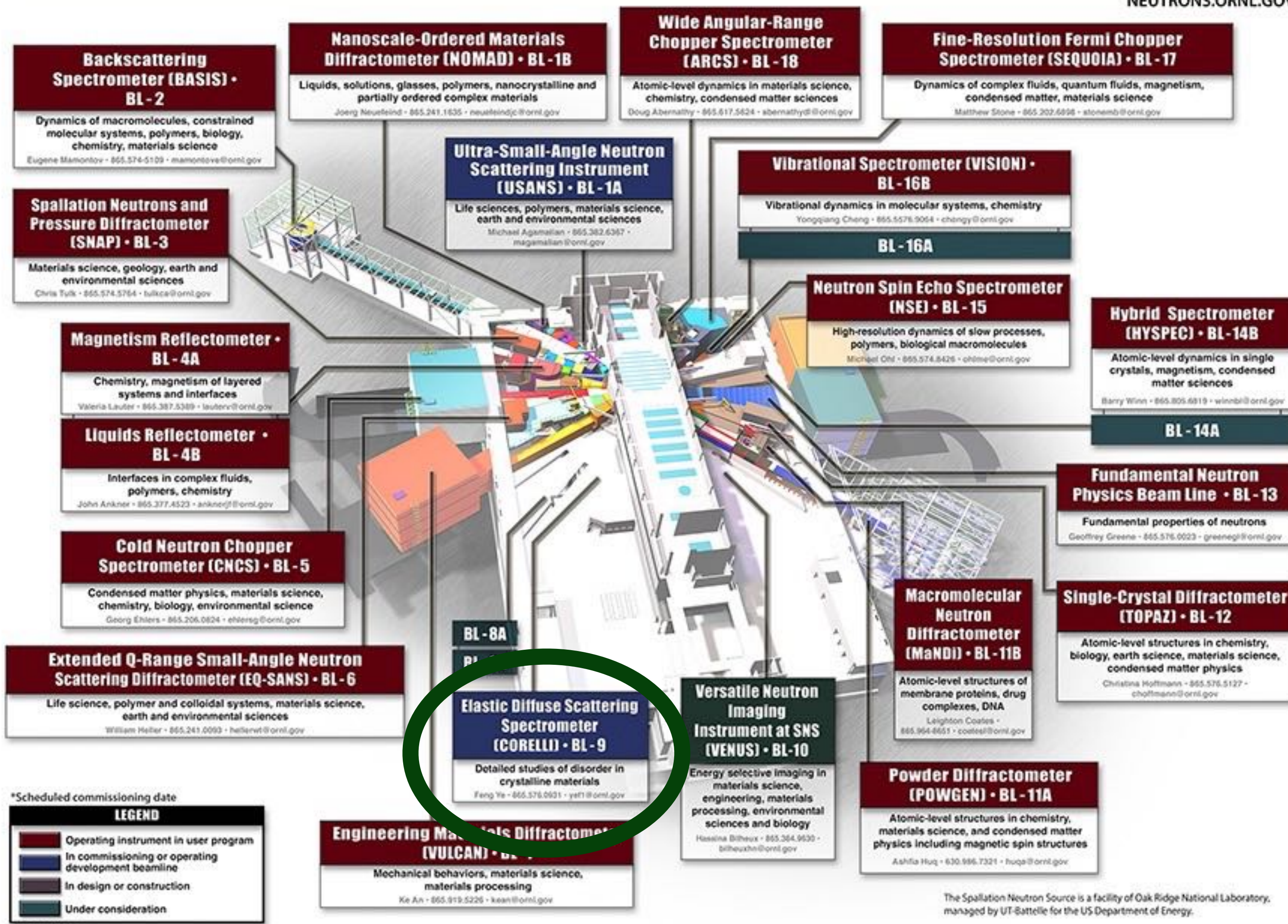
- elastic energy discrimination
- optimum use of white beam

Elastic scattering: $\hbar\omega = 0$

Inelastic scattering: $\hbar\omega = +E_0$

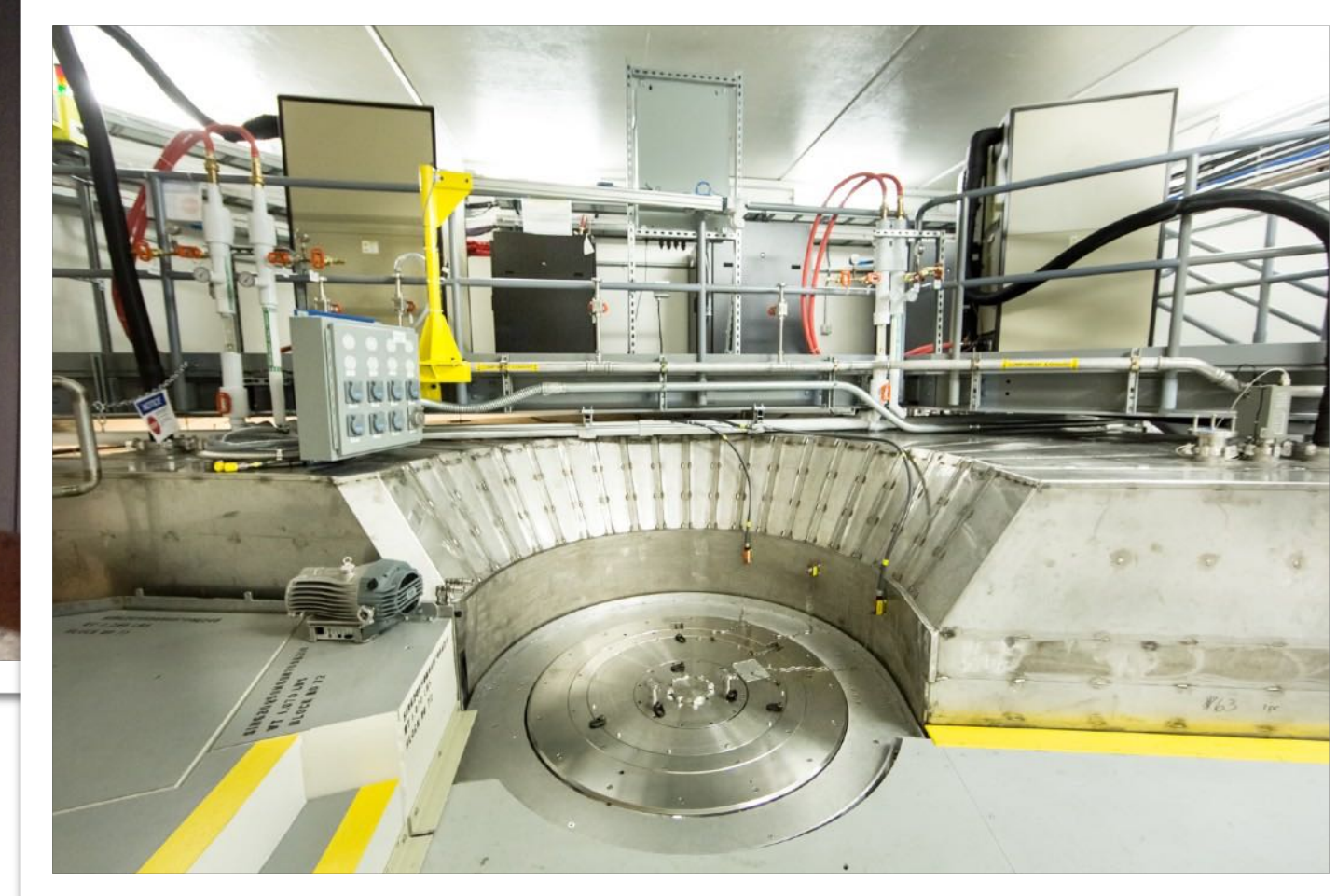
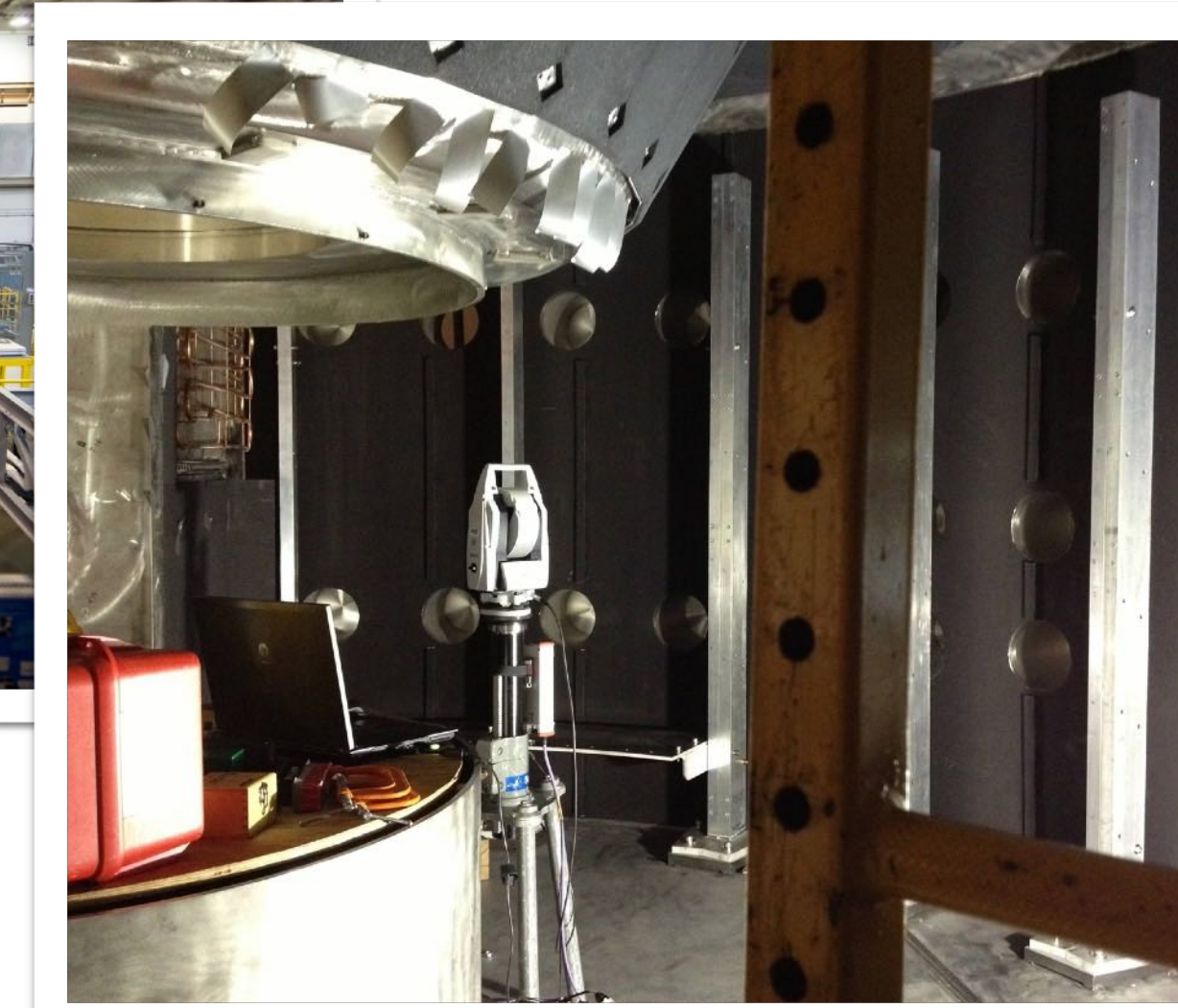
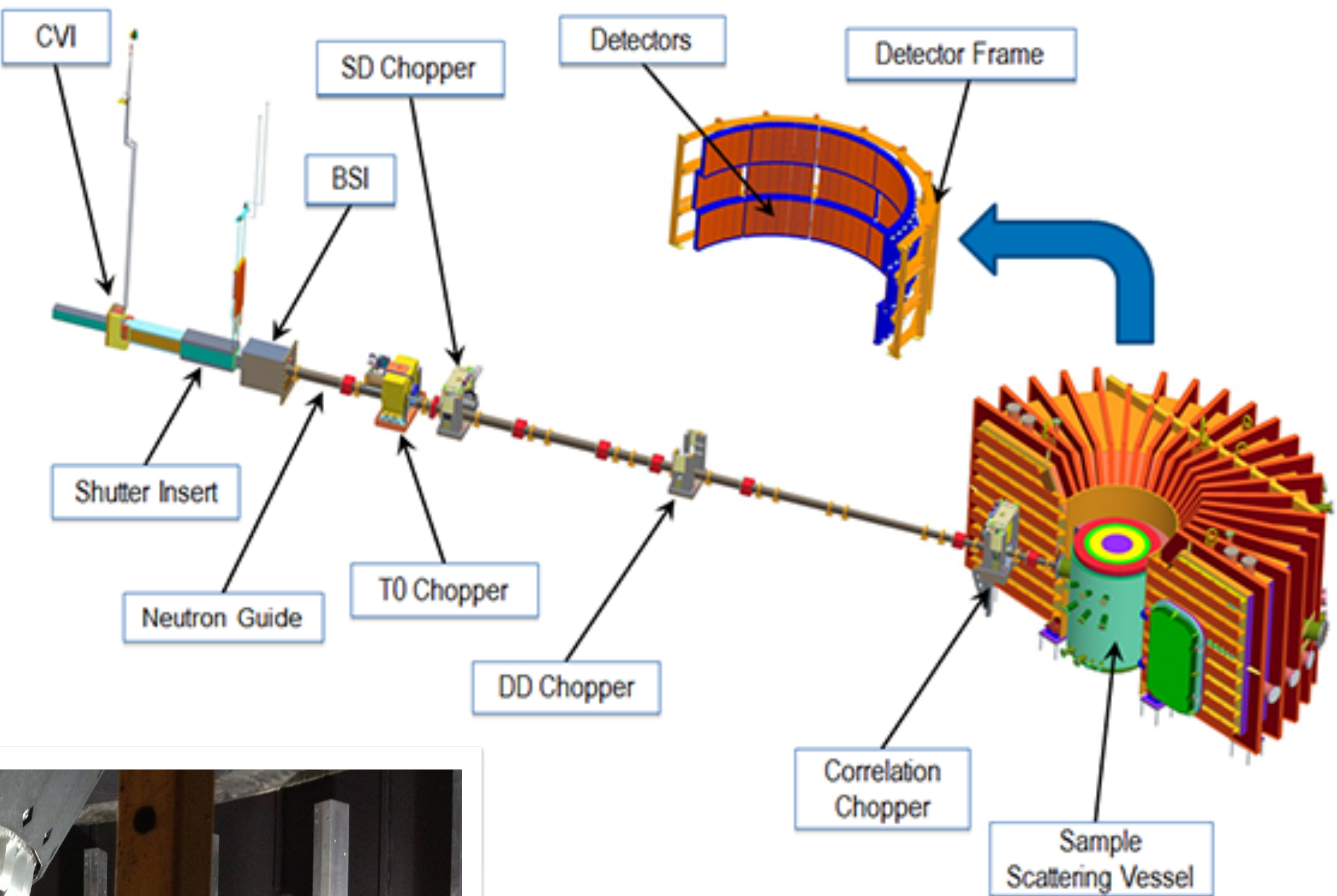
$\hbar\omega = -E_0$





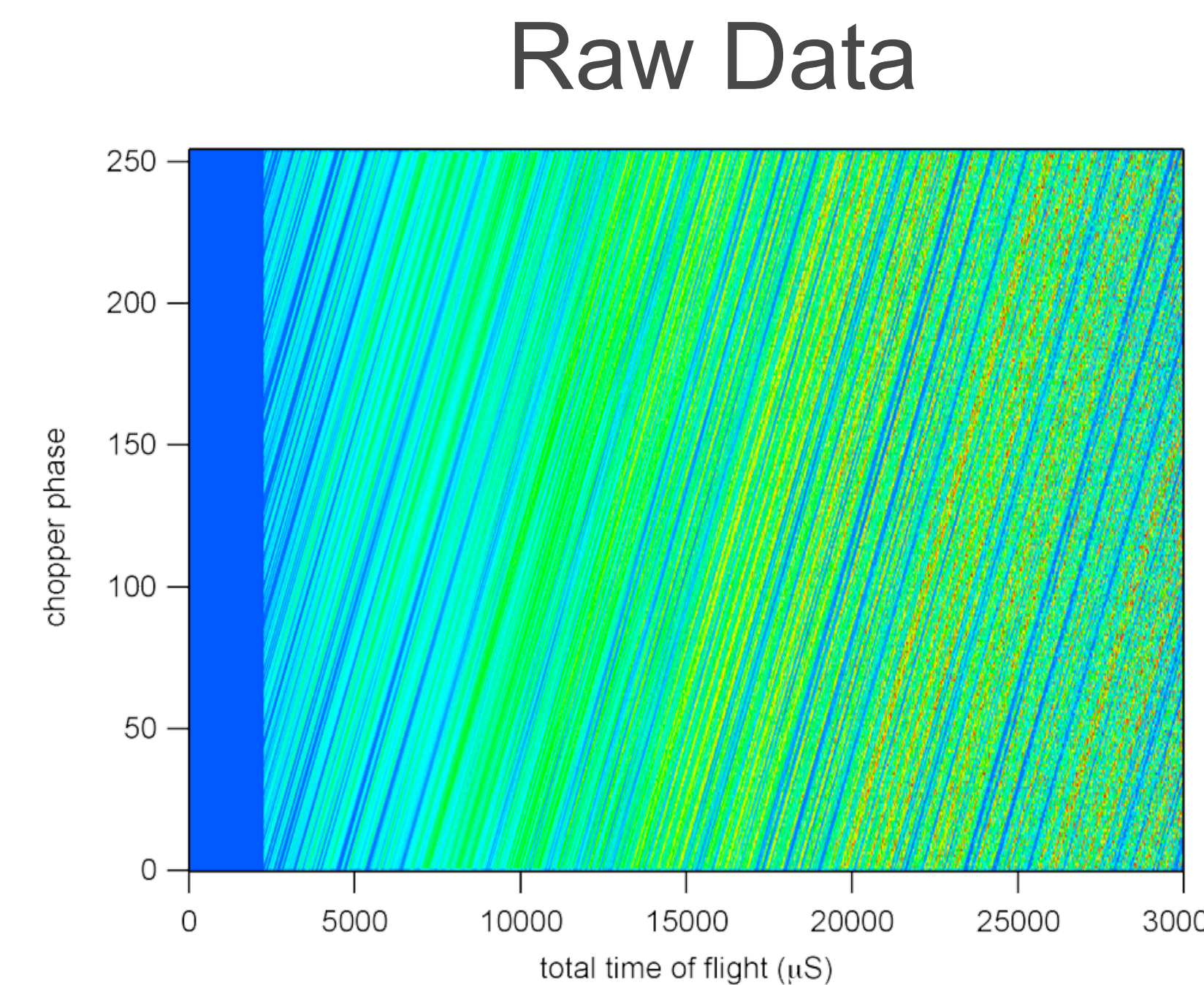
CORELLI

Instrument Scientists
Feng Ye
Yaohua Liu



Instrument Proposers
Stephan Rosenkranz
Ray Osborn

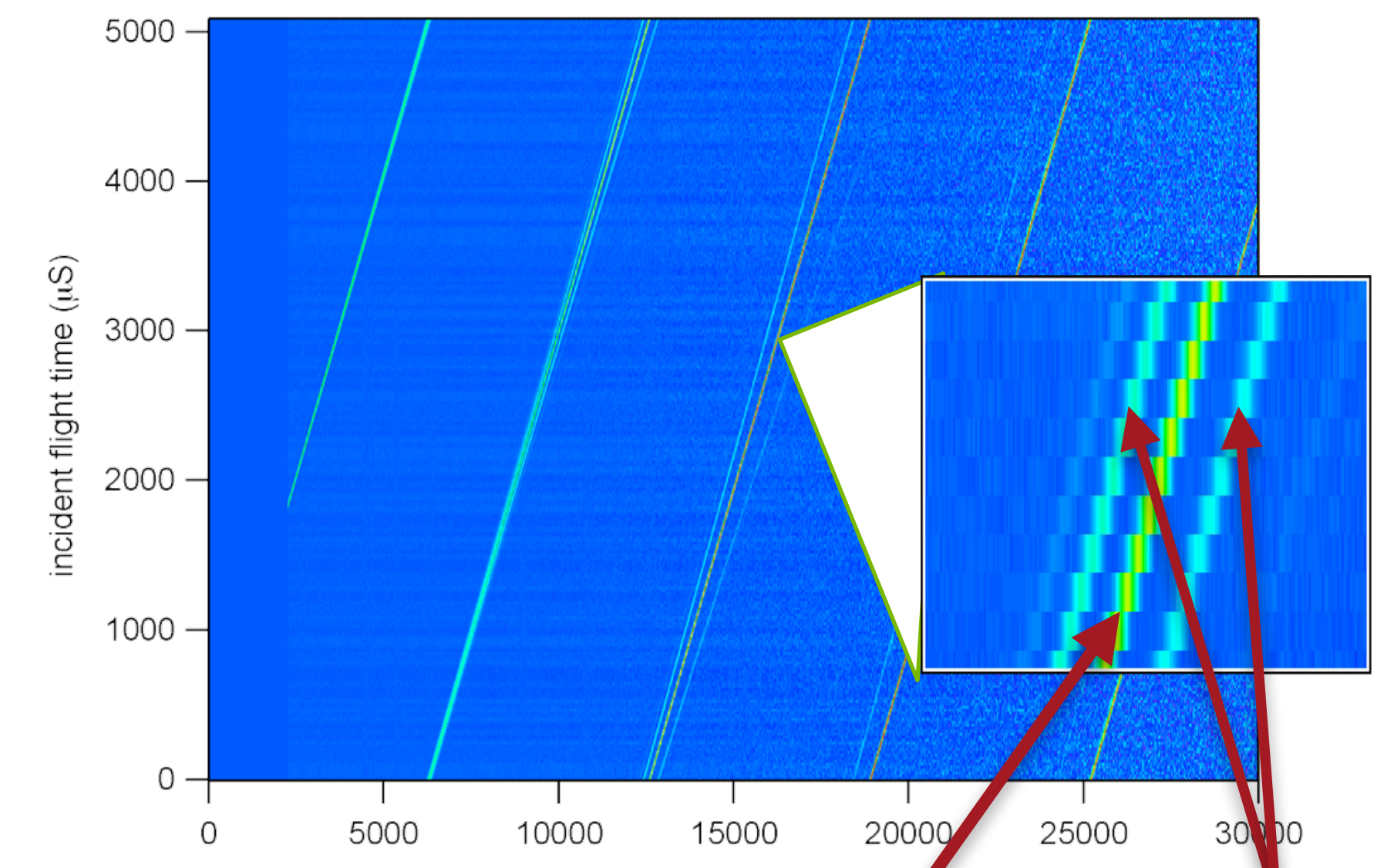
CROSS CORRELATION IN ACTION



Cross
Correlation



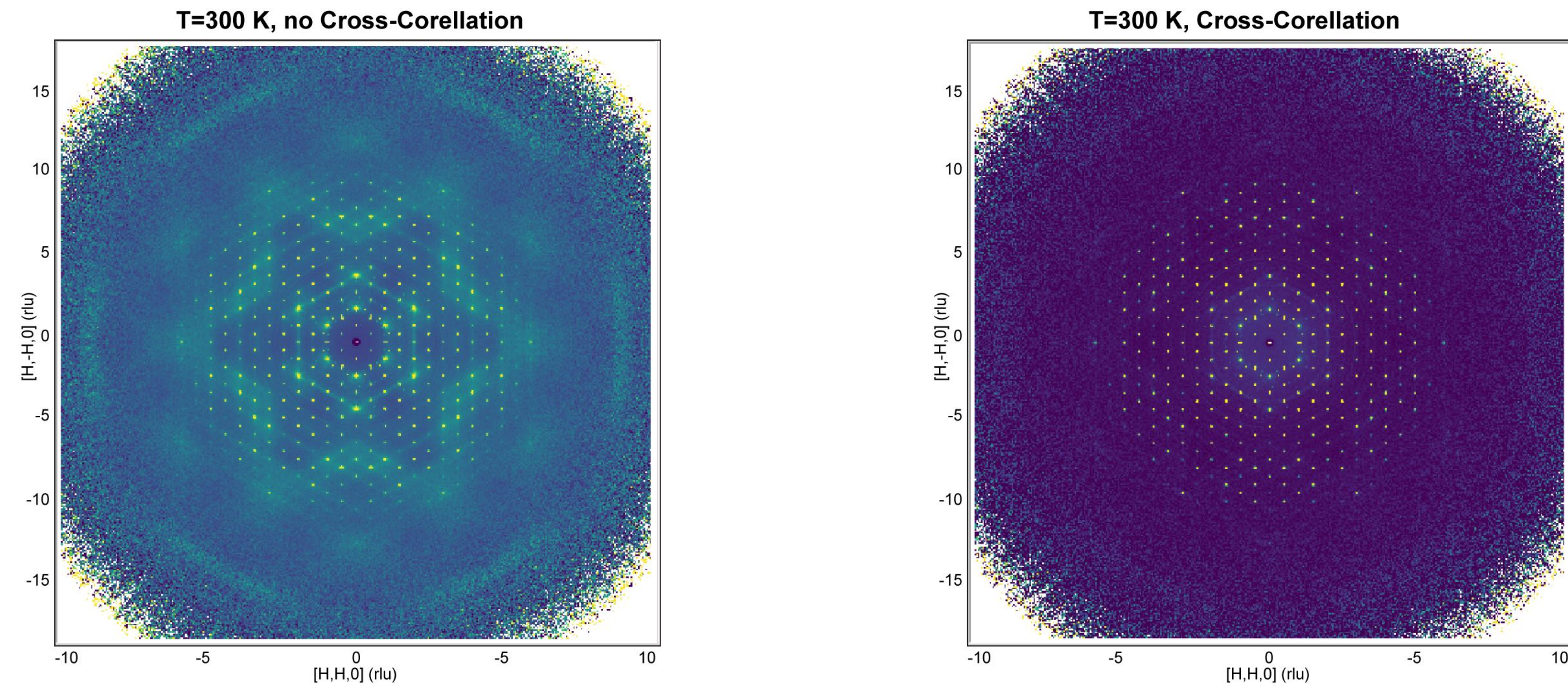
Reconstructed Scattering Function



elastic inelastic

ELASTIC DISCRIMINATION WITH CROSS CORRELATION

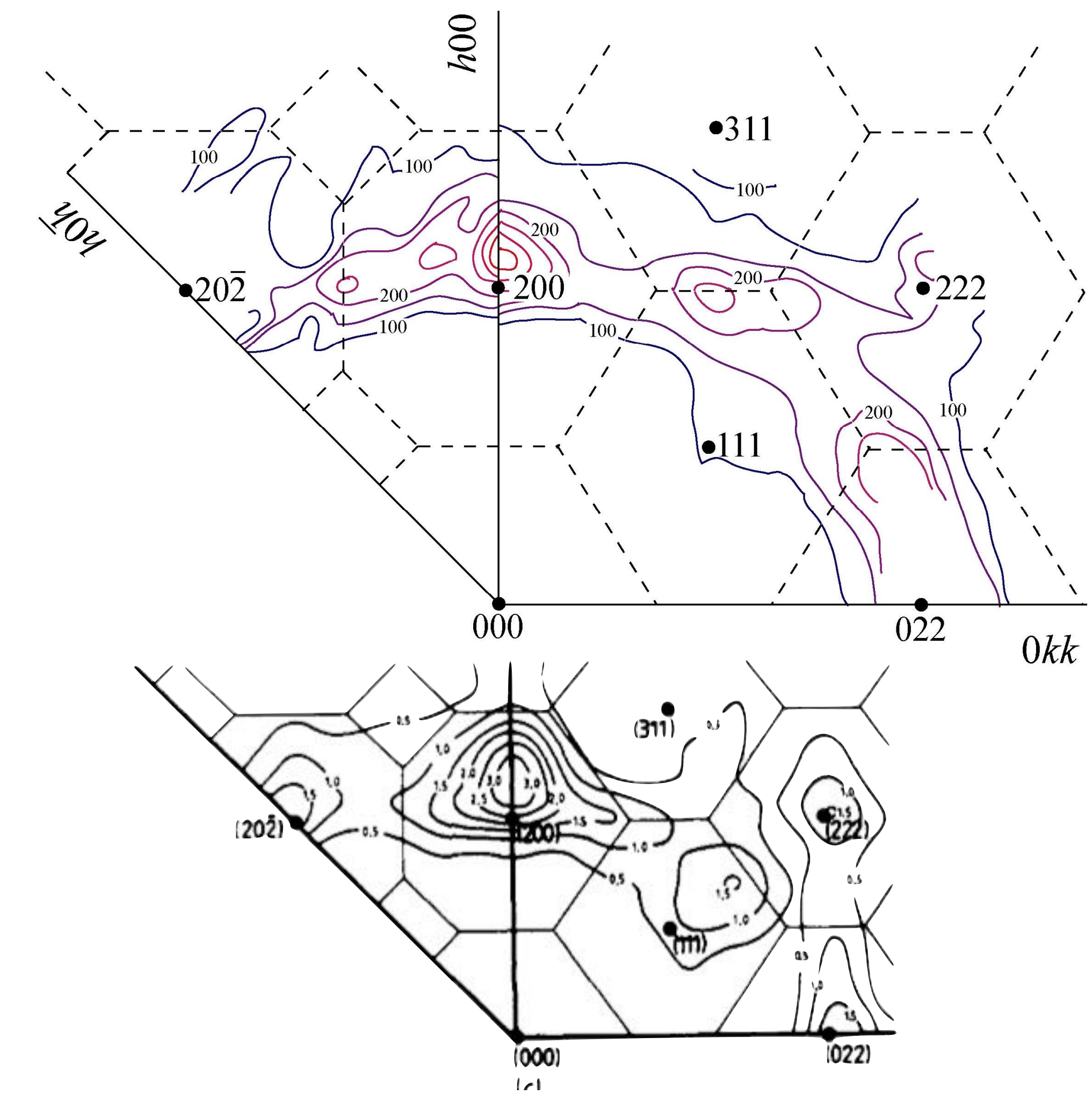
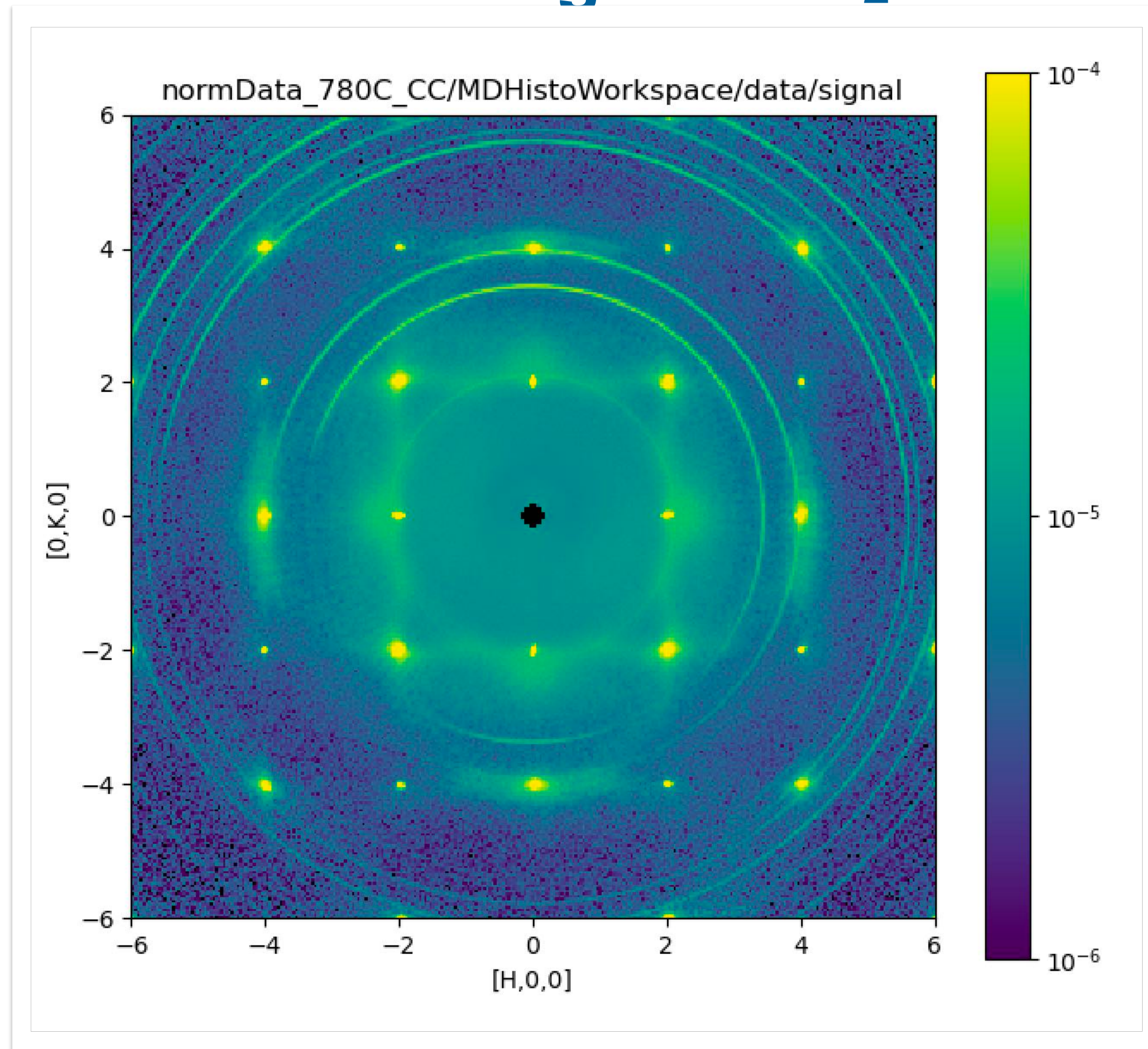
Benzil $C_{14}H_{10}O_2$



T. R. Welberry and R. Whitfield, Quantum Beam Science 2, 2 (2018)

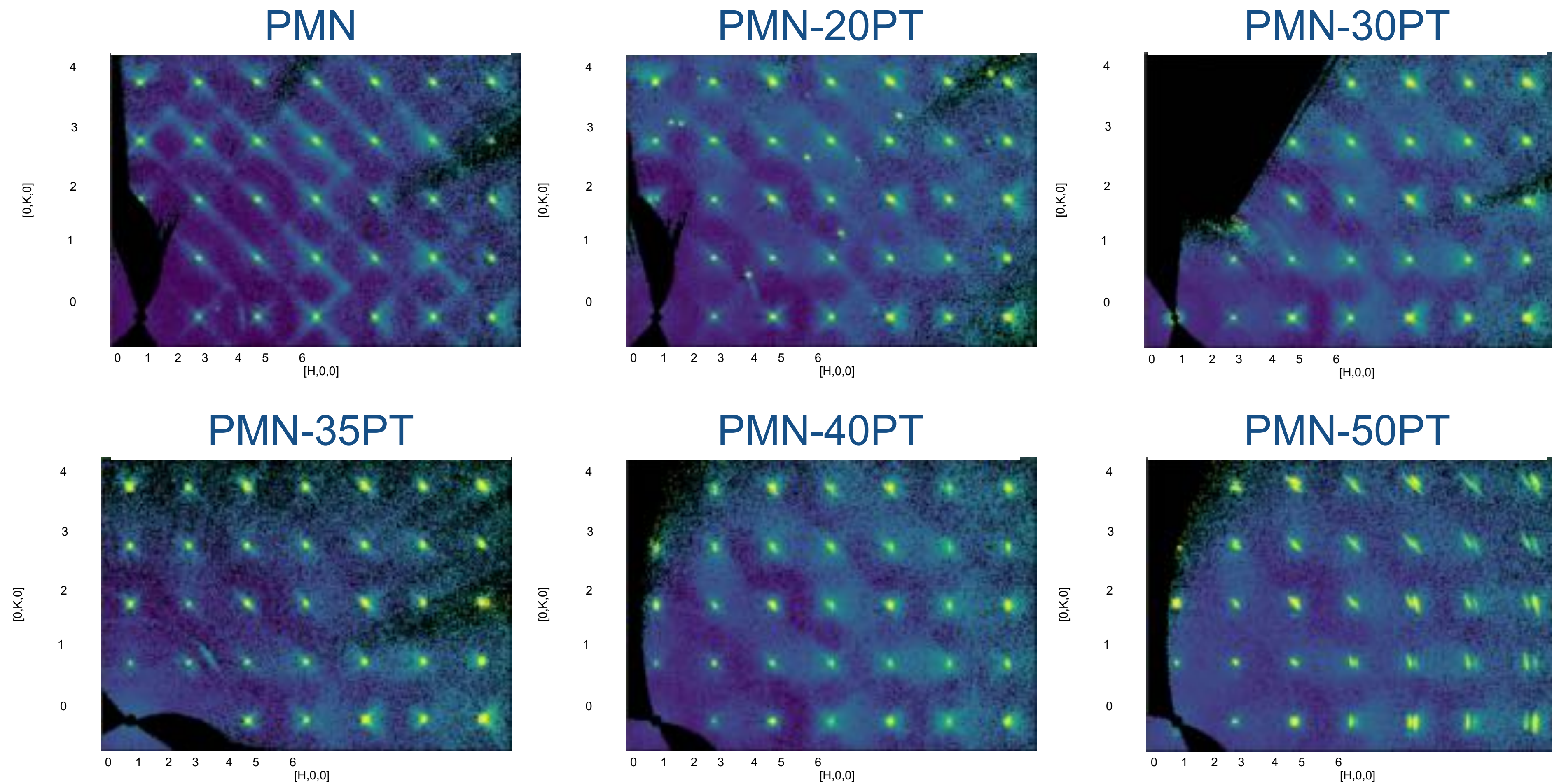
DIFFUSE SCATTERING FROM A FAST-ION CONDUCTOR

Sublattice Melting in SrCl_2



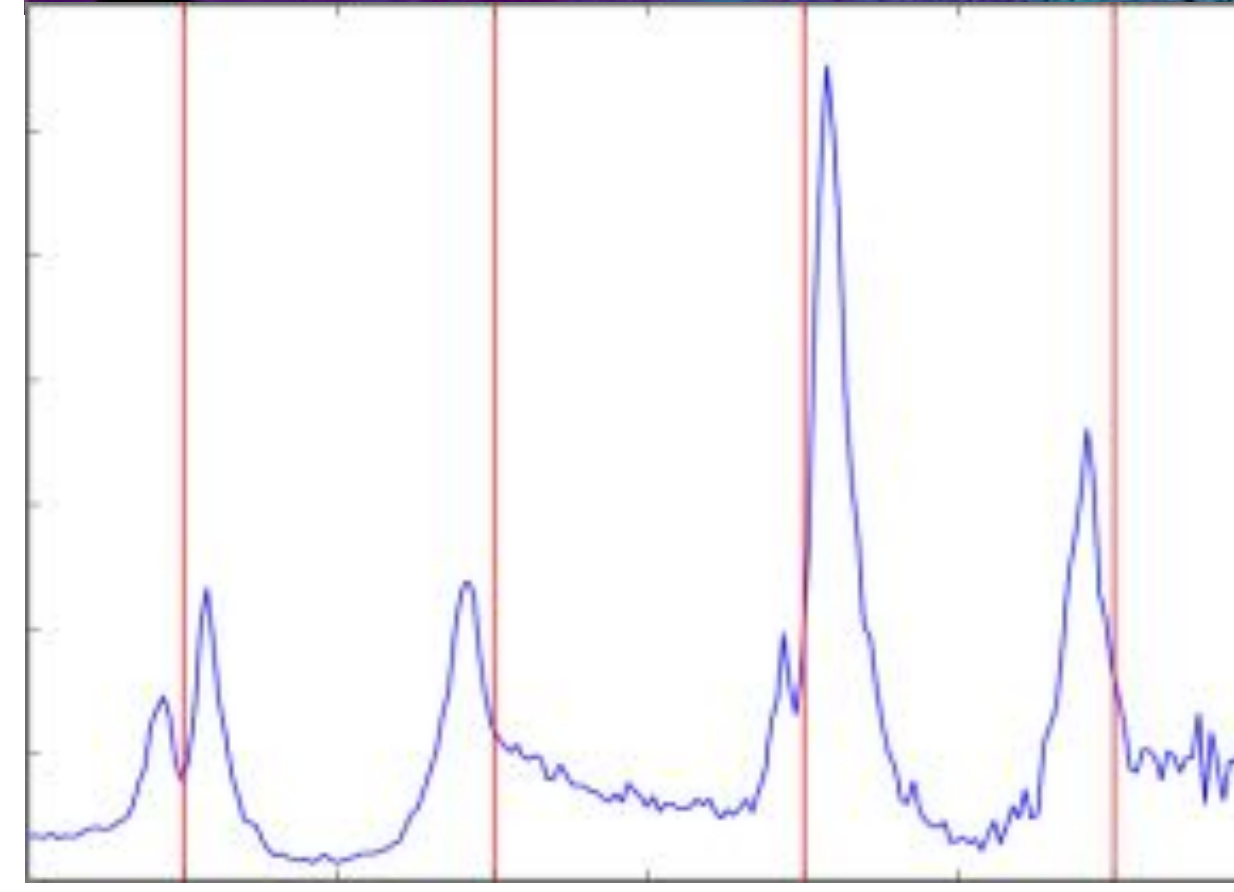
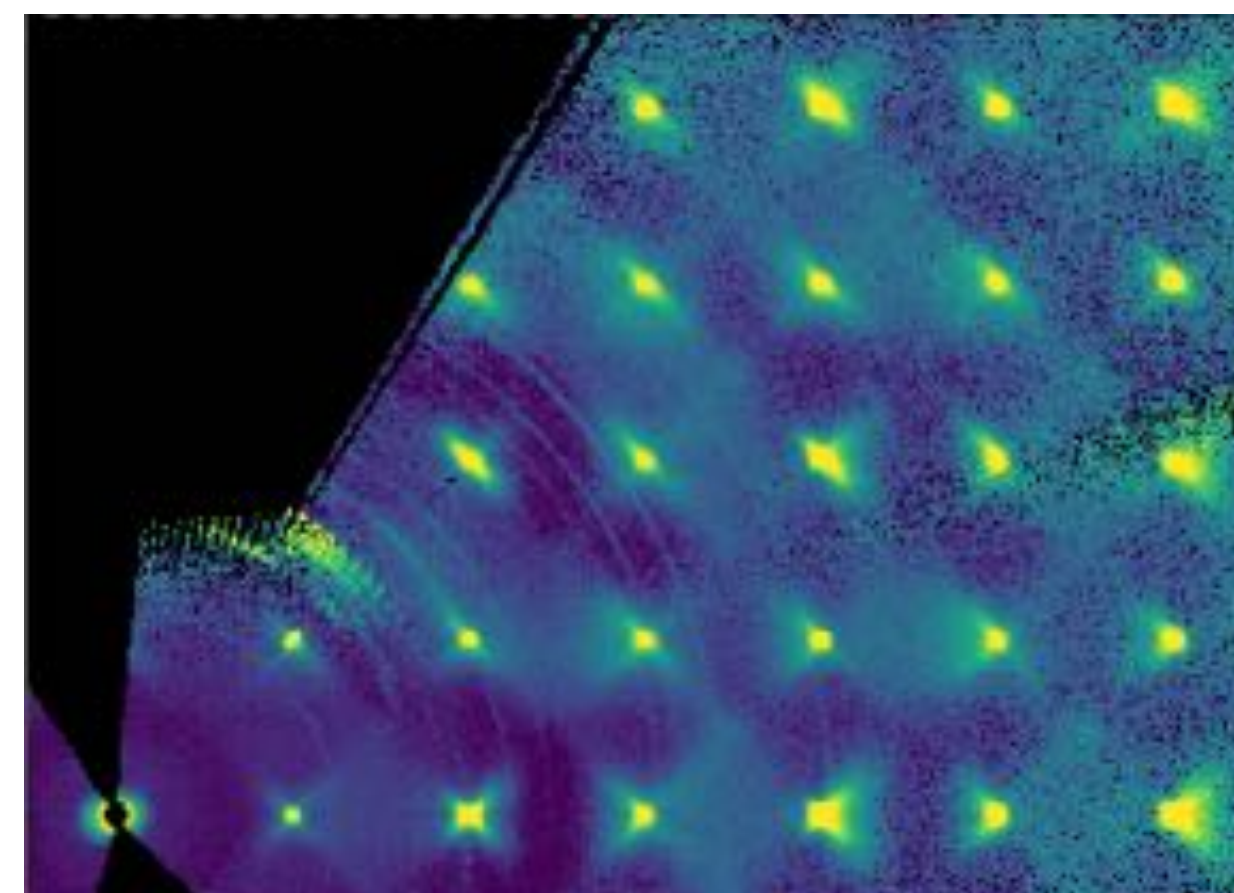
RELAXOR FERROELECTRICS - $\text{Pb}(\text{Mg}_{1/3}\text{Nb}_{2/3})\text{O}_{3-x}\text{PbTiO}_3$

M. J. Krogstad, *et al.*, Nat Mater 48, 1 (2018).

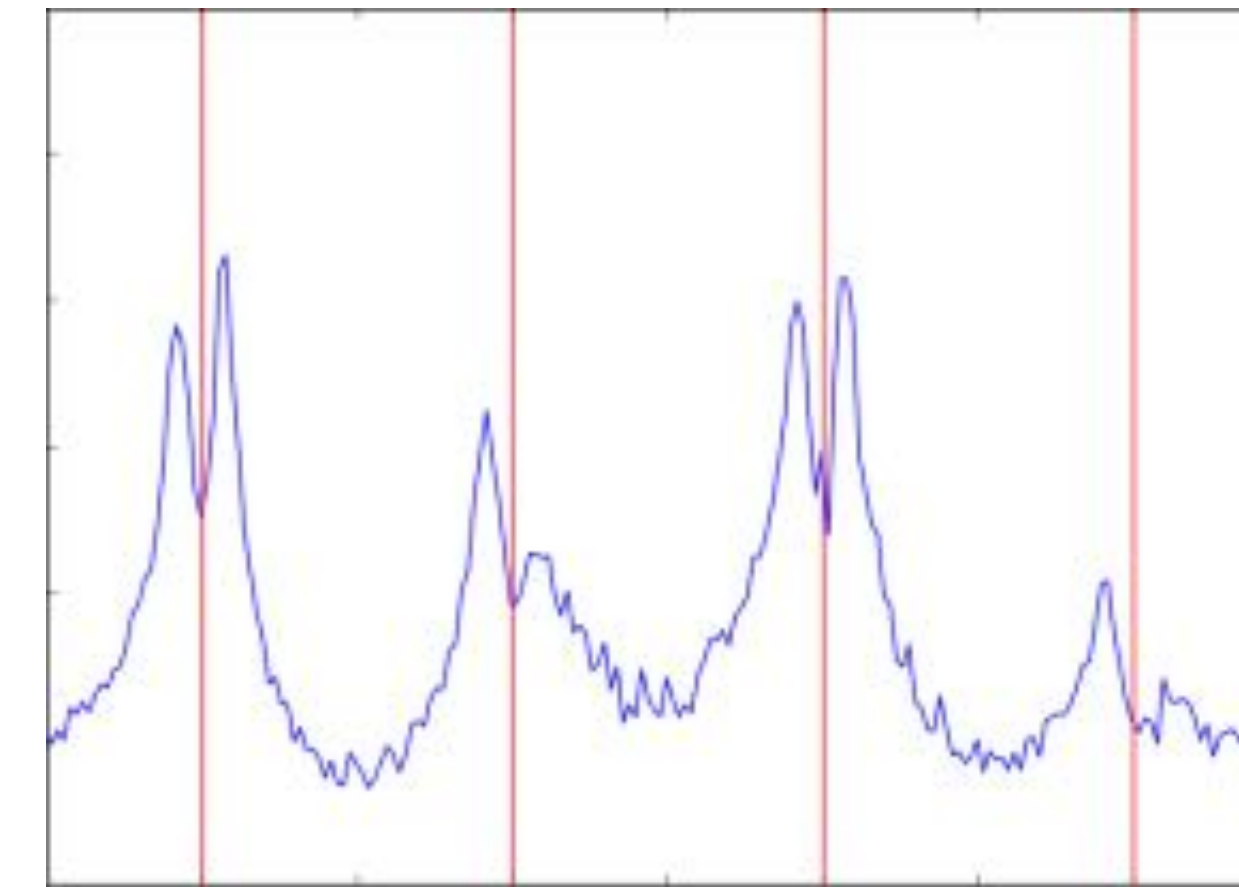
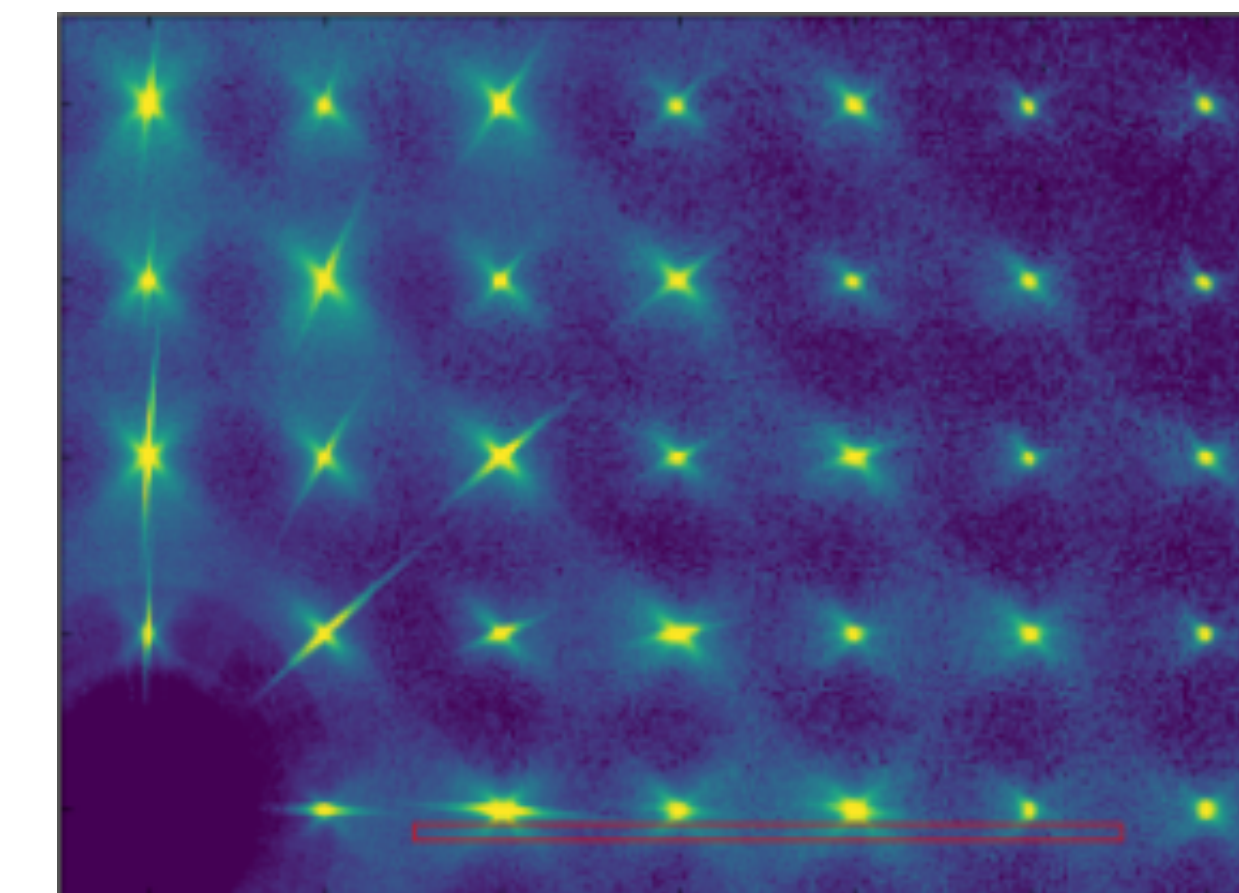


COMPLEMENTARITY OF NEUTRONS AND X-RAYS

$\text{Pb}(\text{Mg}_{1/3}\text{Nb}_{2/3})\text{O}_3$ -30% PbTiO_3



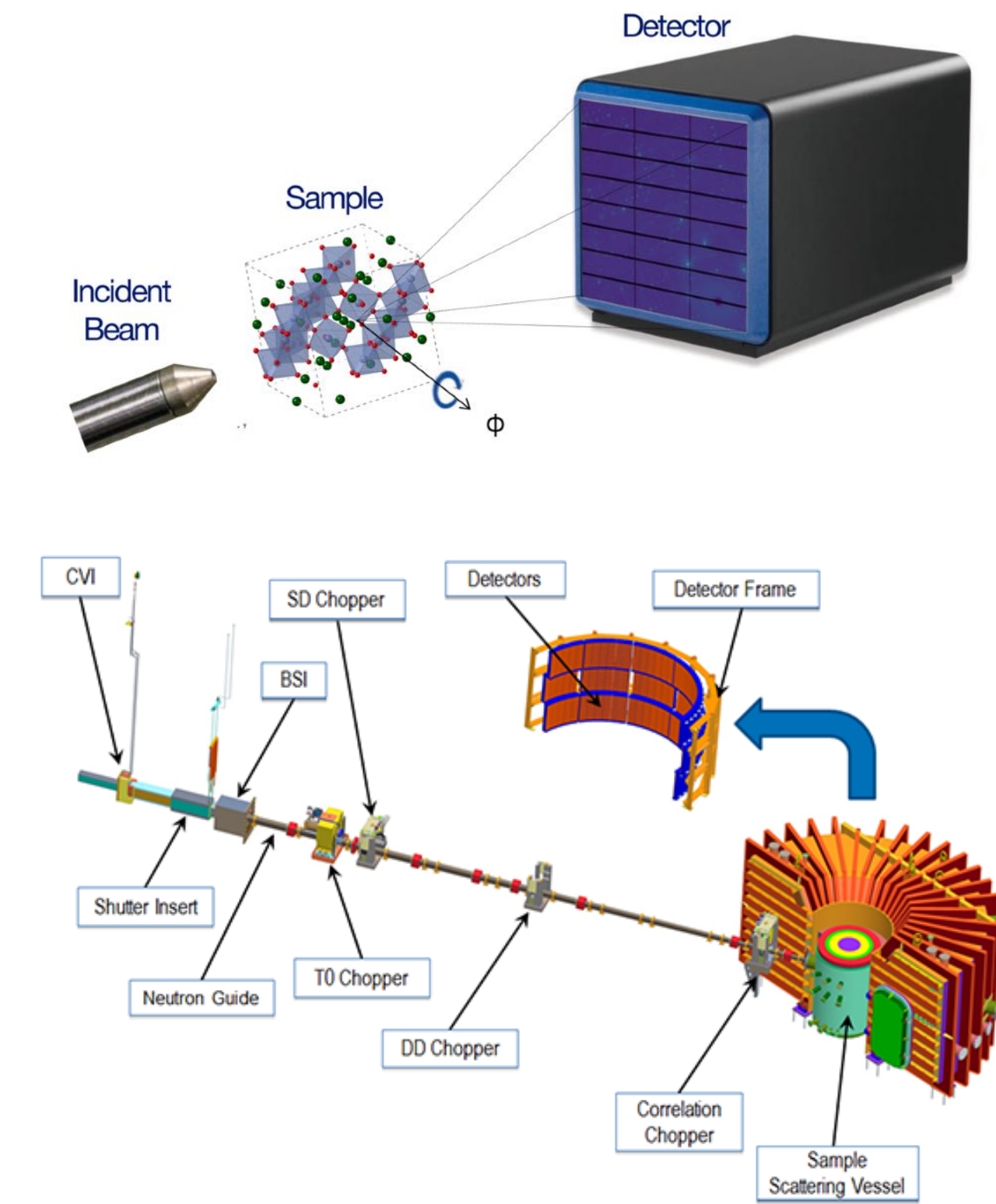
Corelli Neutrons



CHESS 55keV X-rays

THE FUTURE

- Advances in instrumentation have transformed our ability to measure single crystal total scattering over large volumes of reciprocal space.
 - High-Energy X-rays
 - Time-of-Flight Neutrons
- This is enabling new ways of analyzing the data:
 1. Unsupervised machine learning
 2. *ab initio* computational modeling
 3. 3D- Δ PDF - real-space pair distributions
- The results give unique insight into disordered materials
 - Bridging the gap between diffraction and imaging



A FEW REFERENCES

- T. R. Welberry & B. Butler, Chem Rev **95**, 2369–2403 (1995).
- F. Frey, Acta Cryst B **51**, 592–603 (1995).
- T. R. Welberry & D. J. Goossens, Acta Cryst A **64**, 23–32 (2007).
- D. A. Keen & A. L. Goodwin, Nature News **521**, 303–309 (2015).

